CATALOGED BY WCOSI-3

UNCLASSIFIED

4407

[redacted]

AD A075990

WADC TECHNICAL REPORT 52-152

[redacted]

Classification cancelled in accordance with Executive Order 10501 issued 5 November 1953
Document Service Center
Armed Services Tech. Info. Agency
17 Feb 55

DO NOT DESTROY
RETURN TO
TECHNICAL DOCUMENT
CONTROL SECTION
WCOSI-3

FILE COPY

PROPELLER PERFORMANCE AT ZERO FORWARD SPEED

DANA A. WEBB
JACK E. WILLER

PROPELLER LABORATORY

JULY 1952

WRIGHT AIR DEVELOPMENT CENTER

20011016175

RESTRICTED

AF-WP-(B)-O-31 OCT 52 75

UNCLASSIFIED

NOTICES

When Government drawings, specifications, or other data are used for any purpose other than in connection with a definitely related Government procurement operation, the United States Government thereby incurs no responsibility nor any obligation whatsoever; and the fact that the Government may have formulated, furnished, or in any way supplied the said drawings, specifications, or other data, is not to be regarded by implication or otherwise as in any manner licensing the holder or any other person or corporation, or conveying any rights or permission to manufacture, use, or sell any patented invention that may in any way be related thereto.

The information furnished herewith is made available for study upon the understanding that the Government's proprietary interests in and relating thereto shall not be impaired. It is desired that the Judge Advocate (WCJ), Wright Air Development Center, Wright-Patterson Air Force Base, Ohio, be promptly notified of any apparent conflict between the Government's proprietary interests and those of others.

This document contains information affecting the National defense of the United States within the meaning of the Espionage Laws, Title 18, U.S.C., Sections 793 and 794. Its transmission or the revelation of its contents in any manner to an unauthorized person is prohibited by law.

UNCLASSIFIED

[redacted]

WADC TECHNICAL REPORT 52-152 [redacted]

PROPELLER PERFORMANCE AT ZERO FORWARD SPEED

Dana A. Webb
Jack E. Willer

Propeller Laboratory

July 1952

RDO No. 587-141

Wright Air Development Center
Air Research and Development Command
United States Air Force
Wright-Patterson Air Force Base, Ohio

[redacted]

UNCLASSIFIED

FOREWORD

This report was initiated and prepared by the Aerodynamics Branch, Propeller Laboratory, Aeronautics Division, WADC, under R.D.O. No. 587-141, "Propeller Aerodynamic Analysis." Messrs. Dana A. Webb, Jr. and Jack E. Willer acted as project engineers.

ABSTRACT

Static thrust data from propeller whirl tests at Wright-Patterson Air Force Base, and several other sources, on numerous propellers are analyzed and correction factors are derived which correlate these data. Standard curves for static thrust are given for 2, 3, and 4-bladed single rotation propellers, and for 6 and 8-bladed dual-rotation propellers. These standard curves, together with the correction factors, are used to predict the static shaft thrust of any conventional propeller to within about 5%. With the exception of a two-bladed Clark-Y propeller curve, all standard curves are for propellers utilizing NACA 16-series airfoil sections.

The security classification of the title of this report is UNCLASSIFIED.

PUBLICATION REVIEW

Manuscript Copy of this report has been reviewed and found satisfactory for publication.

FOR THE COMMANDING GENERAL:

L. M. TAYLOR
Colonel, USAF
Chief, Propeller Laboratory
Aeronautics Division

CONTENTS

	Page
INTRODUCTION	1
BASIC THEORY	1
DESCRIPTION AND DISCUSSION OF TEST EQUIPMENT	2
PROCEDURE	3
APPLICATION OF METHOD	8
EXAMPLE	8
DISCUSSION OF VARIABLES AFFECTING PROPELLER PERFORMANCE	8
COMPARISONS	12
CONCLUSIONS	12
APPENDIX I - Generalized Data on Blade Angle, Slipstream Velocity and Negative Thrust	13
ILLUSTRATIONS	16
BIBLIOGRAPHY	68
DISTRIBUTION	69

ILLUSTRATIONS

Figure		Page
1	Theoretical Variation of Thrust per Shaft Brake Horsepower Versus Power Coefficient	16
2	Sketch of Whirl Rig 1	17
3	General Arrangement of the Propeller Test Rigs	18
4	Front View of Rig 1	19
5	Quarter View of Rig 1 with Eight Blade Dual	20
6a	Typical Whirl Rig Thrust Curves	21
6b	Typical Whirl Rig Horsepower Curves	22
7	Sketch of NACA Static Test Rig	23
8	Sketch of Engine Test Stand	24
9	Front View of Engine Test Stand	25
10a	Symbols Legend for Figure 10b	26
10b	Thrust per Horsepower Versus Power Coefficient for Seventeen 3-Bladed Propellers	27
11	Power Coefficient Correction for Activity Factor	28
12	Power Coefficient Correction for Integrated Design Lift Coefficient	29
13	Power Coefficient Correction for Thickness Ratio . . .	30
14	Thrust per Horsepower Versus Corrected Power Coefficient for Several Two-Bladed Propellers with Clark-Y Sections	31
15	Thrust per Horsepower Versus Corrected Power Coefficient for Several Two-Bladed Propellers with 16-Series Sections	32
16	Thrust per Horsepower Versus Corrected Power Coefficient for Several Three-Bladed Propellers with 16-Series Sections	33

Figure		Page
17a	Symbols Legend for Figure 17b	34
17b	Thrust per Horsepower Versus Corrected Power Coefficient for Several Four-Bladed Propellers	35
18	Thrust per Horsepower Versus Corrected Power Coefficient for Several Six-Bladed Propellers	36
19	Curves for Static Thrust for Two-Blade Single Rotation Propellers Having Clark-Y Sections	37
20	Static Thrust Curves, Two-Blade, 16-Series Sections . . .	38
21	Static Thrust Curves, Three-Blade, 16-Series Sections . .	39
22	Static Thrust Curves, Four-Blade, 16-Series Sections . .	40
23	Static Thrust Curves, Six-Blade Dual, 16-Series Section	41
24	Static Thrust Curves, Eight-Blade Dual, 16-Series Sections	42
25	View of One-Quarter Scale Model of Rig 3	43
26	Sketch of Configurations for NACA Bluff Body Tests . . .	44
27	Effect of Whirl Rig Shape on Static Performance of a Tractor Propeller	45
28	Effect of Whirl Rig Shape on Static Performance of a Pusher Propeller	46
29	Comparison of Whirl Test Equipment with Engine Thrust and Torquemeters	47
30	Comparison of Whirl [illegible] and F-47 Thrustmeter Values . . .	48
31	Comparison of USAF Whirl Tests and NACA Static Tests . . .	49
32a	Effect of Distance from Plane of Rotation to Rig Face on Shaft Thrust	50
32b	Effect of Distance from Plane of Rotation to Rig Face on Shaft Brake Horsepower	51

Figure		Page
33	Effect of Distance from Plane of Rotation to Rig Face on Thrust per Horsepower	52
34	Comparison of Propulsive Thrust and Shaft Thrust	53
35	Effect of Tip Speed on Thrust per Horsepower	54
36	Comparison of Static Thrust Curves with Momentum Theory	55
37a	Sketch of Three Different Blade Sections.	56
37b	Effect of Trailing Edge Extension on Static Thrust . . .	57
38a	Section Comparison of NACA 16-Series with NACA 65-Series.	58
38b	Static Thrust Comparison of 16-Series with 65-Series Sections	59
39	Effect of Tip Shape on Static Performance	60
40	Comparison of New Static Performance Method with the Previous Method	61
41	Comparison of New Static Performance Method with British Method	62
42	Curve of Blade Angle Versus C_p/TAF Showing Scatter . . .	63
43	Static Blade Angle at 75% Radius	64
44	Average Slipstream Velocity	65
45	Static Thrust, Slipstream Decay	66
46	Ratio of Negative Thrust to Positive Thrust	67

SYMBOLS AND DEFINITIONS

Symbol	Definition	Unit
a	Velocity of Sound	Ft/Sec
AF	Activity Factor $\frac{100,000}{16}\int_{.2}^{1.0}\left(\frac{b}{D}\right)\left(\frac{r}{R}\right)^3 d\left(\frac{r}{R}\right)$	
b	Blade Width	Ft
B	Number of Blades	
C_{l_i}	Section Design Lift Coefficient	
C_{L_i}	Integrated Design Lift Coefficient Sometimes referred to as Camber Factor $4\int_{.2}^{1.0} C_{l_i}\left(\frac{r}{R}\right)^3 d\left(\frac{r}{R}\right)$	
C_p	Power Coefficient $\frac{5x10^{10}SBHP}{\sigma N^3 D^5}$	
$C_{p''}$	Power Coefficient Corrected for Activity Factor and Thickness Ratio	
$C_{p'''}$	Power Coefficient Corrected for Activity Factor, Integrated Design Lift Coefficient and Thickness Ratio	
C_T	Thrust Coefficient $\frac{1.514x10^6 T}{\sigma N^2 D^4}$	

Symbol	Definition	Unit
D	Propeller Diameter	Ft
J	Advance Ratio, $\frac{V}{\pi nD}$, Zero for Static Conditions	
M	Mach Number, $\frac{V}{a}$	
n	Propeller Revolutions per Second	1/Sec
N	Propeller Revolutions per Minute	1/Min
P	Power	Ft-Lb/Sec
P_{AF}	Power Coefficient Correction for Activity Factor	
$P_{C_{L_i}}$	Power Coefficient Correction for Integrated Design Lift Coefficient	
$P_{t/b}$	Power Coefficient Correction for Thickness Ratio	
r	Radius of a Blade Element	Ft
R	Radius to Propeller Tip	Ft
SBHP	Shaft Brake Horsepower, $\frac{P}{550}$	Ft-Lb/Sec
t	Maximum Thickness of Blade Section	Ft
$(t/b)_{.75R}$	Thickness Ratio at 75% of Tip Radius	
T	Propeller Shaft Thrust	Lb
TAF	Total Activity Factor, B x AF/Blade	
V	Velocity	Ft/Sec
V_s	Slipstream Velocity Behind Propeller	Ft/Sec
x	Fraction of Propeller Tip Radius, $\frac{r}{R}$	

Symbol	Definition	Unit
X	Axial Distance	Ft
α	Section Angle of Attack at 75% of Tip Radius	Deg
α_i	Section Induced Angle at 75% of Tip Radius	Deg
β	Propeller Blade Angle at 75% of Tip Radius	Deg
ρ	Density of Air	$Lb\text{-}Sec^2/Ft^4$
ρ_o	Density of Air at Sea Level Standard Conditions	$Lb\text{-}Sec^2/Ft^4$
σ	Density Ratio	
πnD	Propeller Tip Speed	Ft/Sec

PROPELLER PERFORMANCE AT ZERO FORWARD SPEED

INTRODUCTION

For a propeller operating at a given power coefficient, it is known that the shaft thrust per brake horsepower will vary with the number of blades, tip speed, activity factor, integrated design lift coefficient (camber), thickness ratio and distribution, and type of section used (Clark-Y, 16-series, 65-series, etc.). In addition, there are several other factors, such as Mach number, Reynolds number, and amount of blade twist, which influence performance.

A determination of the static thrust and power of a given propeller can be made by use of a strip analysis; however, this would not be expected to be very accurate for the following reasons:

(1) The Goldstein theory, on which the strip analysis is based, was derived on the assumption of a lightly loaded disc. In practice, propellers under static conditions are always heavily loaded. Theodorsen's extension of Goldstein's work appears to fall short of the practical static case also.

(2) The airfoil data used in the strip analysis are not of sufficient range to be accurate over the high angles of attack which are encountered in a static analysis.

Nevertheless, a number of static strip analyses were made for two, three, and four bladed propellers. Although the strip analysis predicted thrust per horsepower at a given power coefficient with acceptable accuracy, it did not satisfactorily predict power coefficient for a given blade angle. In an attempt to remedy this, several modifications to the method and data were tried, but with no success. Therefore, it was concluded that due to one or both of the above reasons, the strip analysis could not be relied upon to present a true picture of static performance.

A more practical approach to the problem appeared to be to correlate the existing test results by suitable correction factors, and then to use these correlated curves and correction factors to determine the static characteristics of any given propeller. This procedure was found to be much more rapid and convenient than a strip analysis approach and was the procedure followed.

BASIC THEORY

The momentum theory may be considered as applying only to a perfect propulsive device acting in a perfect medium. More specifically, it assumes the propeller to be frictionless and to create no rotation of the medium in its wake. Thus, the momentum theory will provide an upper limit to the performance of an actual propeller.

The following form of the momentum theory was taken from an unpublished report by S. D. Black, dated 1944.

$$C_p = 1/2\ C_T\ (J + \sqrt{\frac{8C_T}{\pi} + J^2}\ )$$

Since J = 0 for static conditions, we have

$$C_p = \sqrt{\frac{2}{\pi}} \cdot C_T^{3/2} \qquad \text{or} \qquad C_T^{3/2} = 1.253\ C_p \tag{1}$$

Using this formula, values of C_T/C_P were computed for C_P from .02 to .20. From the definitions for C_T and C_P,

$$T/SBHP = C_T/C_p\ (\frac{33,000}{ND}\ ) \tag{2}$$

For tip speeds (πnD) of 700, 800, 900, and 1000 feet per second, the values of (T/SBHP) were then calculated for the above C_P range. The resulting plot of curves (Figure 1), then, represent the upper limit of any actual test curves, and have some use as a guide in that respect. They also indicate the general shape of the test curves, and may be used to determine an "efficiency factor" for static performance of a given propeller. ("Efficiency" = per cent of ideal thrust per SBHP actually developed.)

DESCRIPTION AND DISCUSSION OF TEST EQUIPMENT

The majority of the data used in this study was obtained from tests on the Electric Whirl Rigs at Propeller Laboratory, Wright-Patterson Air Force Base, Ohio. The general arrangement of Rig 1 is shown in Figures 2, 3, and 4. Rigs 2 and 3 differ from Rig 1 essentially in size only, the general configuration and construction being the same. The power transmitted to the propeller shaft is obtained by measuring the electric power supplied to the driving motor, and subtracting the losses involved; namely, the armature loss, the friction, and windage losses. The propeller shaft thrust is measured by an Emery hydraulic thrust scale, as shown in Figure 3. The "typical dimension" in Figure 2 of 40 in. from the plane of rotation to the rig face changes to about 80 in. to the rear propeller when the special gear box necessary for a dual rotating propeller is used. Figure 5 shows a dual rotating propeller

installed on Rig 1. Speed-increasing gear boxes are available for Rigs 1 and 3. Their appearance is similar to that of the dual rotating gear box. However, no data in this report were taken with speed-increasing gear boxes installed. Typical whirl test curves of thrust and horsepower versus propeller speed are shown in Figures 6a and 6b.

The test equipment used in Reference 1 consists of an electric dynamometer, the same dynamometer as was used in the Langley Eight-Foot High-Speed Tunnel. The shaft thrust and torque were measured by hydraulic capsules. For details, see Reference 1.

A sketch of the test equipment used in References 2 and 3 is shown in Figure 7. It can be seen that the net torque of the driving engine and the net thrust are measured directly by balance scales, and that the thrust measured is propulsive thrust; i.e., the propeller thrust minus the drag of the nacelle and struts due to the propeller slipstream. The setup used in Reference 4 is similar to this except that an electric dynamometer is used for the driving power.

In all the outdoor static tests of References 2, 3, and 4, care was taken not to run the tests in wind velocities greater than five miles per hour. Also, most of the whirl tests at the Propeller Laboratory were run under conditions of low wind velocity, although a few exceptions to this may be encountered.

The engine test stands at Wright-Patterson AF Base were also a source of some of the data used. The general arrangement of the stands is shown in Figure 8, while Figure 9 is a photograph showing more details and the degree of aerodynamic "cleanliness" of a typical installation. The shaft thrust and torque are measured by a thrustmeter and torquemeter installed in the nose of the engine.

The accuracy of all the above torque and thrust measuring devices would be expected to be a nominal one per cent in the range for which the devices were designed.

PROCEDURE

In the past, various methods have been used in an attempt to correct all thrust per horsepower versus power coefficient curves to one standard curve, for any given tip speed and number of blades. Sometimes, this was approached by plotting thrust-coefficient/power-coefficient versus power coefficient, in which case tip speed did not enter directly. The wide variation of the first mentioned curve for seventeen 3-bladed propellers can be [illegible] in Figure 10b.

It will be observed that there were three possible means of correcting these data to bring them into reasonable agreement. These are as follows:

(1) Shift the data horizontally; i.e., apply suitable corrections to power coefficient.

(2) Shift the data vertically; i.e., apply suitable corrections to the thrust per horsepower.

(3) Some combination of the above two.

The usual procedure has been to correct power coefficient for variations in one or more of the following non-dimensional factors: activity factor, integrated design lift coefficient, thickness ratio or thickness ratio factor, and number of blades. The corrections used in the past did not produce good agreement among propellers which varied considerably in the above mentioned characteristics. An attempt was therefore made to develop a more valid method. However, the basic approach of correcting power coefficient (instead of thrust per horsepower, or both) has been retained in this report; this is due partly to the fact that there is little or no experience with "vertical" corrections, and partly to the fact that satisfactory results were obtained with this approach.

In Reference 1, three 2-bladed propellers were tested which differed only in integrated design lift coefficient (hereinafter referred to as camber), and two 2-bladed propellers which differed only in activity factor. The two most important factors were derived principally from these tests.

From the data on propellers differing only in activity factor, a correction factor curve was derived such that when applied to the power coefficient, the thrust per horsepower versus corrected power coefficient curves of the two propellers were coincident for a tip speed of 900 feet per second. This correction factor curve is shown in Figure 11. It will be noted that the factor is in parameters of power-coefficient/total-activity-factor, and that the shifting effect of the factor is largest for large values of this parameter. The reasoning behind this form is that the higher the value of power-coefficient/total-activity-factor, which is a measure of blade loading, the more the static performance will benefit from a higher-than-standard activity factor, and the more it will suffer from a lower-than-standard activity factor.

Similarly, from the data on the propellers differing only in camber, a correction factor curve for camber was derived. This curve, shown in Figure 12, was plotted against power-coefficient/total-activity-factor and is in parameters of integrated design lift coefficient. In the region of very low camber, the curve was determined by whirl tests of blades having lower camber than those of Reference 1. However, since the work on this curve was completed, an NACA Report, Reference 9, was published and the data therein used to check the derivation of the C_p correction for C_{L_i}. Reasonably good correlation was obtained except for values of low camber and low power. The curve was revised slightly in this region, and when used for correcting test data, good correlation was obtained. The reasoning behind the shape of this correction curve is that higher-than-standard camber will enable higher maximum lift coefficients, and hence improve static performance; conversely, lower-than-standard camber will harm static performance. Section drag at high lift coefficients is also helped by camber. It will be noted that the curves all converge to unity at very high blade loadings, the reason being that the blade is stalled along a substantial portion and is therefore not sensitive to changes in camber.

The thickness ratio correction, shown in Figure 13, is the same as that used in a previous report written by Propeller Laboratory (Reference 10, now obsolete) except that the standard or reference thickness ratio was changed to .065.

Examination of the figure shows that the effect of this correction factor is usually considerably smaller than the effect of either of the two previous factors. The reason that increased thickness affects static performance is that it increases the lift-curve slope and maximum lift coefficient slightly.

Having derived these correction factors, all the data were then gathered for each number of blades and plotted as thrust per horsepower versus corrected power coefficient (corrected for activity factor, camber and thickness ratio) for a tip speed of 900 feet per second. (The exceptions to this were the dual-rotation propellers, where a tip speed of 700 feet per second was used, and the two-bladed Clark-Y propeller, where there was no correction for camber.) These plots can be seen in Figures 14 through 18. It can be seen that, although the corrections were derived from two-bladed propeller tests, the degree of correlation obtained, applying these factors to the other number of blades, appears satisfactory. This is believed to be due largely to the fact that the two major correction factors were dependent upon power-coefficient/total-activity-factor, or blade loadings.

Since the data for 900 feet per second tip speed were in good agreement, curves were then plotted for tip speeds of 700, 800, and 1000 feet per second (except the duals, where 600 was used instead of 1000 feet per second). These curves were usually plotted for two or three of the propellers which had been near the center of the scatter of the 900 feet per second plot. The correction factors appeared valid at these other tip speeds; therefore, the curves for the four tip speeds of each number of blades were cross-plotted, faired, and extrapolated to higher powers using the method of Reference 10 as a guide. The resulting curves of thrust per horsepower versus corrected power coefficient, are shown in Figures 19 through 24.

The above six "Curves for Static Thrust," plus the three correction curves, constitute the principal result of this investigation.

One of the first questions which arose in the use of data from several different test setups was that of how closely two different test setups would agree on the thrust-power characteristics of the same propeller. As has been mentioned, sometimes the equipment measured shaft thrust, and sometimes propulsive thrust. Also, some setups were "clean" (such as a thrustmeter-torquemeter installation on an F-47 airplane), and some were definitely of a type which would be suspected of affecting the propeller's characteristics (such as the electric whirl rigs, with their flat forward face, Figures 2, 3, and 4).

In 1937, according to unpublished information, an attempt was made to determine the effect of whirl rig No. 3 at Wright-Patterson AF Base on the static thrust and power characteristics of a propeller. A one-fourth scale model of the whirl rig was constructed and placed 4.5 inches from the plane of rotation of a one-fourth scale model of a ten-foot, three-bladed propeller which was electrically driven through a long extension shaft. A picture of the test setup, which was in the Five-Foot Wind Tunnel at Wright-Patterson AF Base, is shown in Figure 25. The whirl rig model was then in the same position relative to the model propeller as the full-scale whirl rig would be to a ten-foot propeller. The propeller was run with the whirl rig model 4.5 inches (15% of propeller diameter) from the disc, and then with the whirl

rig model removed. According to the investigator, the effects of the presence of the whirl rig on the propeller characteristics were "so small that they lie within the accuracy of the thrust and torque measuring instruments." It should be noted that this investigation was most probably done at low power coefficients, and the thrust and torque measuring instruments were probably not as accurate as those of the full-scale whirl rigs.

Very recently, similar tests have been run by the NACA to determine the effect of a bluff body such as the whirl rigs on the static performance of a propeller (Reference 9). Specifically, the bluff body was a half-scale model of a 30,000 hp electric whirl rig soon to be constructed at the Propeller Laboratory, Wright-Patterson AFB. This whirl rig will be quite similar to that shown in Figures 2 and 4.

A ten-foot propeller was run on one unit of the NACA 6000 hp propeller dynamometer as both a pusher and a tractor. Then, the propeller was similarly run in the presence of the model of the whirl rig, and a model of the whirl rig with speed increaser installed. These six model configurations are illustrated in Figure 26. In configurations III and IV, the propeller plane of rotation was 15 inches from the speed increaser face, and in configurations V and VI, it was 15 inches from the rig face.

The results of these tests for tractor configurations are shown in Figure 27. Although the test points for the three different configurations (II, IV, and VI) lie on essentially the same thrust per horsepower versus power coefficient curve (for a given tip speed), the propeller absorbs more power at a given blade angle when the "blocking" area behind it is increased. This effect will be noted and discussed in some of the following correlations.

The results for pusher configurations, at one tip speed, are shown in Figure 28. Unlike the tractor case, the three configurations do not result in the same thrust per horsepower versus power coefficient curve. The exact cause of the improvement in performance due to the presence of a bluff body is not understood; however, it is believed due to a significant change in the magnitude and/or direction of the inflow. There are actually three variables to be considered: the blocking effect of dynamometer and bluff bodies, the flow-straightening effect of the dynamometer pylon and the bluff bodies, and the power or disc loading of the propeller. Unfortunately, these variables could not be separated in the subject tests. It can therefore only be concluded from these tests that the prediction of the static performance of pusher propellers from whirl rig tests will be more difficult than for tractor propellers, and should be further investigated.

It should be noted that this ten-foot propeller on a half-scale model represents a twenty-foot propeller on the full scale rig. Since most propellers to be tested will be smaller than this, the effect of the rig presence will be even greater than that shown by these tests.

A comparison of static characteristics of the same four-bladed propeller obtained from an electric whirl rig and from thrustmeter and torquemeter measurements on the engine test stands at Wright-Patterson AFB is shown in Figure 29. Although the test points from the two different sources lie on the same curve for a given blade angle, the propeller on the whirl rig absorbs more power. Thus, this comparison indicates that the presence of the whirl rig increases the effective blade angle, in that the propeller absorbs more power and produces more thrust than if it were at the same angle on the engine test stand. However, the thrust per horsepower versus power coefficient curves are coincident for the two test setups. This is in agreement with the previously discussed NACA tests.

Figure 30 shows a comparison for thrust-coefficient/power-coefficient versus power coefficient from an electric whirl rig test and from an F-47 thrustmeter-torquemeter static calibration, for the same propeller. This comparison indicates that there is no large, consistent difference between the two test methods.

Although no direct comparison is available between the electric whirl rig tests and the NACA tests using the Eight-Foot High-Speed Tunnel dynamometer, Figure 31 shows a comparison of the corrected results for several two-bladed propellers from each source. The whirl rig test points represent four different propellers, and the NACA tests, four propellers. It will be observed that the scatter between the corrected whirl rig test results and the corrected NACA results is less than the scatter among the four corrected NACA results.

To investigate the effect of distance from plane of rotation to the whirl rig face on static performance, and also to determine the agreement among the three whirl rigs at Wright-Patterson AFB, a four-bladed 13-foot propeller was tested on each whirl rig, and at two different distances from the rig on one of the rigs. The results of these four different tests, all made at the same blade angles, are shown in Figures 32a and 32b. It will be observed that almost without exception, the closer the propeller to the rig face, the higher the thrust produced and the power absorbed; however, the difference between the 45 inch distance and the 36 inch distance is less than the experimental scatter. Altogether, Figures 32a and 32b show definitely that the whirl tests on the different rigs can be quite accurate and are consistent with one another.

The results of these seven separate tests, plotted as thrust per horsepower versus power coefficient, are shown in Figure 33. This supports the earlier conclusion that although the [illegible]st and power at a given blade angle may vary slightly with different test setups, the final result of thrust per horsepower versus power coefficient will be essentially the same for tractor propellers.

As mentioned previously, some of the reference data were in terms of propulsive thrust, not propeller shaft thrust (References 2, 3, and 4). The relation of propeller shaft thrust to propulsive thrust is a study within itself, and will not be discussed in detail here. Figure 34 has been prepared to give an indication of the magnitude of the difference. It can be seen that propulsive thrust for the particular setup involved (Figure 7) appears to be between .90 and .95 of the shaft thrust.

The particular value depends, of course, on the installation, and in general will be between .85 and 1.00; see Reference 6. The value to be used for a given airplane must be determined by the airplane designer.

APPLICATION OF METHOD

The procedure in determining the static shaft thrust of a given propeller at a given power and rotational speed can now be stated as follows:

(1) Calculate C_p and πnD of the propeller.

(2) Calculate C_p/TAF, and knowing C_{L_i}, AF, and $(t/b)_{.75R}$ read P_{AF}, P_{CL}, and $P_{t/b}$ from Figures 11, 12, and 13 respectively.

(3) Calculate $C_{p'''} = C_p \times P_{AF} \times P_{C_{L_i}} \times P_{t/b}$.

(4) From the appropriate "Curves for Static Thrust" read (T/SBHP) at the calculated $C_{p'''}$ and πnD, interpolating as necessary.

(5) Multiply (T/SBHP) by SBHP delivered to the propeller to obtain propeller shaft thrust under static conditions.

EXAMPLE

Four-bladed propeller; D = 16 Ft. 6 In.; AF = 113; C_{L_i} = .379; $(t/b)_{.75R}$ = .073; SBHP = 3500 at 2700 engine rpm; Gear Ratio = .375.

$$C_p = \frac{5.10^{10} SBHP}{\sigma N^3 D^5} = .1376; \quad \pi nD = 875; \quad C_p/TAF = \frac{.1376}{4 \times 113} = .000305; \quad P_{AF} = 1.045$$

$$P_{C_{L_i}} = 1.010; \quad P_{t/b} = .977; \quad C_{p'''} = .1376 \times 1.045 \times 1.010 \times .977 = .1418;$$

T/SBHP = 3.21, from Figure 22;

Static shaft thrust = 3.21 x 3500 = 11,230 pounds.

DISCUSSION OF VARIABLES AFFECTING PROPELLER PERFORMANCE

TIP SPEED

The effect of tip speed on the static performance of a two-bladed propeller can be seen in Figure 35, together with the effect as given by the simple momentum theory. This theory (Equations 1 and 2, Page 2) states that for a fixed power coefficient, thrust per horsepower varies inversely as the tip speed. The figure shows this to be generally true for the test data in the higher tip speed range, but the curves are not of hyperbolic shape in the 900-1100 feet per second range. This indicates favorable Reynolds and Mach number effects up to the section critical speed. Above approximately 1100 fps, the effect of section Mach number reduces the thrust per brake horsepower. The effect is not as drastic as might be expected, however, and the $C_p = .04$ curve follows the theoretical shape quite closely, indicating small compressibility effects. Because of the relatively minor effect of Mach number, no attempt was made to correct for this effect other than the tip speed correction itself, and the data used were assumed to fall within the temperature range of 15-100 F.

NUMBER OF BLADES

Figure 36 shows the effect of number of blades on static performance of propellers for a tip speed of 800 feet per second. It is clear that, with the exception of the eight-bladed dual, the static performance improves as the number of blades is increased. For power coefficient above approximately .22, the eight-bladed dual is consistent with this trend. Cross-overs of other numbers of blades occur in the low power coefficient range. The figure conclusively shows that when operating in moderate and high power loadings, it is advantageous to static performance to use a large number of blades. It will be observed that the six-bladed dual curve approaches rather close to the momentum theory curve at one point. Upon checking this, some of the actual experimental points were found to be even closer to the momentum curve. However, no source of error could be found, and it was concluded that the curve was correct as it stands.

POWER COEFFICIENT

The effect of this variable can also be seen from Figure 36. It shows that for a given propeller and tip speed, this thrust per horsepower decreases with increasing power coefficient, and that the values are always below those given by the momentum theory. Further examination of the curves will show that, in the ranges considered, an increase in power coefficient (at constant tip speed) will always result in an increase in thrust, even though the thrust per horsepower decreases.

ACTIVITY FACTOR

The effect of activity factor on static performance can be shown using Figure 11. It can be seen that the lower the activity factor, the larger the correction factor. In other words, a propeller with a low activity factor has its thrust per horsepower

values shifted to the right in order to coincide with those of standard activity factor. Thus, increasing activity factor increases the thrust per horsepower of a propeller under normal operating conditions. Furthermore, as discussed under "Procedure," the correction factor for high loadings is larger (farther from unity) than for light loadings. Changing the activity factor of a heavily loaded propeller, then, will cause a larger change in static performance than changing that of a lightly loaded propeller.

INTEGRATED DESIGN LIFT COEFFICIENT

From Figure 12, the effect of blade camber can be seen. Increasing the camber means shifting the thrust per horsepower curve to the left; thus, increasing camber increases the thrust per horsepower. The correction factor is only slightly dependent upon power-coefficient/total-activity-factor, except at the very high values where the factor becomes unity. As mentioned under "Procedure," this represents the stall condition over most of the blade, and so the blade is insensitive to changes in camber.

THICKNESS RATIO

Figure 13 shows the variation of thickness ratio correction with thickness ratio. From this it can be seen that increasing the thickness ratio will increase the thrust per horsepower. It should be noted that this correction is smaller than either of the preceding ones; hence, the effect of increasing thickness ratio will, in general, be less than that of increasing activity factor or camber (see discussion of Figure 13 under Procedure).

TRAILING EDGE EXTENSION

During the preceding study, the inclusion of blades not having 16-series sections with those having 16-series sections was avoided in establishing the standardized curves. The following discussion will indicate the reason for this.

A comparison of typical sections of three different related blades is shown in Figure 37a. These three blades are closely related in that No. 2 was obtained from No. 1 by adding to it a trailing edge extension which increased the chord 20%. The No. 3 blade is similar to the No. 2 except that the thickness along the chord has been redistributed to make a more normal looking section. The No. 1 section was 16-series, having a design lift coefficient of .50; however, it is obvious that a design lift coefficient, in the same sense, cannot be assigned to the two sections resulting from the modifications described.

These three blades were tested as two-bladed propellers of the same diameter; the results, corrected only for activity factor, are shown in Figure 37b. It is clear from this figure that the correlation is of no value compared to the previous correlations for 16-series blades. Also, it is to be noted that if the thickness ratio correction were applied, the curves would be shifted further apart.

Thus, it was decided that if blades having sections as closely related as the preceding would not correlate well, it would be even more difficult to correlate 16-series blades with non-16-series blades of different diameters, thicknesses, planforms, etc. While these non-standard, extended trailing edge sections offer greater static performance than the basic 16-series, little data are available as to their performance at forward flight conditions and these data indicate some performance loss for the same planform.

NACA 65-SERIES SECTIONS

A further, and possibly more important aspect of non-16-series sections can be seen in Figures 38a and 38b. Two propellers, identical in all respects except type of blade section, were tested for static performance. One of the propellers embodied 16-series sections, and the other, 65-series sections of the same thickness and camber. A visual comparison of two types of sections can be seen in Figure 38a. The static test results, shown in Figure 38b, indicate that the 65-series sections definitely have better static performance. To support this result, there are some wind tunnel tests at moderately high forward speeds which indicate that the 65-series sections are superior to the 16-series section in L/D ratio.

Although the 65-series section may be aerodynamically superior to the 16-series, it can be seen from Figure 38a that it is structurally inferior. Its area is approximately 87% of that of a 16-series section of the same chord and thickness, and the minor moment of inertia is approximately 82% of the corresponding 16-series section. Thus, structural considerations may limit its use on thin blades.

It should be noted that some of the potential of the 65-series section may be lost due to the fact that the cusp near the trailing edge would probably have to be faired out to permit practical fabrication. (Conversely, some methods of fabrication introduce this cusp to 16-series sections.)

TIP SHAPE

This study has not considered blade planform geometry as a variable, although activity factor does, to some extent, describe the planform. In the past, there has been some discussion as to the relative merits of square-tipped and round-tipped blades, thus inferring that the tip shape is one of the major variables when comparing different planforms. Figure 39 shows thrust per horsepower versus power coefficient of two propellers which are identical except that one has square tips and the other round tips. The comparison shows that any effect of tip shape on static thrust performance is negligible, and lies well within the experimental error. This indicates that, at least for activity factors up to 110 (AF of test blades = 110), planform geometry in itself is not a major variable in static thrust considerations.

COMPARISONS

A comparison of the static thrust curves developed herein, and those of the method previously used at the Propeller Laboratory, Reference 5, is shown in Figure 40. For the propeller chosen for comparison, the curves are in close agreement for the working ranges of the 3, 4, and 6-bladed propellers, but are substantially different in the case for the 2-bladed propeller. This previous method was derived largely from tests of blades having Clark-Y sections, and thus had no correction for camber. The data were presented as curves of thrust-coefficient/power-coefficient versus total activity factor, and used the same thickness ratio correction as used in this development. Hence, the comparisons shown in Figure 40 would not necessarily hold for propellers differing widely from that chosen.

One of the chief advantages of the method developed herein over the former is the inclusion of a correction factor for camber.

A spot comparison of the method developed herein with a British method as given in Reference 7 is shown in Figure 41. For the blade chosen, the two methods agree within 4% over the range considered; however, as pointed out above, this agreement could not necessarily be expected for blades or conditions differing widely from those chosen. It is interesting to note that the British method gives propulsive thrust, with the note to increase it 2.8% to obtain shaft thrust. Further, the British correction factor for thickness ratio is more than twice the factor used in this report.

CONCLUSIONS

The method developed for predicting the static performance of a propeller is satisfactory over the ranges considered. The values of thrust per horsepower from the included curves should be correct to within 5% for the working ranges of all except the two-bladed propellers, for which the error may be somewhat greater.

The method predicts propeller shaft thrust only; any allowances to convert this to propulsive thrust must be made in accordance with the particular configuration involved. Also, with the exception of the two-bladed Clark-Y static thrust curve, all curves apply only to propellers incorporating 16-series sections.

The effect of bluff bodies on the static tests of tractor propellers can be eliminated by the proper presentation of the data; however, the effect of a bluff body on the pusher propeller needs further investigation. In either case, the blade angle for a given power indicated by the whirl tests will be less than that required when the propeller is installed in an airplane.

APPENDIX I

GENERALIZED DATA ON BLADE ANGLE, SLIPSTREAM VELOCITY AND NEGATIVE THRUST

BLADE ANGLE

The blade angle at which a given propeller will operate, under given conditions of power and rpm, at zero forward velocity, is desired to enable determination of low angle stop settings, angle for minimum starting torque, and propeller relationship to a given flutter boundary.

Blade angle increases with power; but at a given power, a wider blade, a larger camber, or a higher rpm should tend to decrease the blade angle. Ignoring Reynolds and Mach number effects, a given blade angle will represent one value of power absorbed for a given propeller at a certain rpm. By converting power to the non-dimensional quantity, C_p, and plotting a curve of β versus C_p for a constant tip speed (πnD), the power, rpm, Mach number, and density relationships, are described at a particular blade angle. Plotting β versus C_p/TAF is the first step in arriving at a generalized blade angle curve. A given value of C_p/TAF may be obtained from either a wide blade at a high C_p, or a narrow blade at a low C_p. As a general rule, the greater the C_p, the greater the thrust produced and the greater the thrust, the larger the induced flow. Hence, while C_p/TAF is a good index of section angle of attack α, it may not be a valid index of section induced angle of attack α_i; therefore, β versus C_p/TAF curves could be subject to some error because they do not represent unique values of α_i (in addition to errors introduced by ignoring shape variables other than AF).

The data for the β versus C_p/TAF study were taken from seven whirl tests, chosen indiscriminately from Propeller Laboratory files. These tests included three 4-blade, two 3 blade, and two 2-blade propellers, all single rotation. For these propellers the ranges of blade characteristics were as follows: Thickness ratio at 75% radius $(t/b)_{.75R}$ = .050 to .084, inclusive; activity factor (AF) = 86 to 137, inclusive; and integrated lift coefficient (C_{L_i}) = .155 to .50, inclusive. The whirl test data were reduced to read blade angle (β) at the same representative blade section, which was chosen to be the 75% radius. The data were then plotted in the form of $\beta_{.75R}$ versus C_p/TAF at πnD = 700 ft/sec (see Figure 42). Because

of the small amount of scatter, this curve suggested that, for the range of the blade characteristics studied, the quantity TAF was a sufficient correction of C_p to obtain good correlation of the test data, and that further blade characteristic corrections were not needed. To check this, the data were plotted in the same form for πnD's of 800, 900, and 1000 ft/sec and the same correlation was obtained. Thus, on the basis of these data, for the range of $(t/b)_{.75R}$ and C_{L_i} and power studied, it can be safely assumed that thickness ratio, camber, and pitch distribution have little or no effect on the blade angle at a constant power and rotational speed. The expected error due to differences in number of blades and induced flow was not in evidence. This is a very interesting result which deserves additional attention. To obtain the final curves of $\beta_{.75R}$ versus C_p/TAF (Figure 43), a curve was faired through the scatter for each πnD; cross-plotted against πnD at a constant C_p/TAF; then replotted in final form for πnD's = 700, 800, 900, and 1000 ft/sec.

It is concluded that these curves are a good index of blade angle at constant power and tip speed, provided the blade characteristics are within the range of those used in determination of the standard curves; namely,

$$(t/b)_{.75R} \geq .05 \leq .085$$

$$(C_{L_i}) \geq .155 \leq .50$$

$$(AF) \leq 150$$

Blades are relatively stiff in torsion. Blade angle at which minimum torque occurs is -1° for all πnD's (700-1000). The blade angle at a given power from the β versus C_p/TAF curves is falsely high due to the effect of whirl rig blocking area, when compared to an actual airplane installation. This was pointed out in NACA study of bluff bodies in September 1951.

SLIPSTREAM VELOCITY

For various reasons, it is sometimes necessary to know the slipstream velocity behind a propeller, and the simple momentum theory gives the following relationship between slipstream velocity, thrust, and propeller diameter for the static case:

$$V_s = \frac{32.7}{D} \sqrt{\frac{T}{\sigma}}$$

In the actual case, however, the slipstream velocity will be somewhat less than the ideal, primarily because the slipstream cross sectional area is greater than the theory indicates. Reference 11 gives results of some slipstream measurements made behind a pusher propeller mounted on the WADC whirl rigs. Figure 44 shows the

velocity distribution in the wake. Figure 45 gives the relationship between the actual and theoretical velocity as derived from these tests. To determine slipstream velocity, first determine shaft thrust for the particular propeller and condition; second, determine theoretical slipstream velocity from the above formula; and third, multiply the theoretical velocity by the appropriate percentage given on Figure 45. The velocity so calculated will be further reduced by any body in the slipstream.

REVERSE THRUST

A propeller operating in "reverse pitch" will produce negative thrust which is useful for braking or maneuvering an airplane. The values of negative T/BHP for a given condition would not be expected to be as great as the positive case, however, since the inboard blade sections are at low or positive angles of attack and cambered sections are operating in the negative lift coefficient regime. Figure 46 is a plot of the ratio of +T/BHP to -T/BHP versus C_p/TAF for several propellers and serves to establish a correction factor to be applied to the T/BHP curves of this report when negative thrust values are desired. Knowing the negative thrust, the slipstream velocity may be determined in the same manner as the positive thrust case.

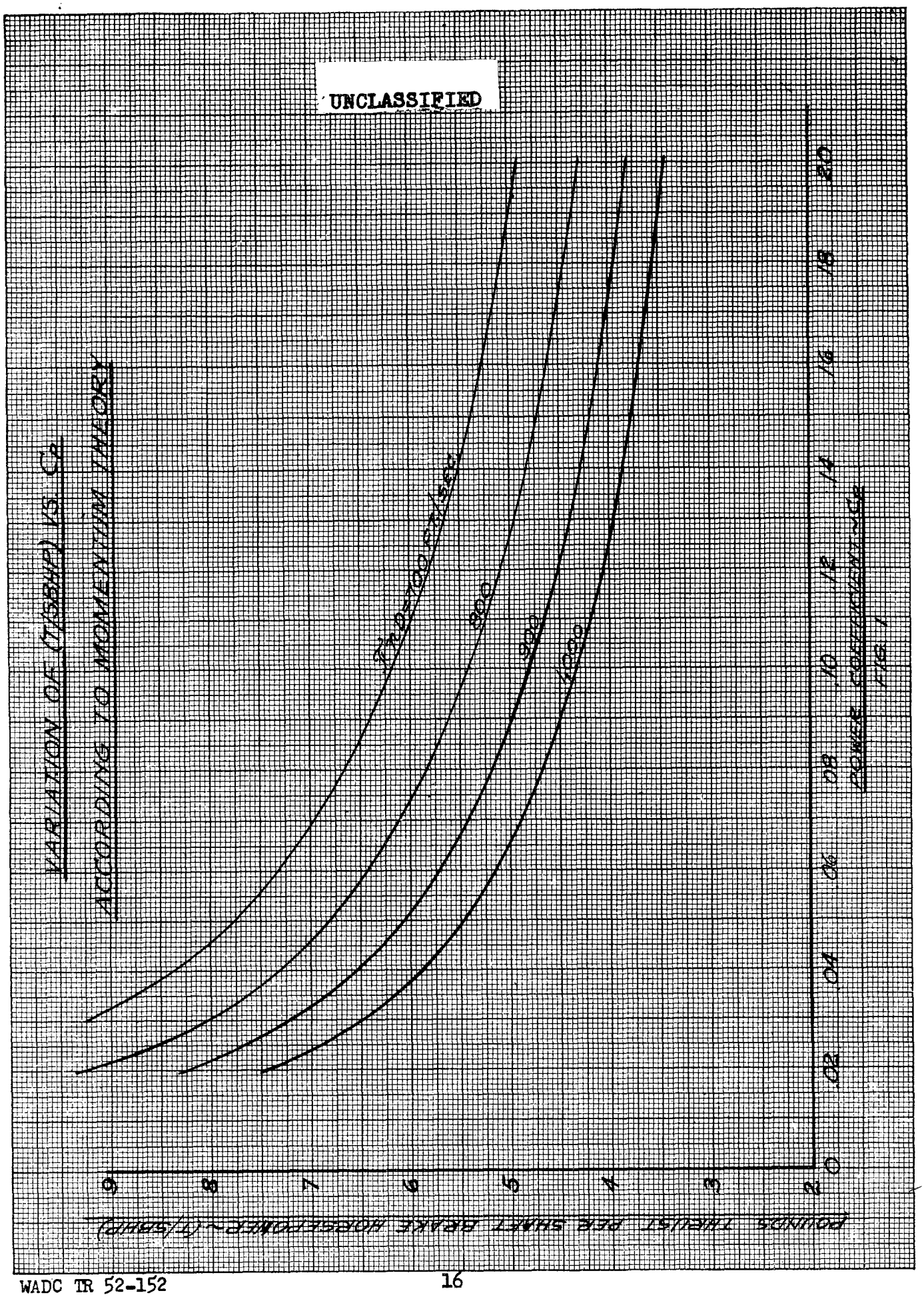
VARIATION OF (T/SHP) VS. CP
ACCORDING TO MOMENTUM THEORY
POWER COEFFICIENT ~ CP
POUNDS THRUST PER SHAFT BRAKE HORSEPOWER ~ (T/SHP)
0
.02
.04
.06
.08
.10
.12
.14
.16
.18
.20
2
3
4
5
6
7
8
9
2700 FT/SEC
800
900
1000

FIG. 1

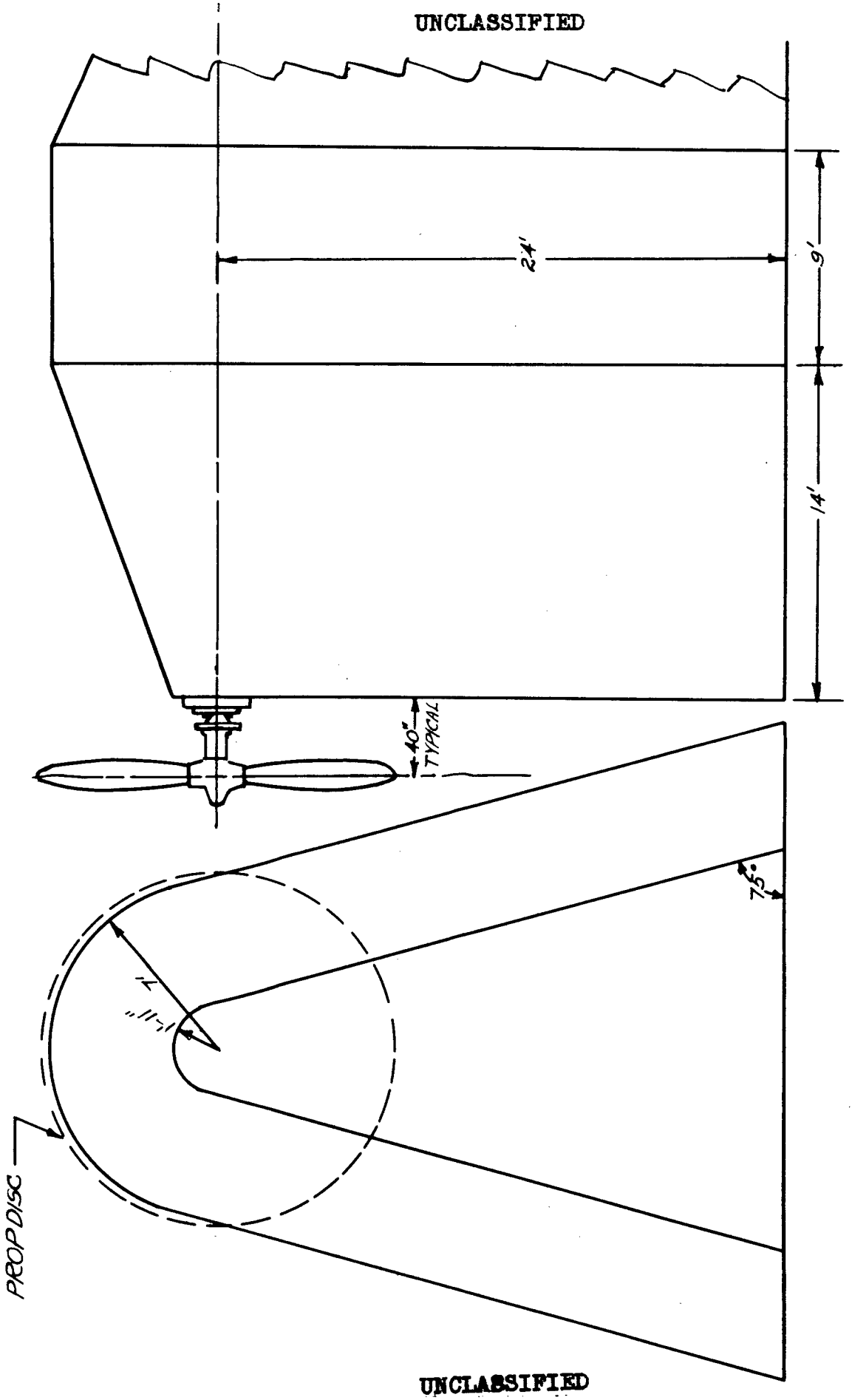

SKETCH OF WHIRL RIG 1

FIG. 2

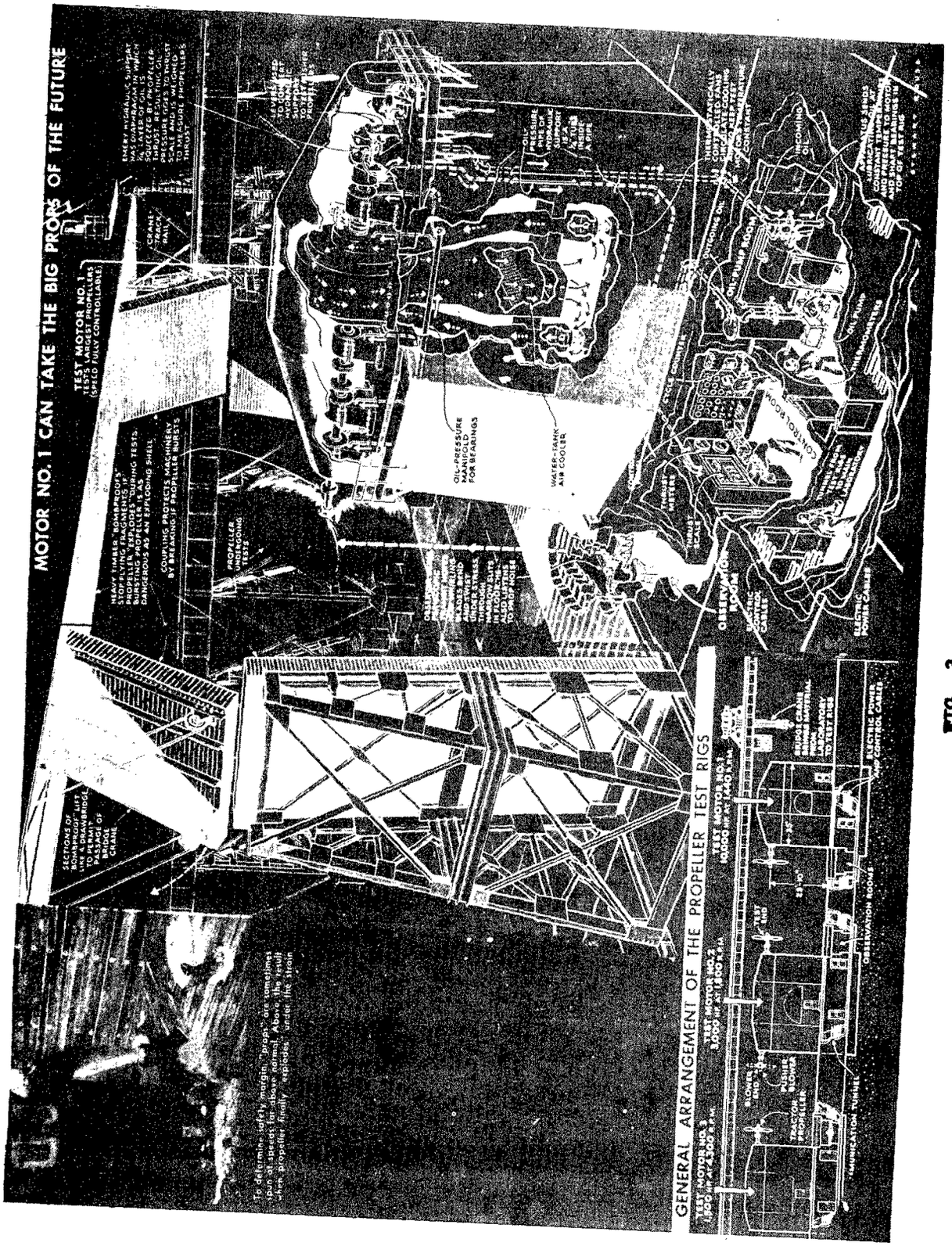

FIG. 3
General Arrangement of the Propeller Test Rigs

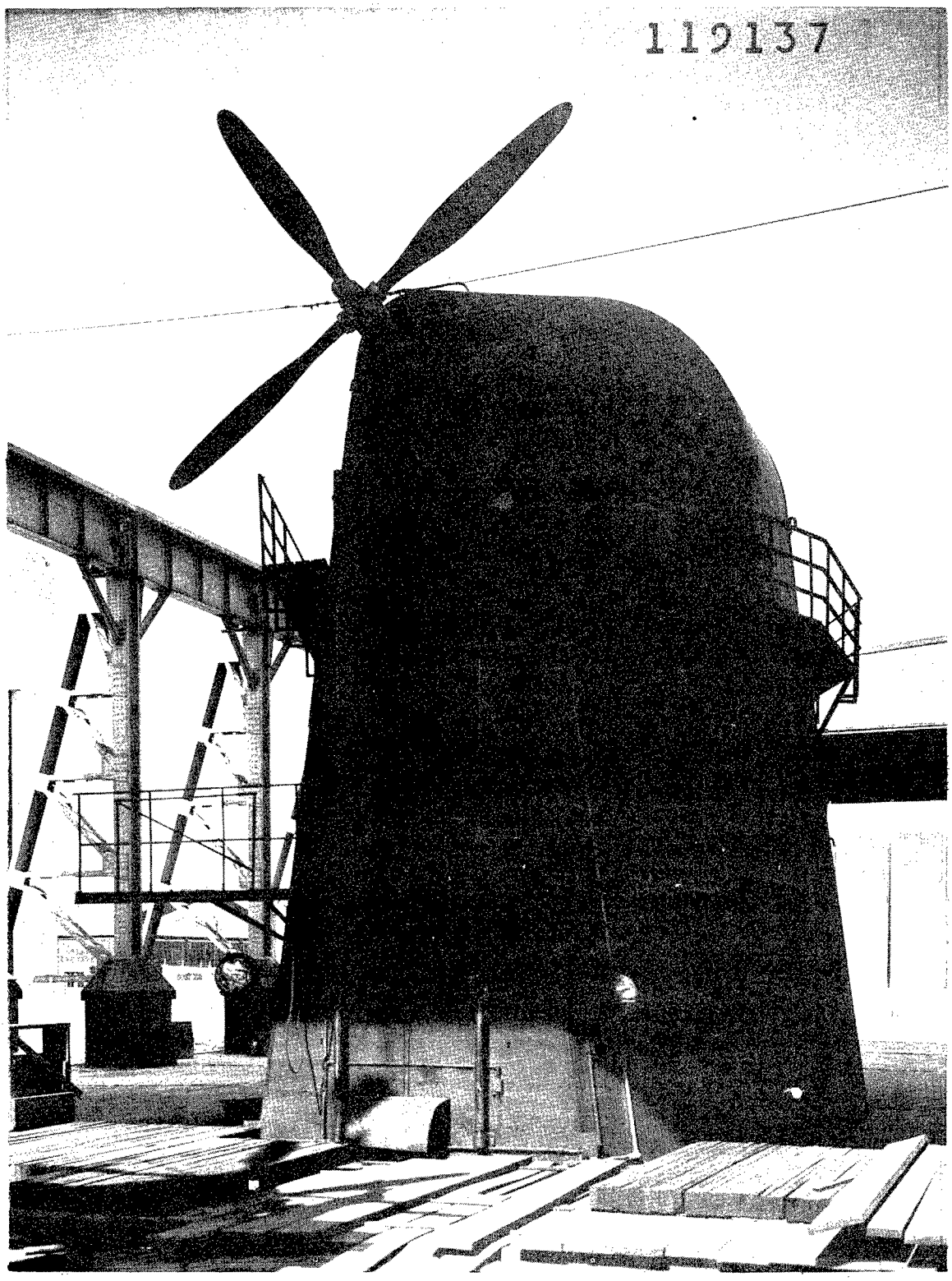

FIG. 4

Front View of Rig 1

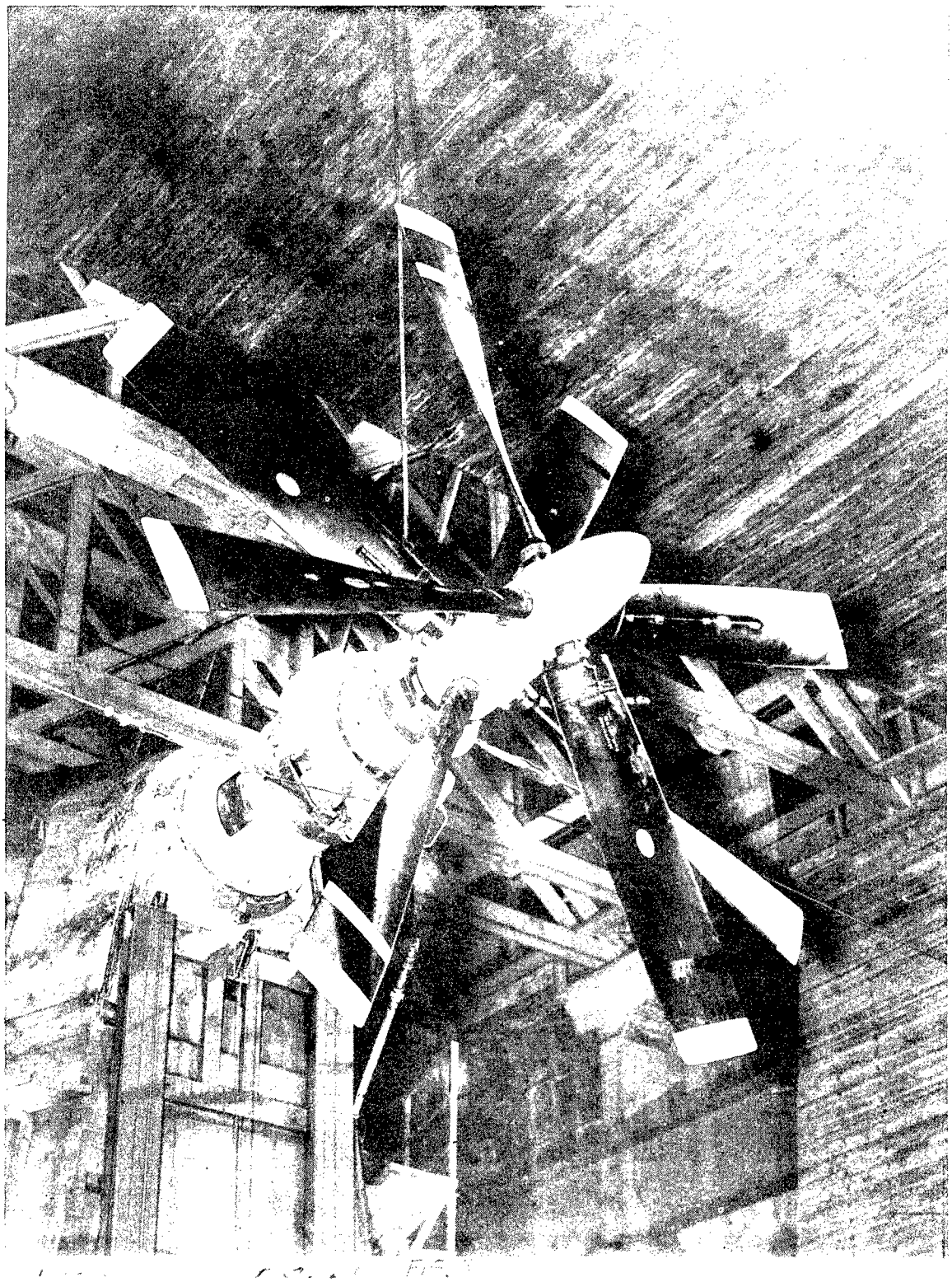

FIG. 5

Quarter View of Rig 1 with Eight Blade Dual

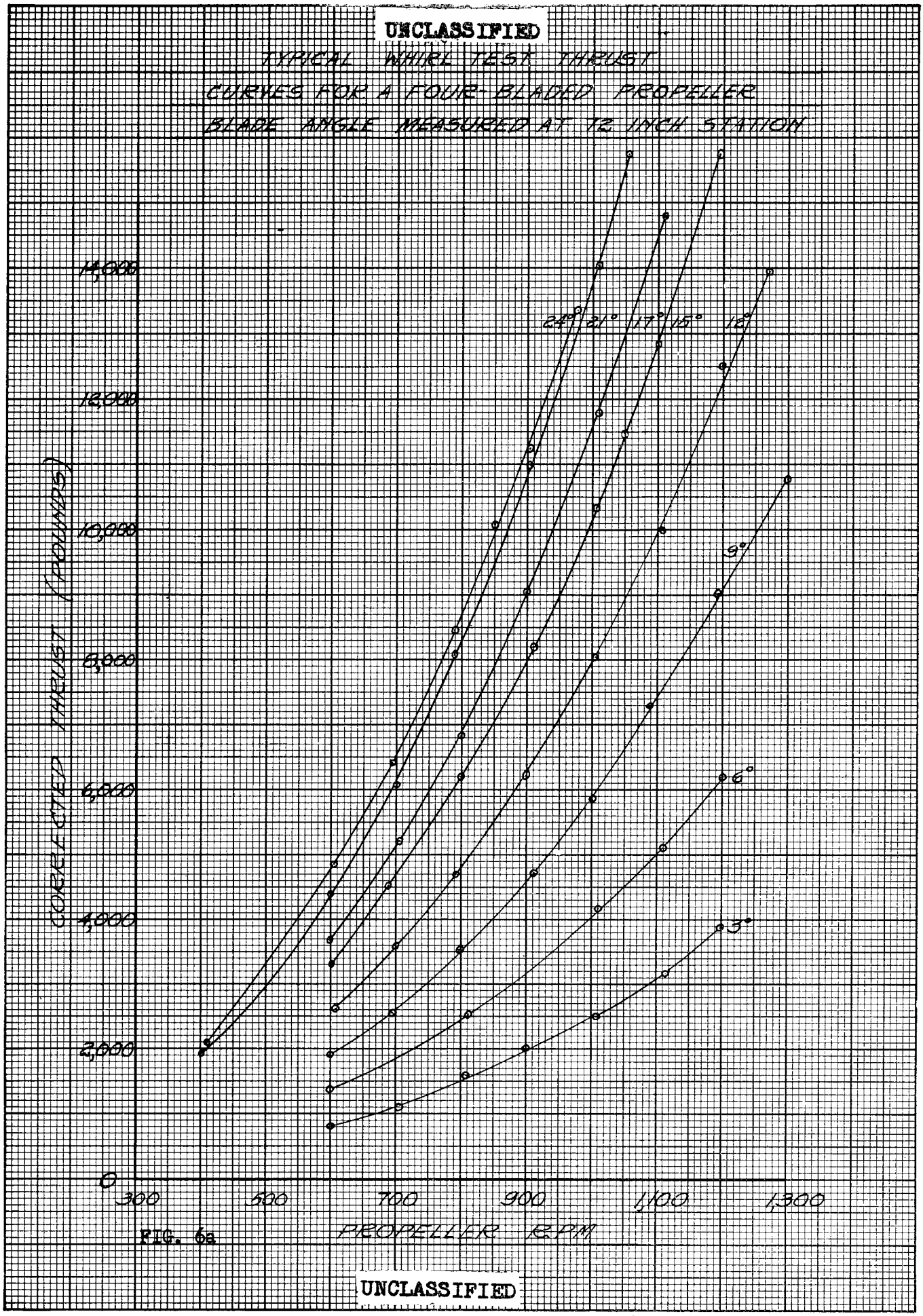
TYPICAL WHIRL TEST THRUST
CURVES FOR A FOUR-BLADED PROPELLER
BLADE ANGLE MEASURED AT 12 INCH STATION
CORRECTED THRUST (POUNDS)
14,000
12,000
10,000
8,000
6,000
4,000
2,000
0
300
500
700
900
1,100
1,300
PROPELLER RPM
24°
21°
17°
15°
12°
9°
6°
3°

FIG. 6a

TYPICAL WHEEL TEST HORSEPOWER CURVES FOR A FOUR-BLADED PROPELLER BLADE ANGLES MEASURED AT 72 INCH STATION

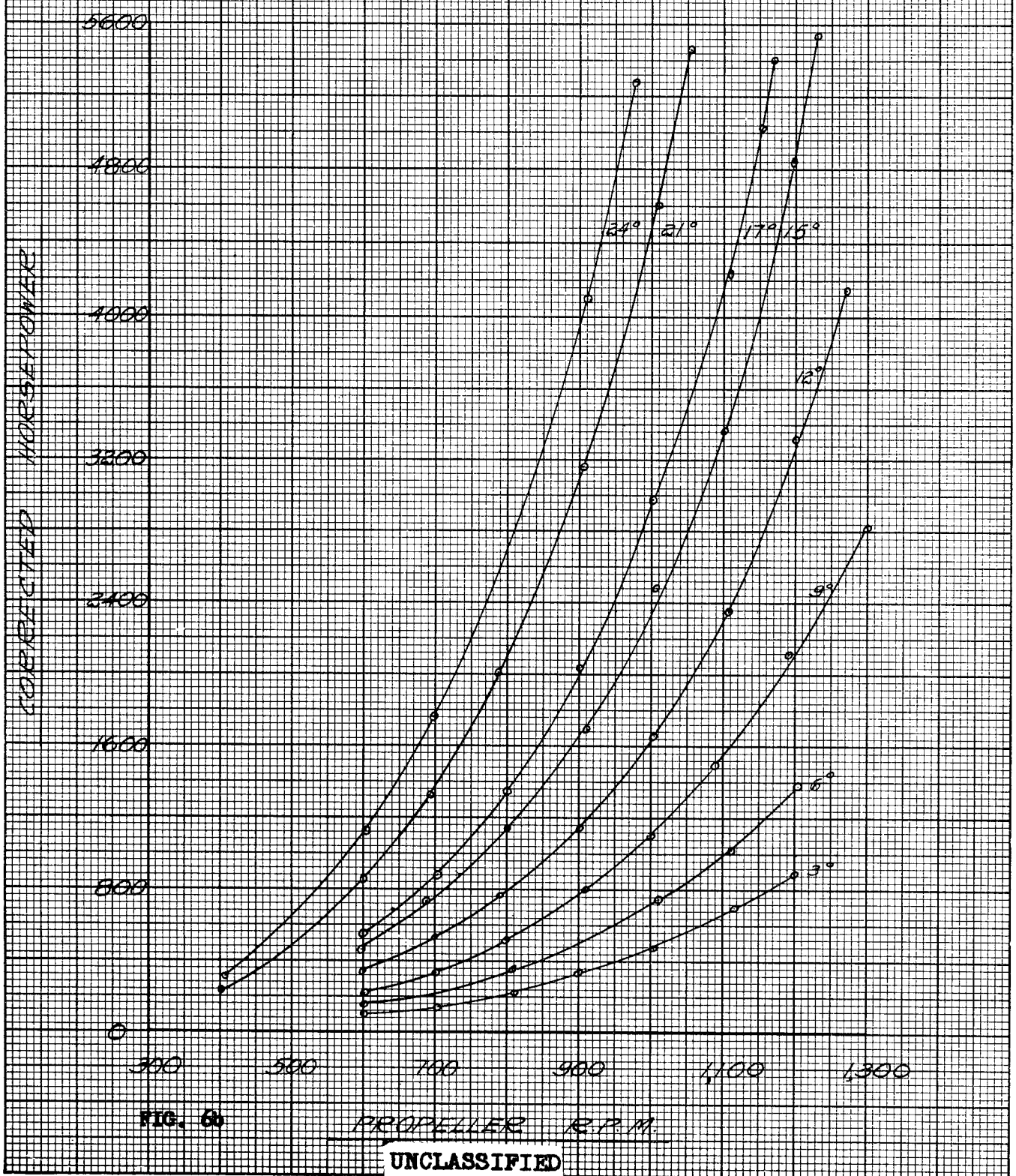

FIG. 6b

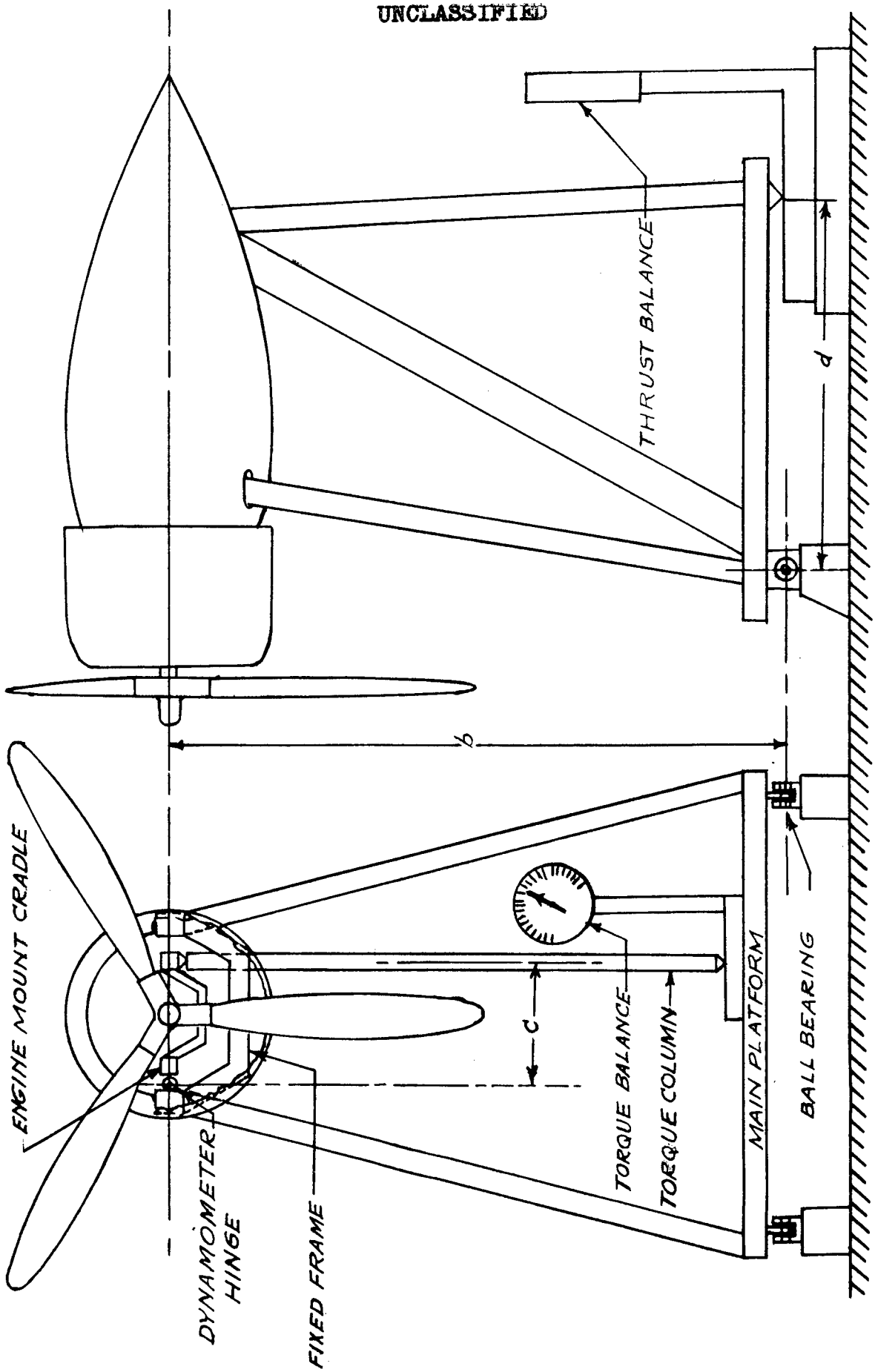

FIG. 7
SKETCH OF NACA STATIC TEST RIG

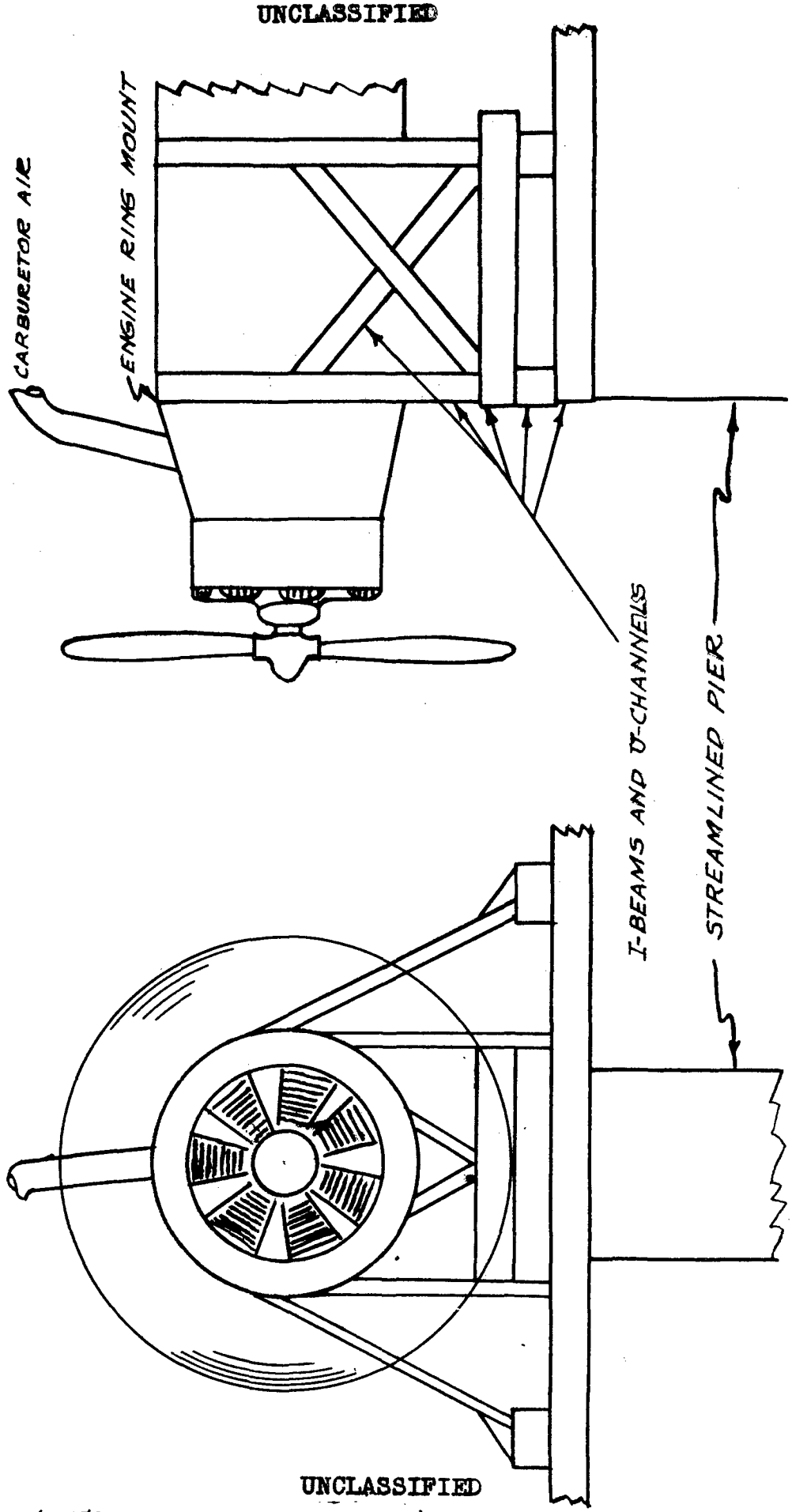

FIG. 8

SKETCH OF ENGINE TEST STAND

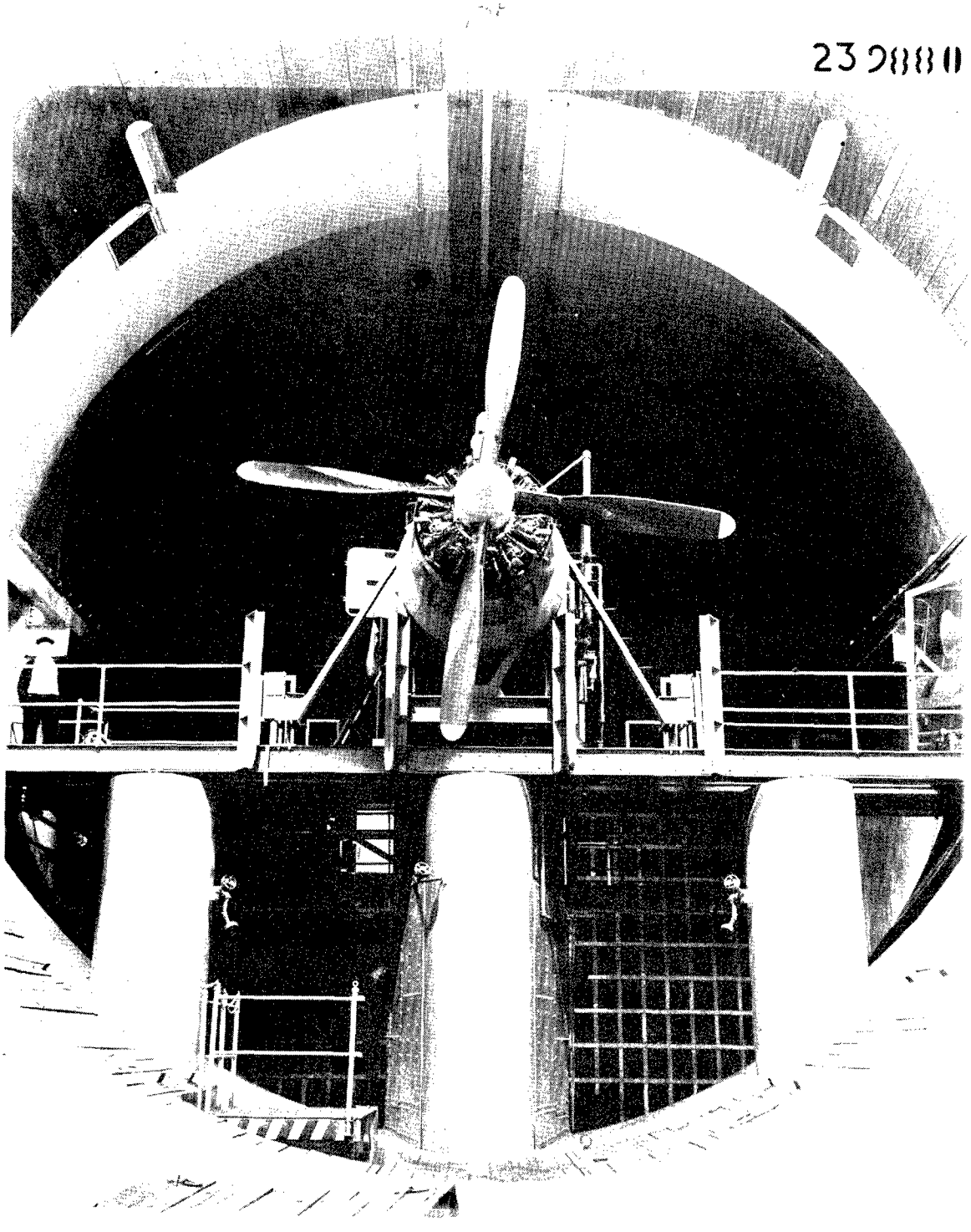

FIG. 9

Front View of Engine Test Stand

FIG. 10a

LEGEND OF SYMBOLS FOR FIG. 10b

BLD NO.	SYMBOL	DIAMETER	A.F.	$(t/b)_{.75R}$	C_{L_i}	SOURCE
1	⊙	19'-0"	121	.073	.604	USAF
2	△	12'-10"	112	.060	.432	
3	⊡	12'-10"	112	.049	.379	
4	◇	15'-8"	121	.067	.500	
5	◺	14'-4"	81	.070	.571	
6	◐	19'-0"	121	.073	.604	
7	▷	10'-1"	84	.075	.324*	
8	◨	19'-0"	118	.063	.361	
9	◆	19'-0"	134	.050	.370	
10	◭	15'-0"	84	.070	.437	
11	✦	17'-0"	74	.068	.438	
12	◹	12'-0"	95	.045	.258	
13	▽	12'-0"	100	.045	0 †	
14	⊙	10'-2"	103	.050	.547	
15	⊙	13'-2"	125	.057	.639	
16	◁ ‡	10'-1"	79	.088	.380	NACA
17	✕ ‡	10'-4"	82	.079	.320	NACA

* FOR CLARK-Y SECTION; NOT COMPARABLE TO OTHER C_{L_i}'S.

† SYMMETRICAL DOUBLE WEDGE SECTIONS

‡ PROPULSIVE THRUST AS COMPARED TO SHAFT THRUST MEASURED IN USAF TESTS.

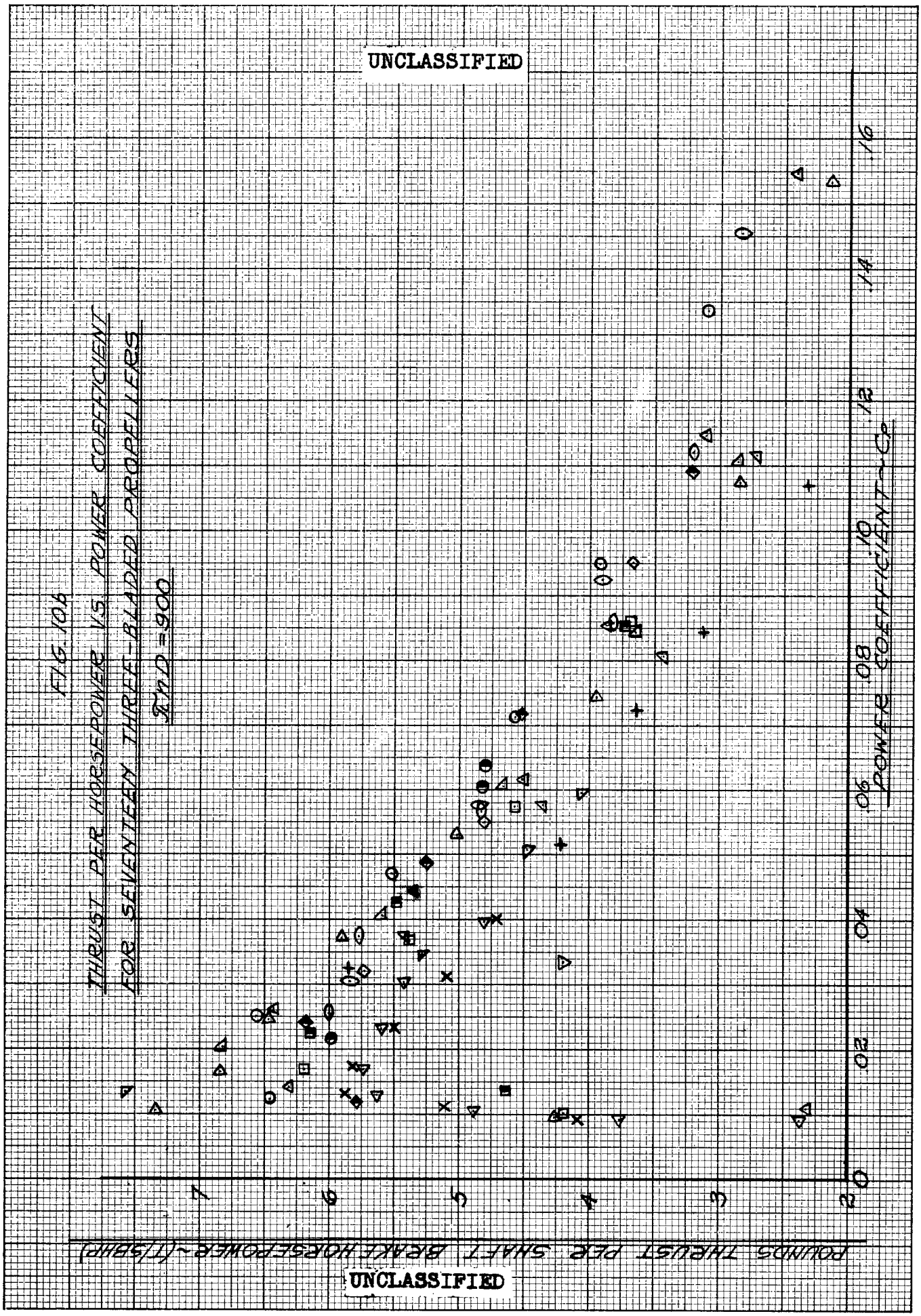

FIG. 106
THRUST PER HORSEPOWER VS. POWER COEFFICIENT
FOR SEVENTEEN THREE-BLADED PROPELLERS
$\pi n D = 900$

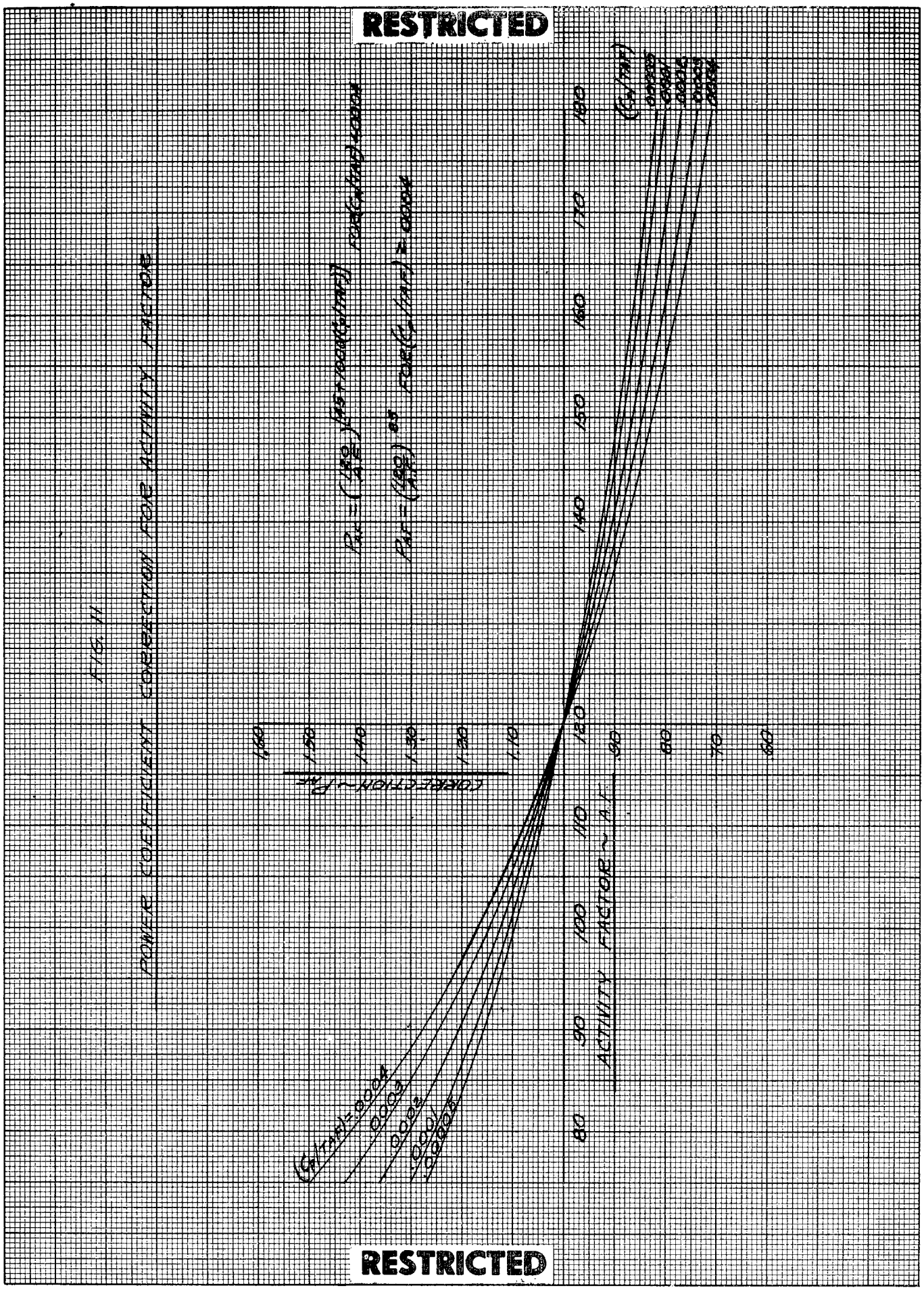
POWER COEFFICIENT CORRECTION FOR ACTIVITY FACTOR
FIG. 11
CORRECTION - %
ACTIVITY FACTOR ~ A.F.
(Cp/Pa)
(Cp/Pa) = 0.004
0.003
0.002
0.001
0.0005
0.0001
100
90
80
70
60
110
120
130
140
150
160
170
180

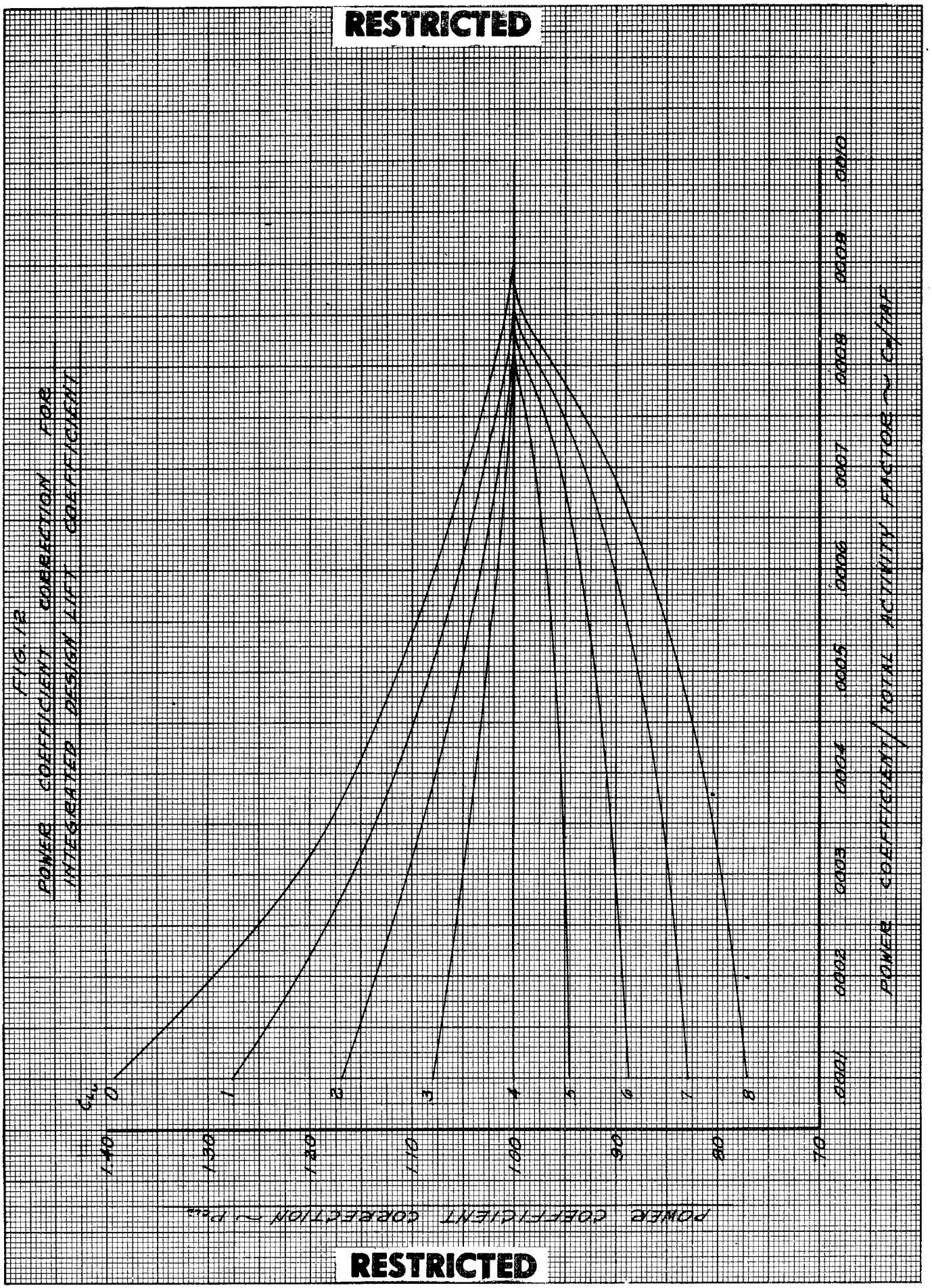
POWER COEFFICIENT CORRECTION FOR
INTEGRATED DESIGN LIFT COEFFICIENT
C_{L_D}
0
1
2
3
4
5
6
7
8
1.40
1.30
1.20
1.10
1.00
.90
.80
.70
.0001
.0002
.0003
.0004
.0005
.0006
.0007
.0008
.0009
.0010
POWER COEFFICIENT / TOTAL ACTIVITY FACTOR ~ C_P/σ
POWER COEFFICIENT CORRECTION ~ P_{CC}

FIG. 12

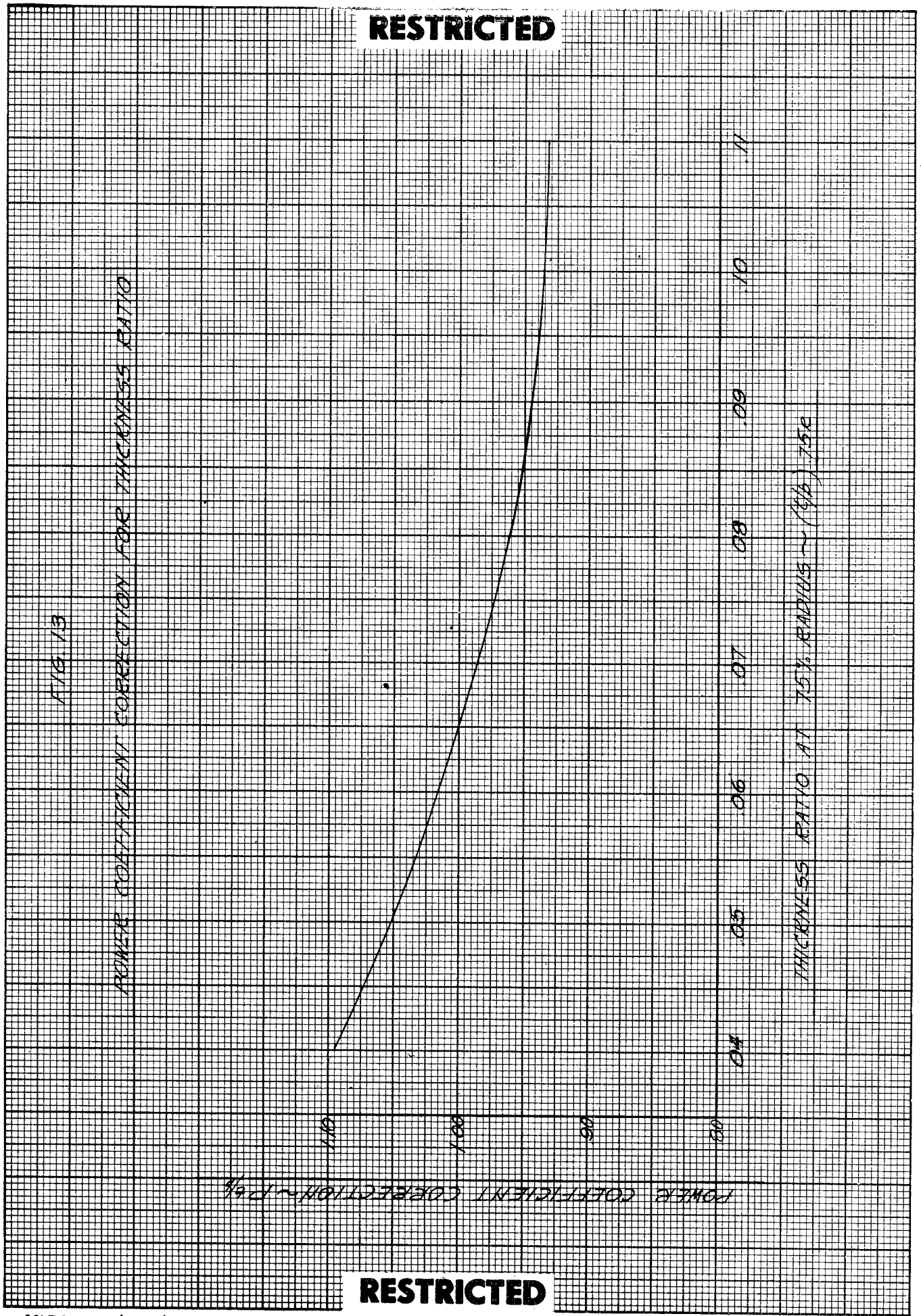

FIG. 13
POWER COEFFICIENT CORRECTION FOR THICKNESS RATIO

UNCLASSIFIED

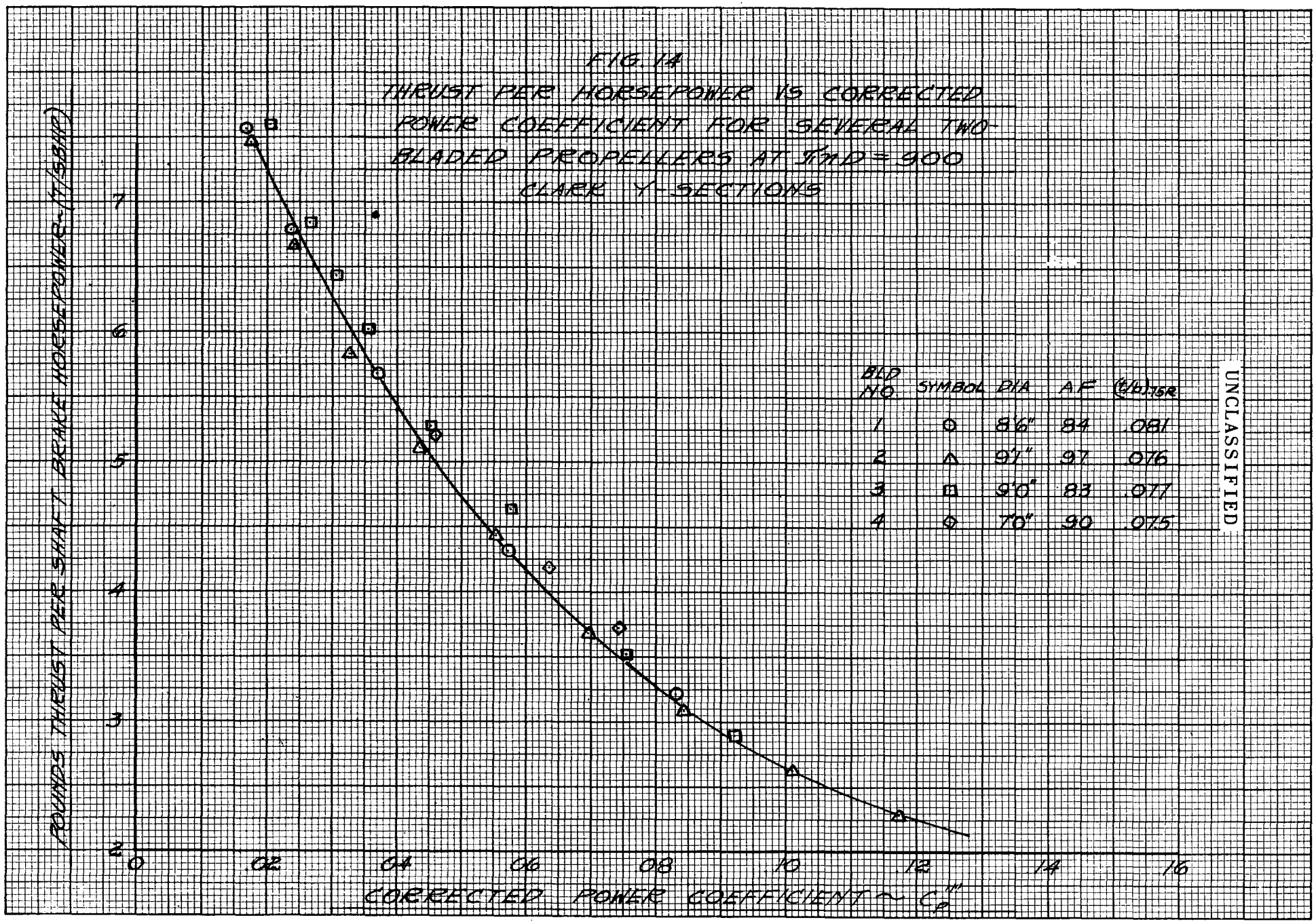

FIG. 14
THRUST PER HORSEPOWER VS CORRECTED POWER COEFFICIENT FOR SEVERAL TWO-BLADED PROPELLERS AT $\pi nD = 900$
CLARK Y-SECTIONS

UNCLASSIFIED

UNCLASSIFIED

FIG. 15

THRUST PER HORSEPOWER VS CORRECTED POWER COEFFICIENT FOR SEVERAL TWO-BLADED PROPELLERS AT $\pi nD = 900$

16-SERIES SECTIONS

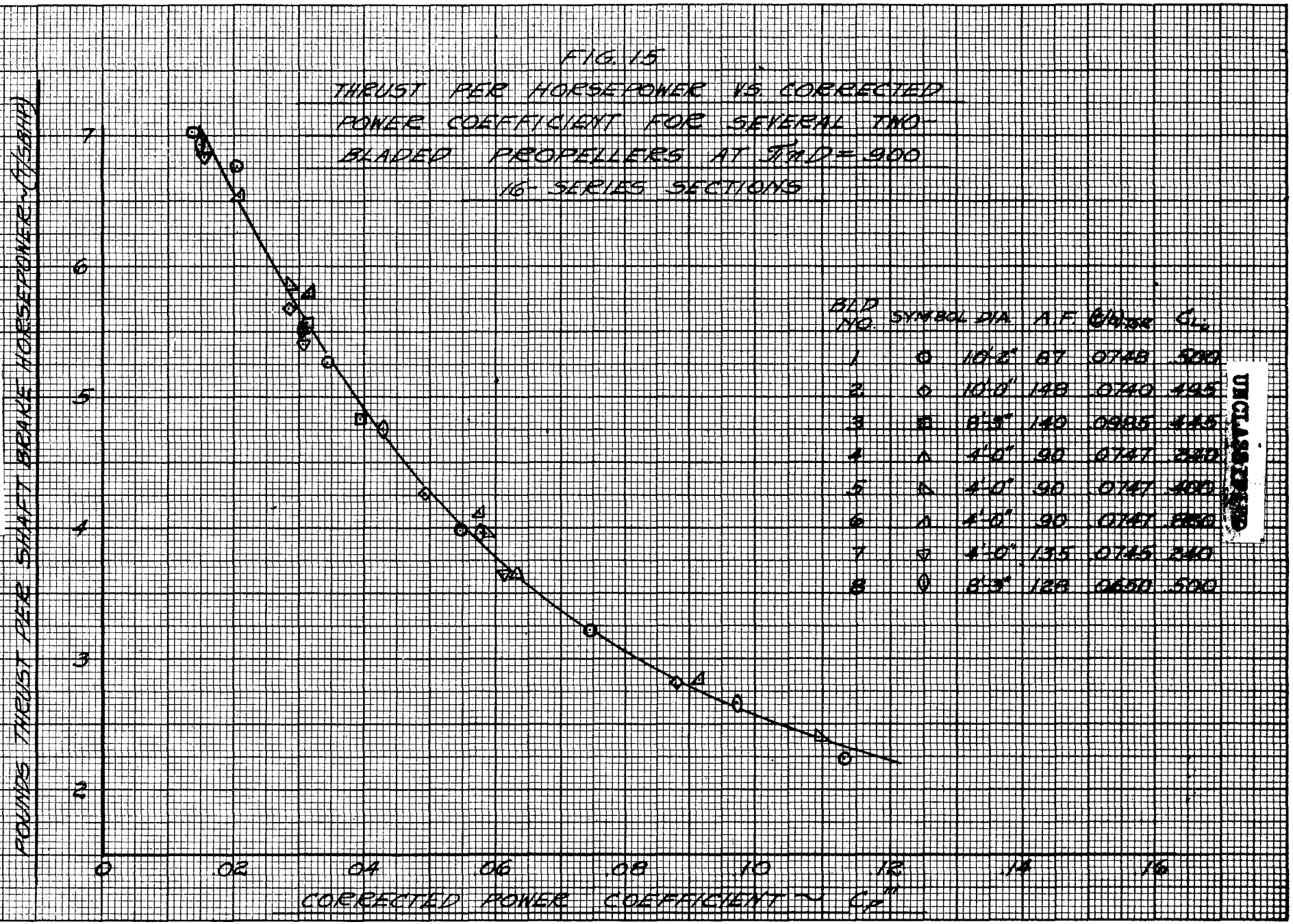

UNCLASSIFIED

UNCLASSIFIED

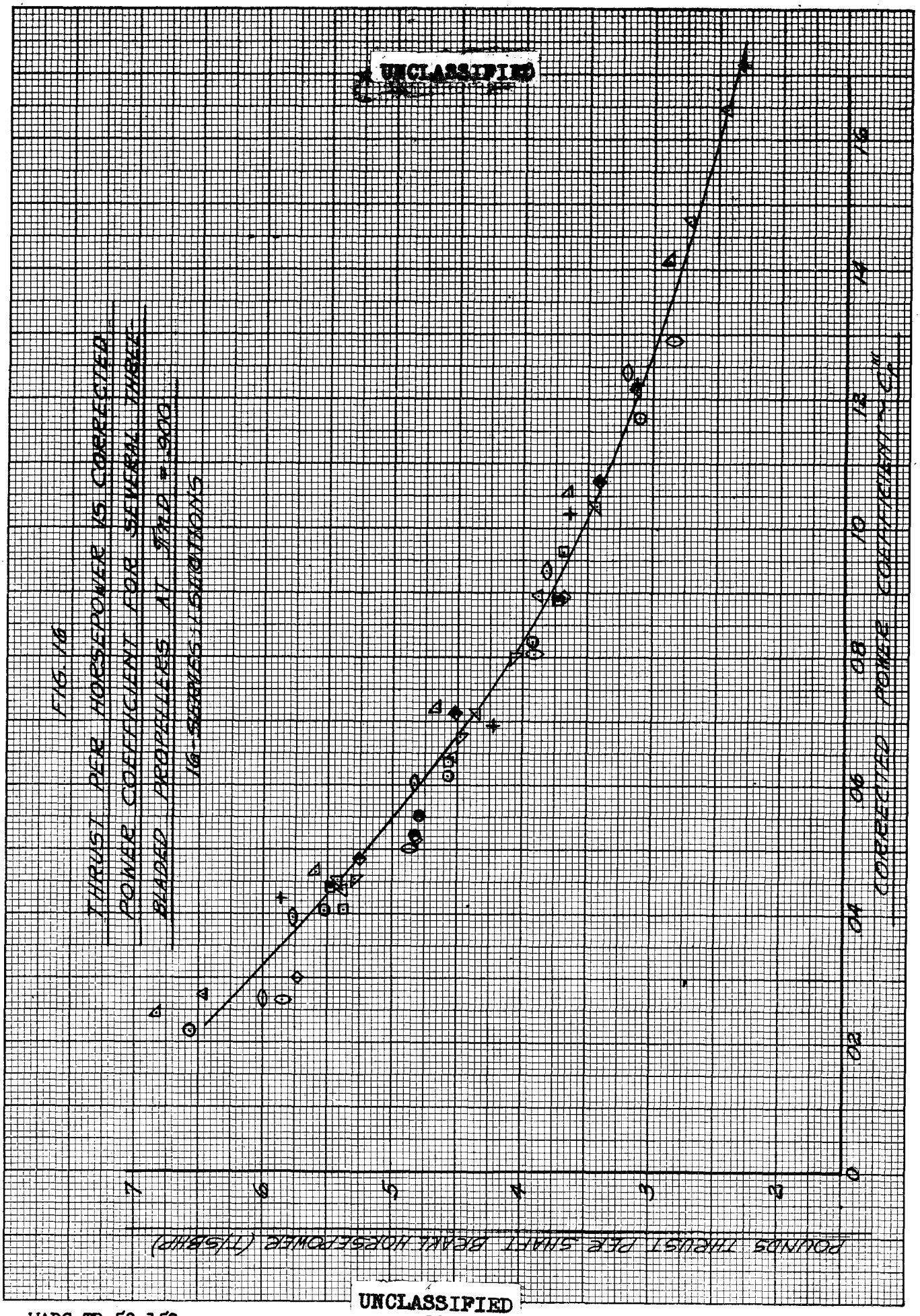

UNCLASSIFIED

FIG. 17a

LEGEND OF SYMBOLS FOR FIG. 17b

BLD NO.	SYMBOL	DIAMETER	AF	$(t/b)_{.75R}$	C_{L_i}	SOURCE
1	⊙ *	16'-6"	113.0	.0724	.501	USAF
2	⊡	19'-0"	80.0	.0675	.489	
3	△	14'-8"	80.8	.070	.571	
4	◇	14'-8"	128.0	.069	.491	
5	⬭	15'-2"	103.0	.050	.547	
6	◺	16'-7"	135.0	.0527	.375	
7	⊗	16'-6"	112.5	.0575	.400	
8	⊠	13'-0"	177	.0523	.284	
9	◆	13'-1"	103	.053	.500	
10	◊	13'-2"	125	.0571	.639	
11	◘	13'-0"	111	.078	.485	
12	✦	13'-0"	111	.078	.485	
13	◐	13'-0"	164	.063	.415	
14	▽	11'-2"	125.5	.0746	.355	

* EXTENDED TRAILING EDGE

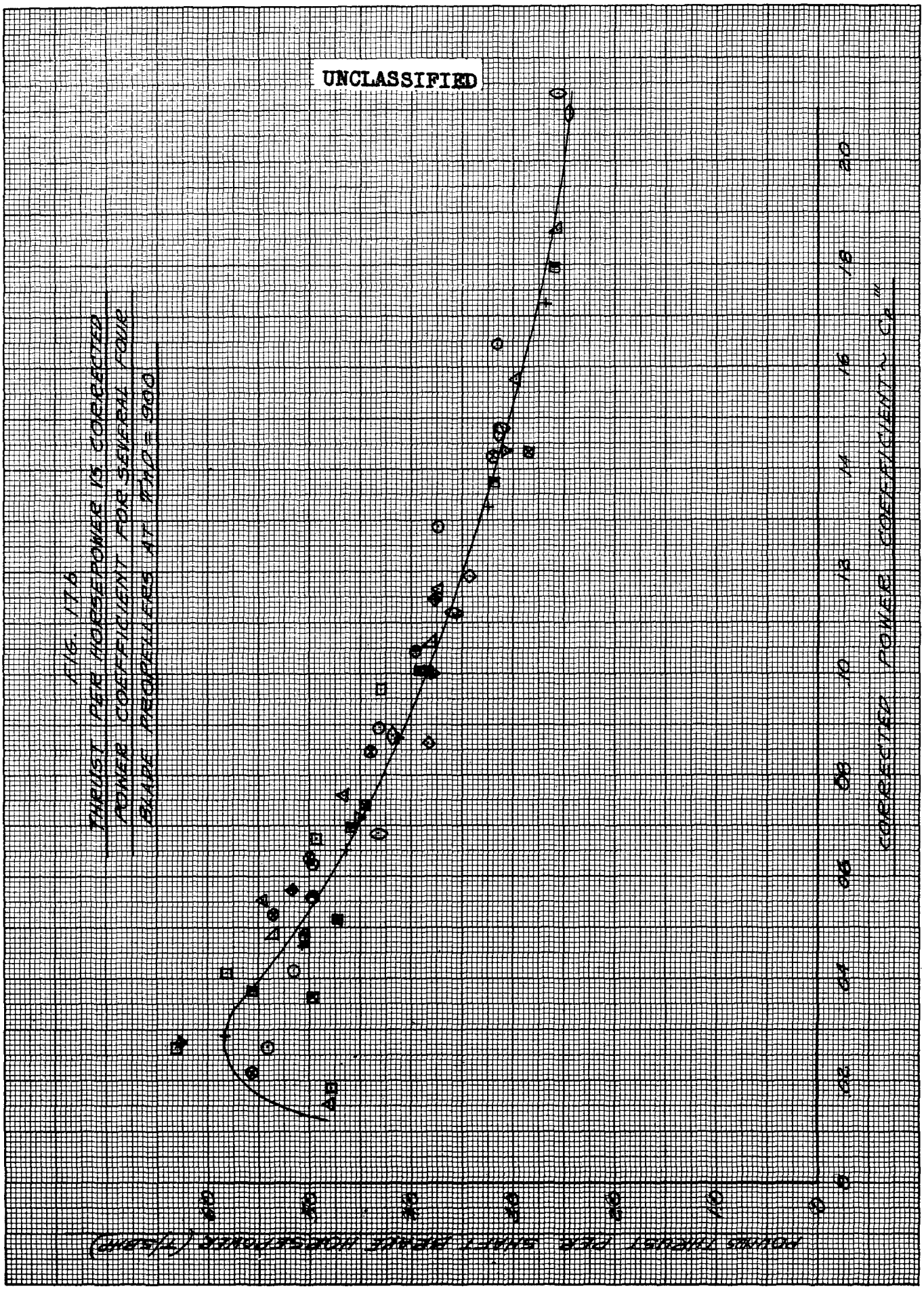
THRUST PER HORSEPOWER IS CORRECTED
POWER COEFFICIENT FOR SEVERAL FOUR
BLADE PROPELLERS AT M_TIP = 900
CORRECTED POWER COEFFICIENT ~ C_{P_m}
0
.02
.04
.06
.08
.10
.12
.14
.16
.18
.20
.90
.92
.94
.96
.98
1.00

FIG. 17a

UNCLASSIFIED

FIG. 18

THRUST PER HORSEPOWER VS. CORRECTED POWER COEFFICIENT FOR SEVERAL SIX-BLADED DUAL ROTATION PROPELLERS

$\pi n D = 700$

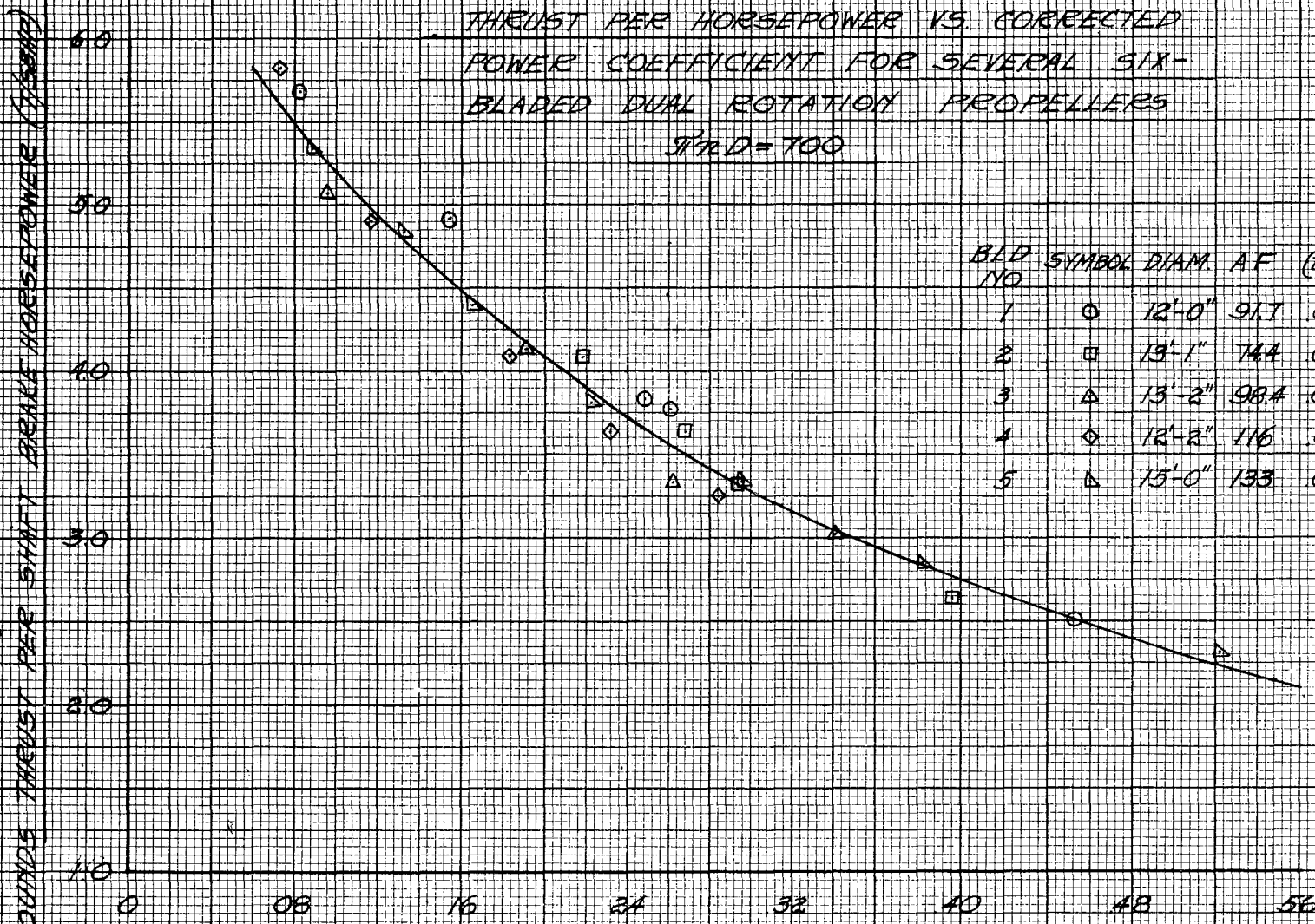

BLD NO	SYMBOL	DIAM.	AF	$(t/b)_{.75R}$	C_{L_i}
1	○	12'-0"	91.7	.0775	.50
2	□	13'-1"	74.4	.0730	.50
3	△	13'-2"	98.4	.0730	.533
4	◇	12'-2"	116	.0765	.47
5	◭	15'-0"	133	.0675	.50

UNCLASSIFIED

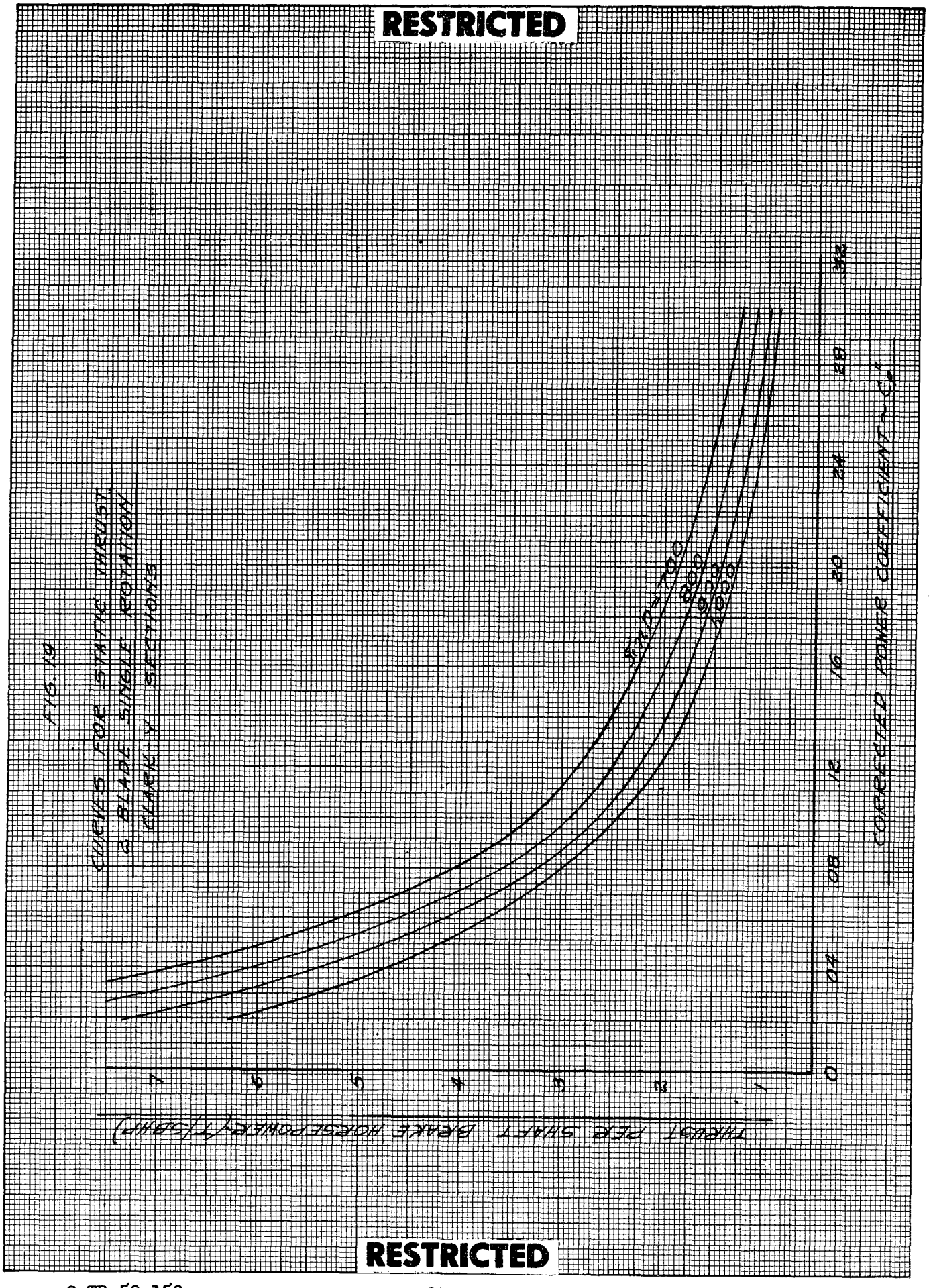
CURVES FOR STATIC THRUST
3 BLADE SINGLE ROTATION
CLARK Y SECTIONS
$\Phi = 0.7$
$\Phi = 0.8$
$\Phi = 0.9$
$\Phi = 1.0$
CORRECTED POWER COEFFICIENT C_P
0
.04
.08
.12
.16
.20
.24
.28
.32
THRUST PER SHAFT BRAKE HORSEPOWER (T/SHP)
1
2
3
4
5
6
7

FIG. 19

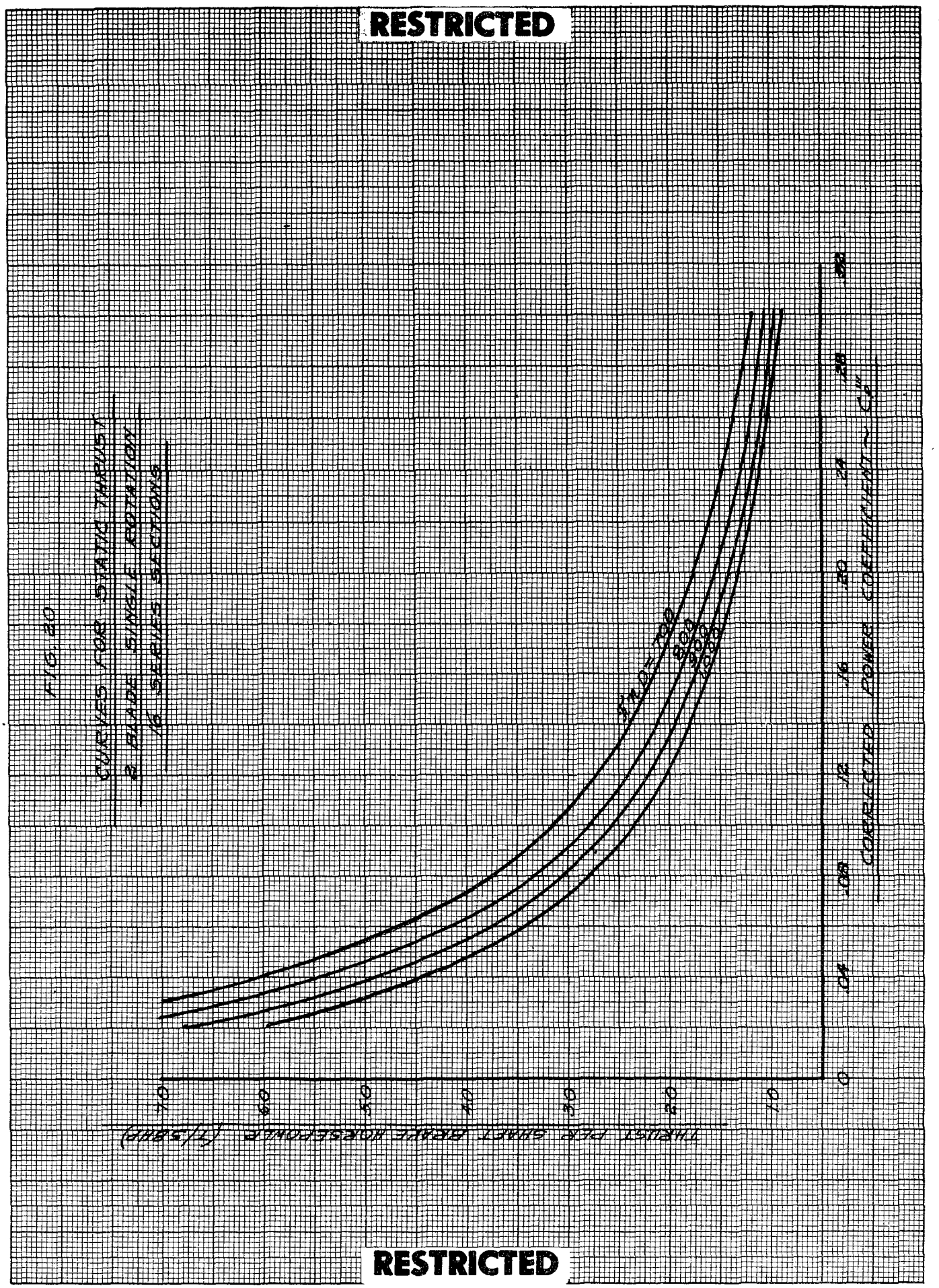
CURVES FOR STATIC THRUST
2 BLADE SINGLE ROTATION
16 SERIES SECTIONS
$\sigma_{TIP} = .200$
.300
.400
.500
THRUST PER SHAFT BRAKE HORSEPOWER (T/SBHP)
70
60
50
40
30
20
10
0
.04
.08
.12
.16
.20
.24
.28
.32
CORRECTED POWER COEFFICIENT C_P''

FIG. 20

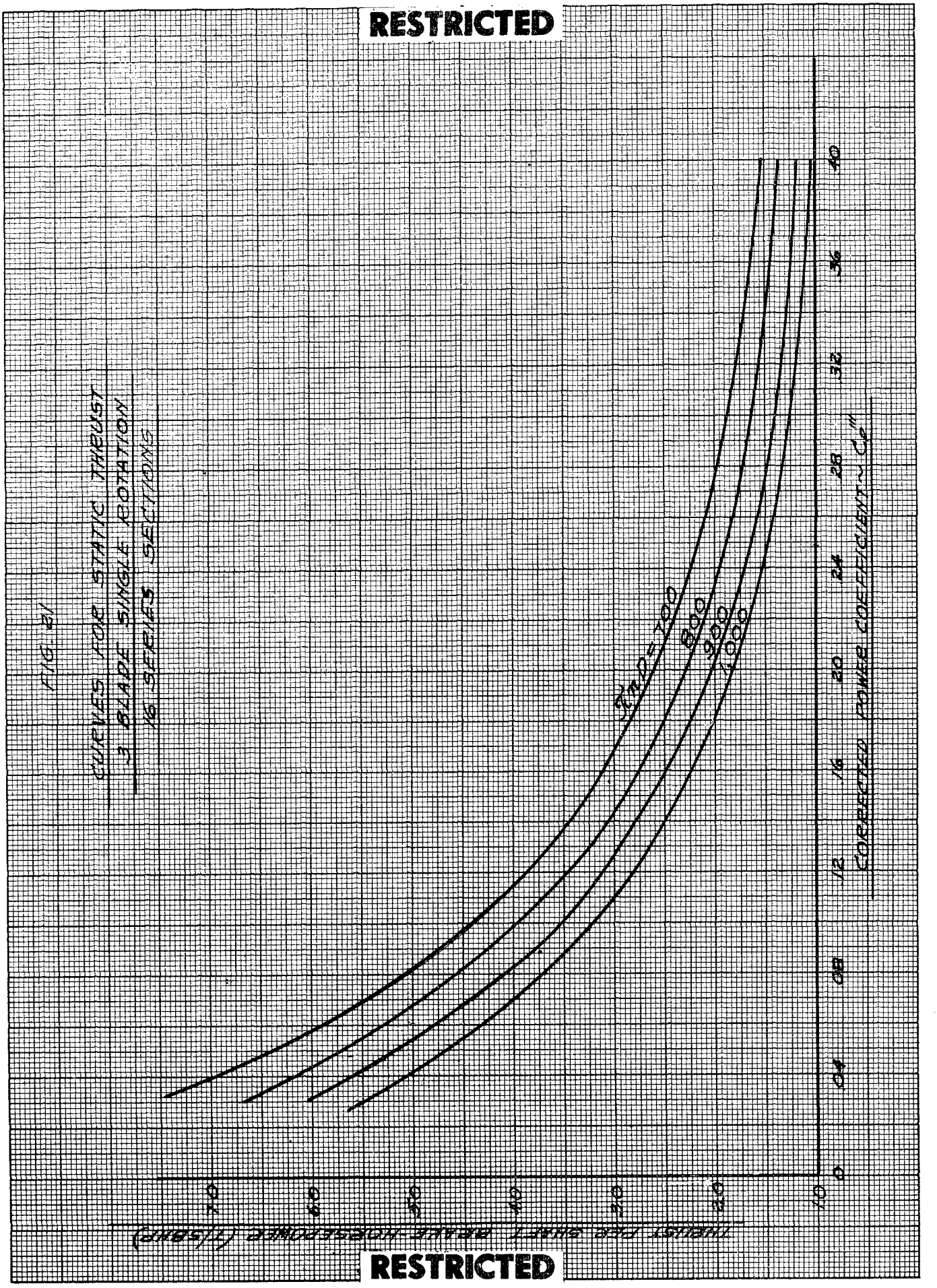
FIG. 21
CURVES FOR STATIC THRUST
3 BLADE SINGLE ROTATION
16 SERIES SECTIONS
700
800
900
1000
0
.04
.08
.12
.16
.20
.24
.28
.32
.36
.40
CORRECTED POWER COEFFICIENT ~ C_P'''
10
20
30
40
50
60
70
INDICATED FOR SHAFT BRAKE HORSEPOWER (HP)

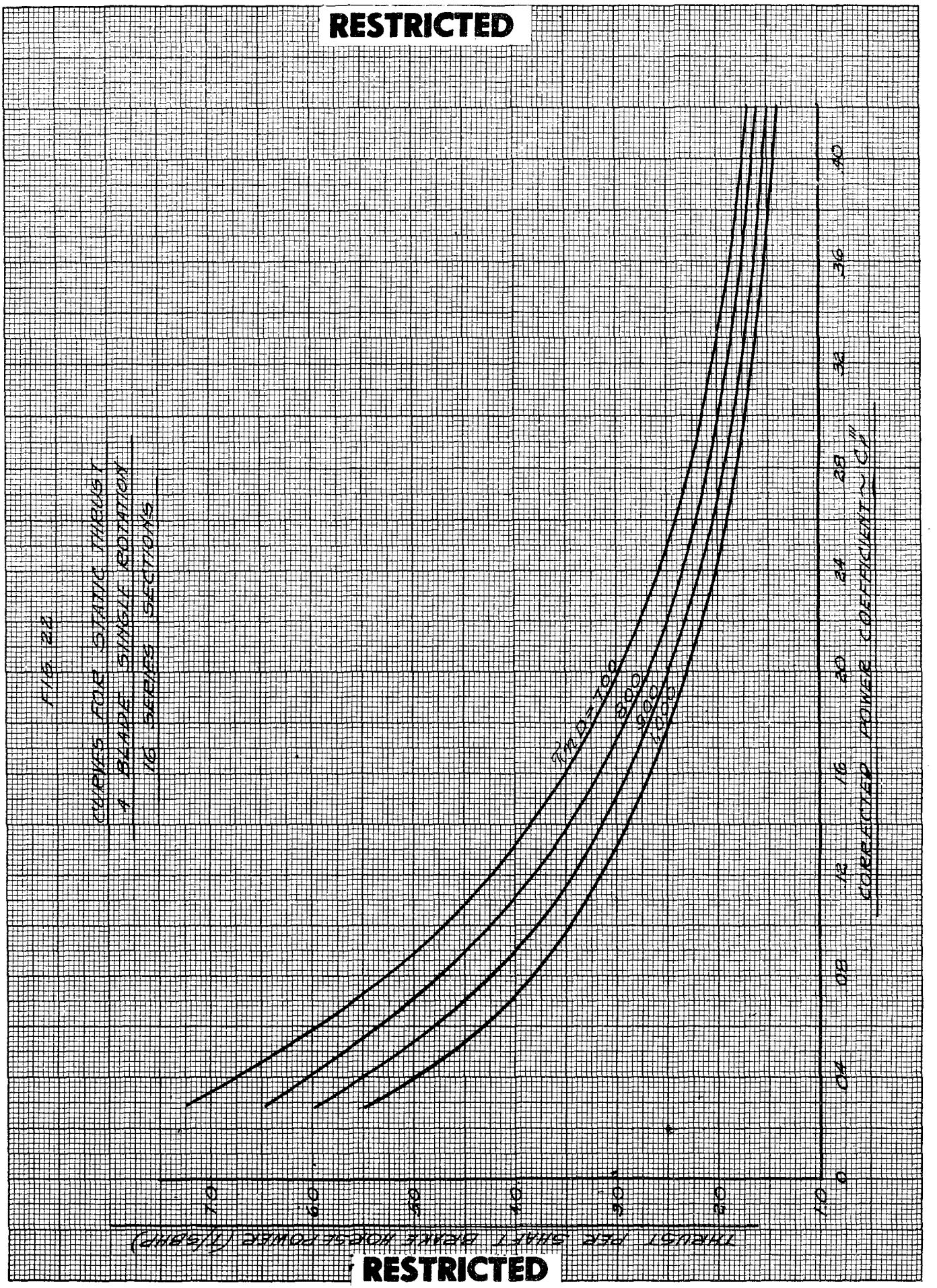
CURVES FOR STATIC THRUST
4 BLADE SINGLE ROTATION
16 SERIES SECTIONS
RPM=700
800
900
1000
CORRECTED POWER COEFFICIENT ~ $C_{P''}$
THRUST PER SHAFT HORSE POWER (lb/shp)
0
.04
.08
.12
.16
.20
.24
.28
.32
.36
.40
10
20
30
40
50
60
70

FIG. 22

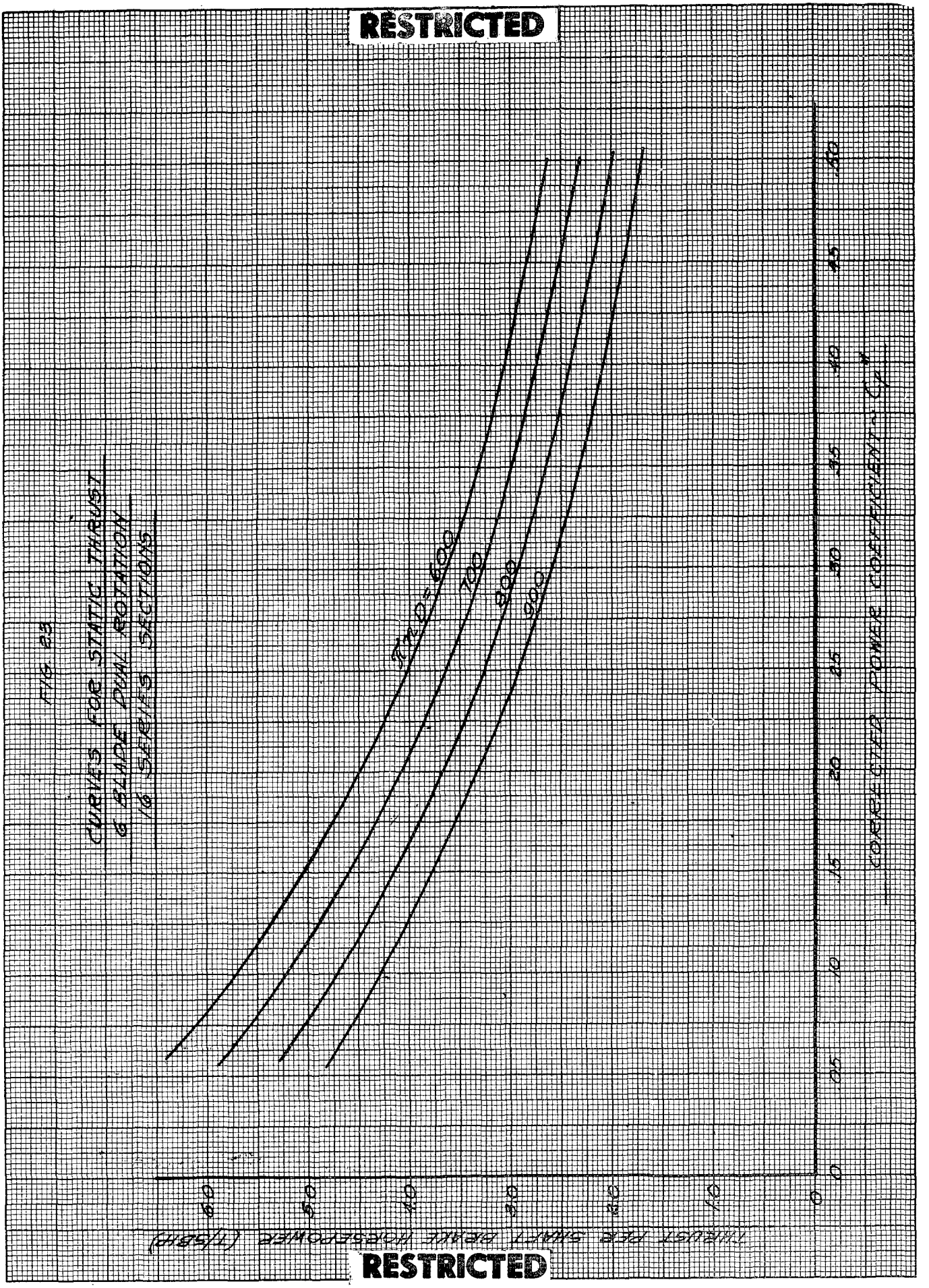
CURVES FOR STATIC THRUST
6 BLADE DUAL ROTATION
16 SERIES SECTIONS
FIG 23
RPM = 600
700
800
900
CORRECTED POWER COEFFICIENT - $C_{P'}$
0
.05
.10
.15
.20
.25
.30
.35
.40
.45
.50
THRUST PER SHAFT PER HORSEPOWER (lb/shp)
0
10
20
30
40
50
60

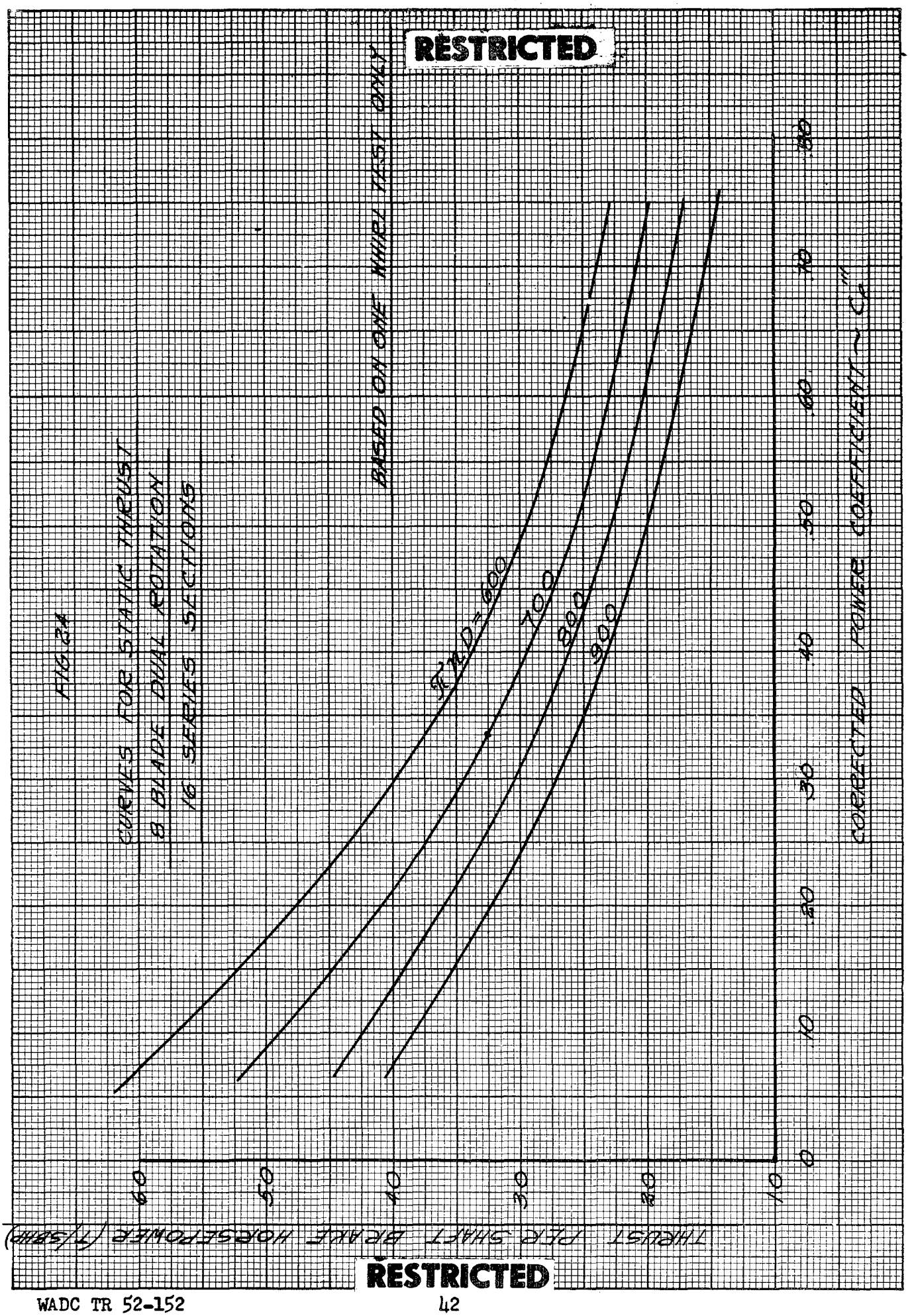
FIG. 24
CURVES FOR STATIC THRUST
8 BLADE DUAL ROTATION
16 SERIES SECTIONS
BASED ON ONE WHEEL TEST ONLY
RPM = 600
700
800
900
CORRECTED POWER COEFFICIENT ~ C_P'''
0
10
20
30
40
50
60
THRUST PER SHAFT BRAKE HORSEPOWER (T/SHP)
60
50
40
30
20
10

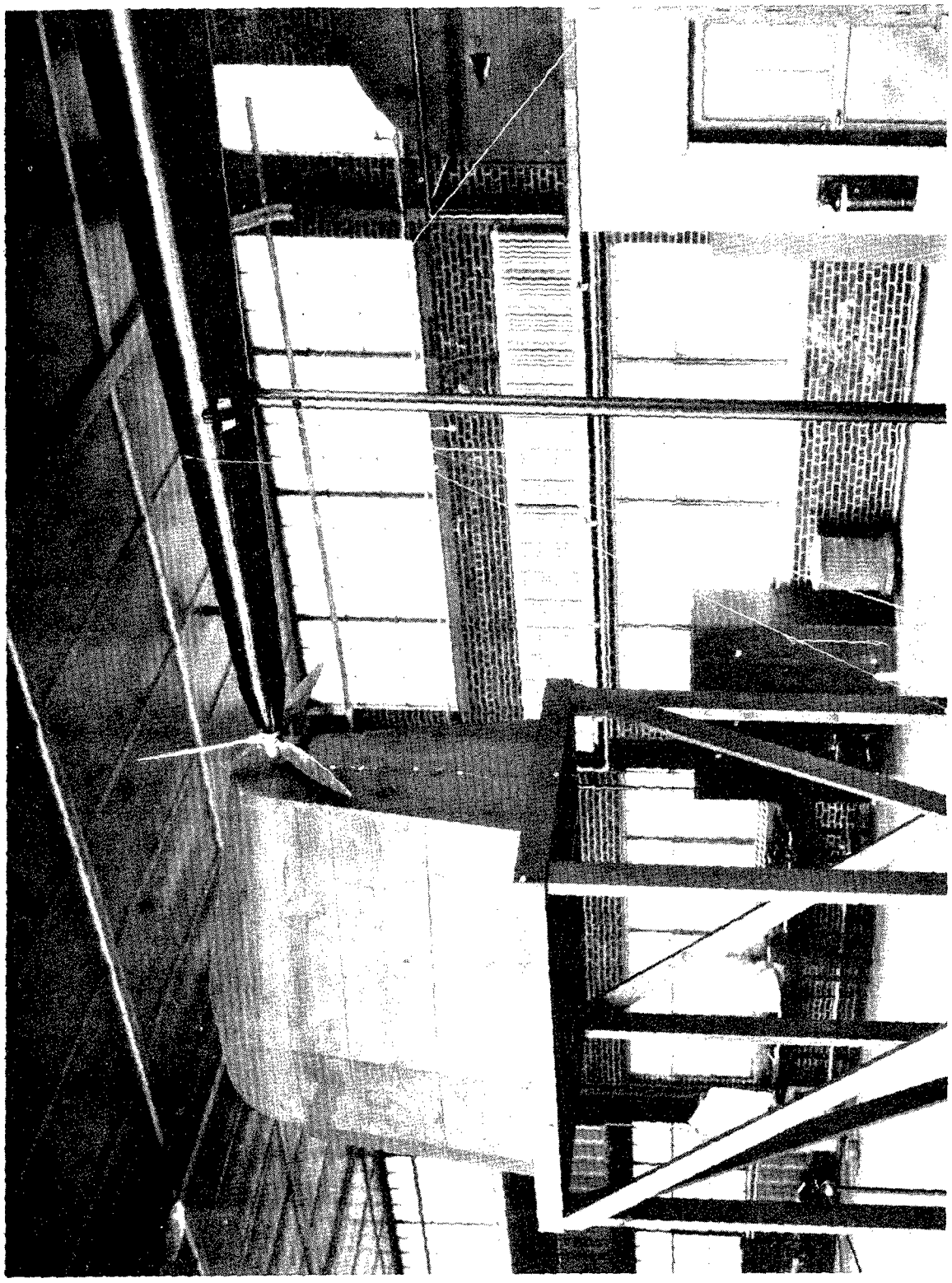

FIG. 25
View of One-Quarter Scale Model of Rig 3

SKETCH OF CONFIGURATIONS FOR NACA BLUFF BODY TESTS

ARROW DENOTES DIRECTION OF SLIPSTREAM

CONFIG I ← PUSHER
CONFIG II → TRACTOR

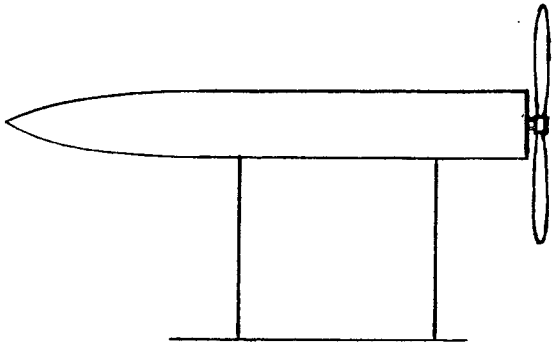

DYNAMOMETER

CONFIG III ← PUSHER
CONFIG IV → TRACTOR

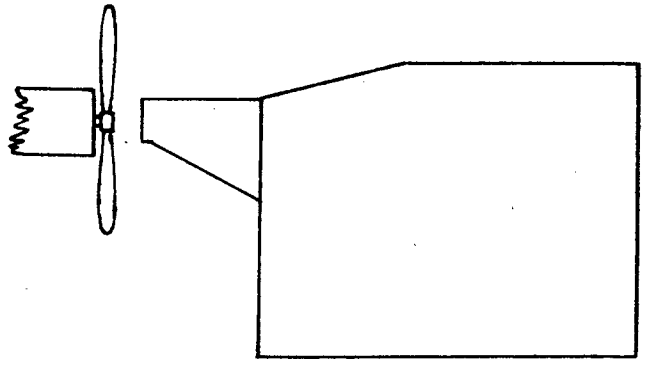

RIG WITH SPEED INCREASER

CONFIG V ← PUSHER
CONFIG VI → TRACTOR

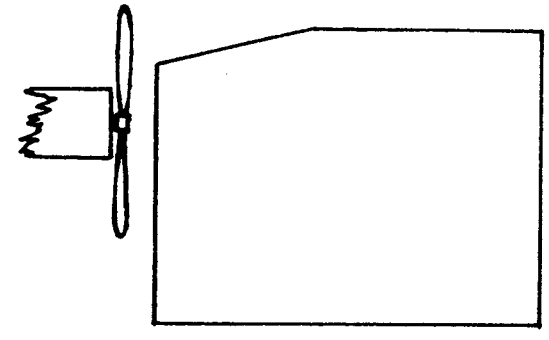

RIG ONLY

FIG. 26

UNCLASSIFIED

FIG. 27

EFFECT OF WHEEL RIG SHAPE ON STATIC PERFORMANCE OF A TRACTOR PROPELLER

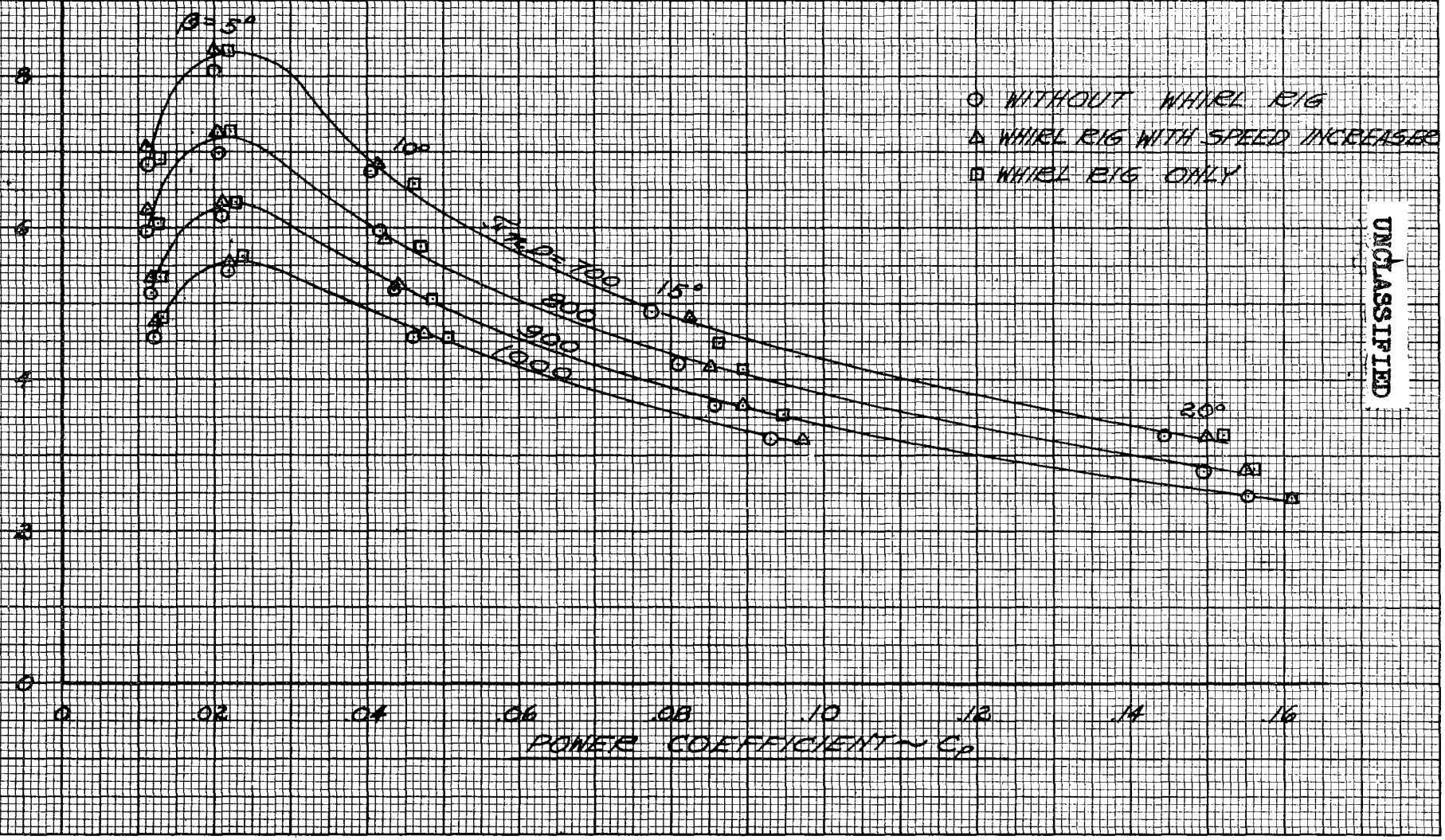

UNCLASSIFIED

UNCLASSIFIED

FIG. 28

EFFECT OF WHIRL RIG SHAPE ON STATIC PERFORMANCE OF A PUSHER PROPELLER

$\pi' n D = 900$

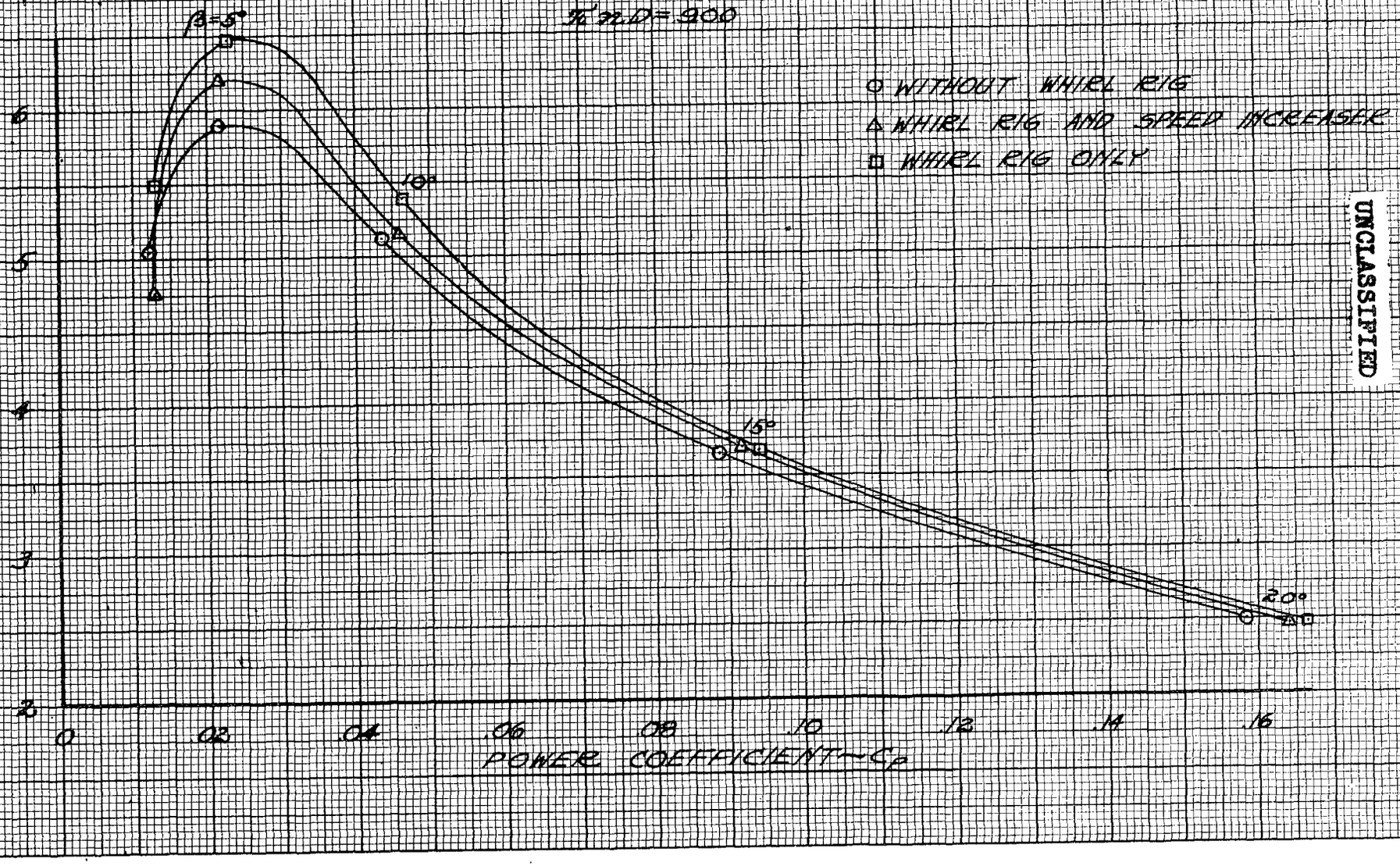

UNCLASSIFIED

UNCLASSIFIED

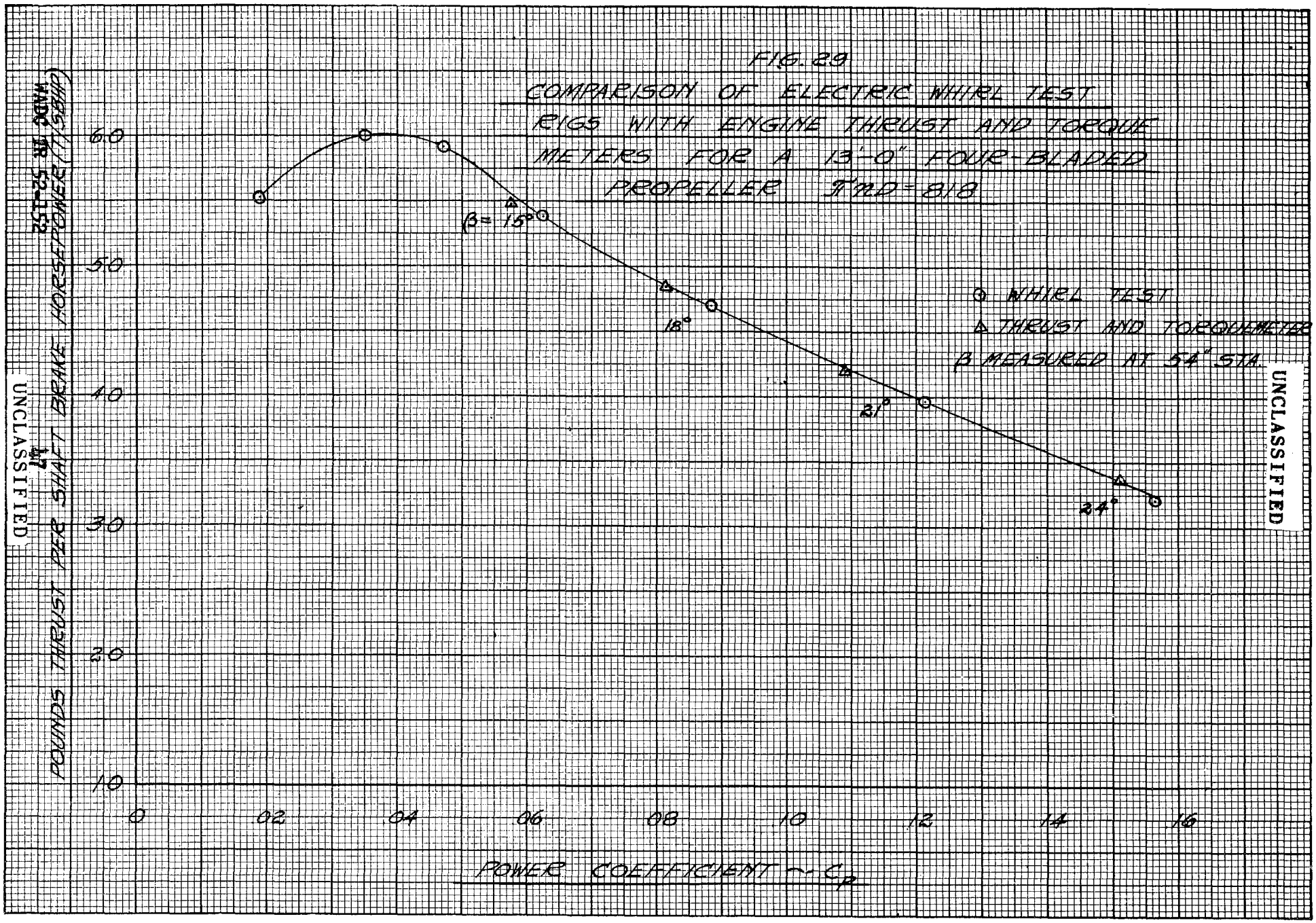

FIG. 29
COMPARISON OF ELECTRIC WHIRL TEST RIGS WITH ENGINE THRUST AND TORQUE METERS FOR A 13'-0" FOUR-BLADED PROPELLER $\pi nD = 8/8$

UNCLASSIFIED

FIG. 30

COMPARISON OF WHIRL RIG AND F-47 THRUSTMETER VALUES FOR A THREE BLADED PROPELLER

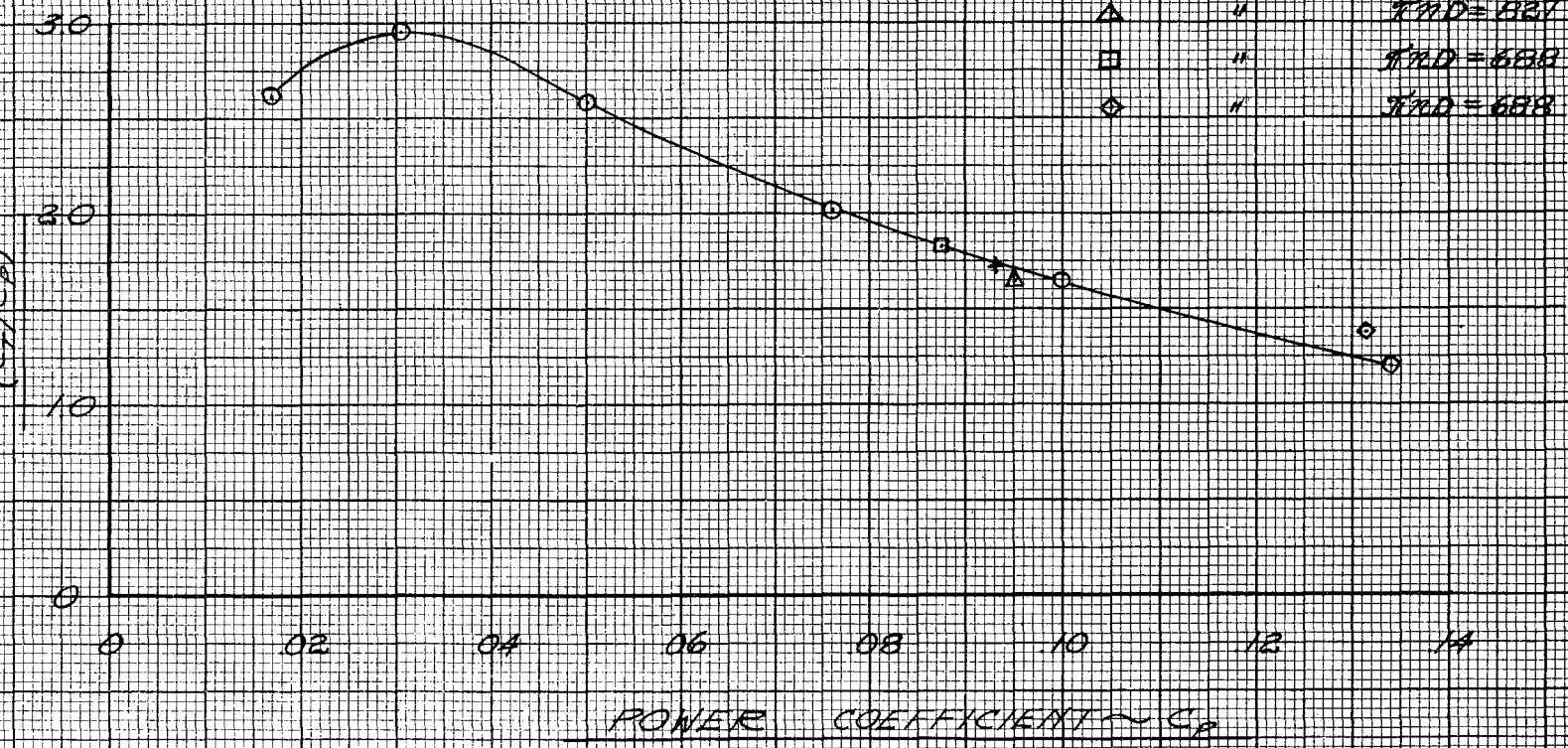

UNCLASSIFIED

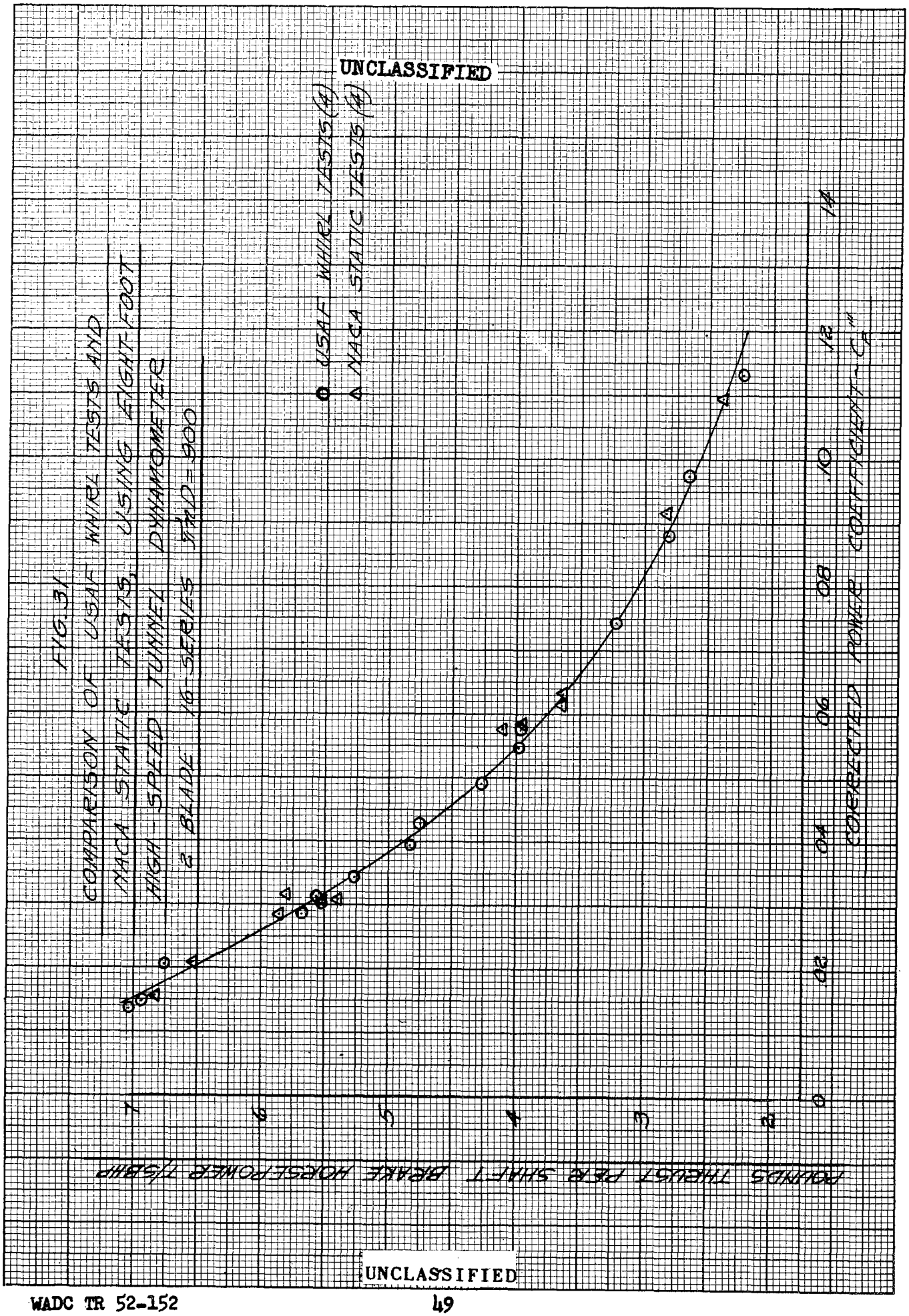
FIG. 31
COMPARISON OF USAF WHIRL TESTS AND
NACA STATIC TESTS, USING EIGHT-FOOT
HIGH-SPEED TUNNEL DYNAMOMETER
2 BLADE 16-SERIES $\pi D^2 = 900$
USAF WHIRL TESTS (4)
NACA STATIC TESTS (4)
POUNDS THRUST PER SHAFT BRAKE HORSEPOWER T/SBHP
0
1
2
3
4
5
6
7
0
.02
.04
.06
.08
.10
.12
.14
CORRECTED POWER COEFFICIENT ~ C_P'''

FIG 32a

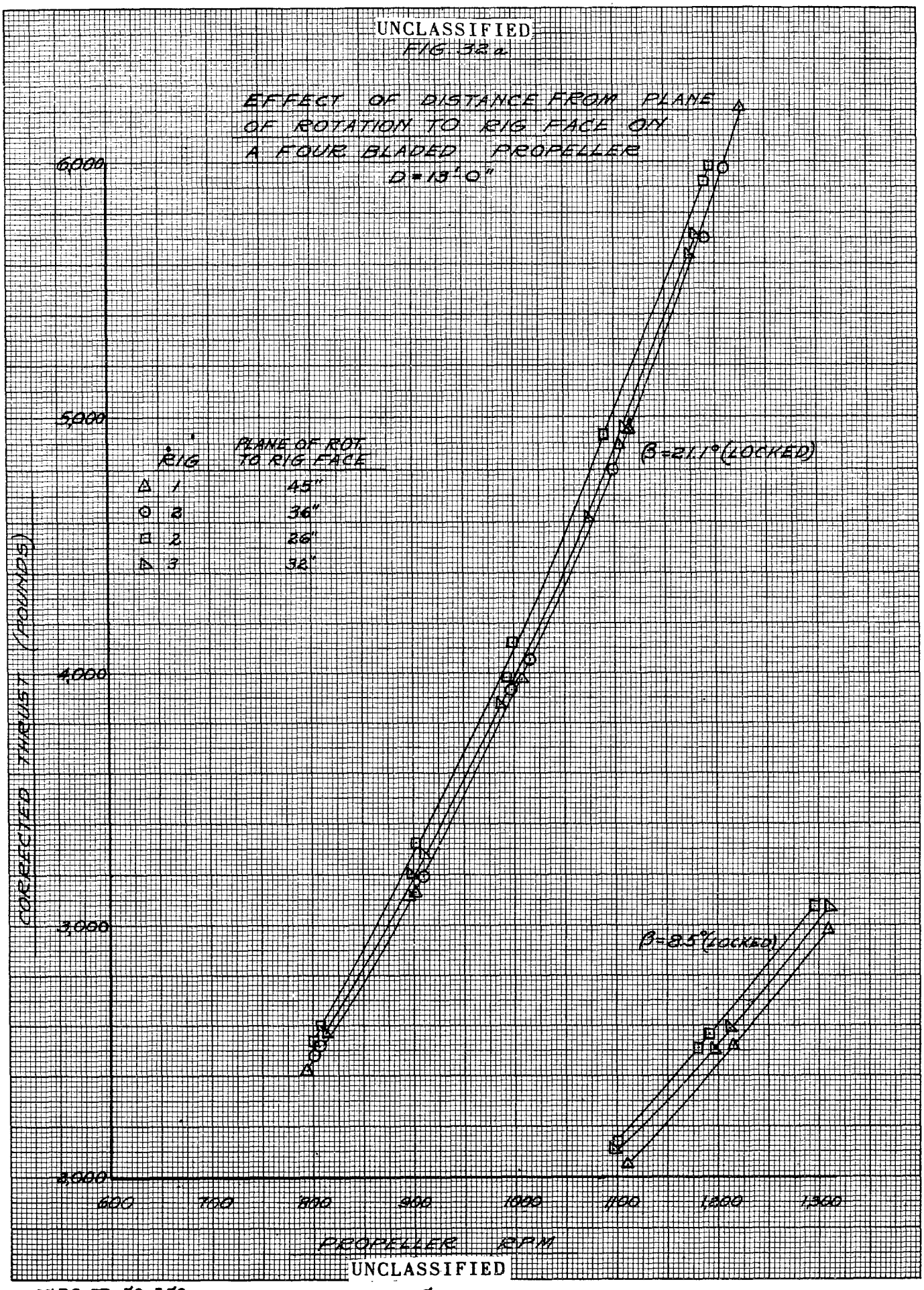
EFFECT OF DISTANCE FROM PLANE OF ROTATION TO RIG FACE ON A FOUR BLADED PROPELLER
D = 13'-0"
RIG
PLANE OF ROT. TO RIG FACE
1 45"
2 36"
2 26"
3 32"
β = 21.1° (LOCKED)
β = 8.5° (LOCKED)
CORRECTED THRUST (POUNDS)
6,000
5,000
4,000
3,000
2,000
600
700
800
900
1000
1100
1200
1300
PROPELLER RPM

FIG. 32 b

EFFECT OF DISTANCE FROM PLANE OF ROTATION TO RIG FACE ON A FOUR BLADED PROPELLER

D = 13'-0"

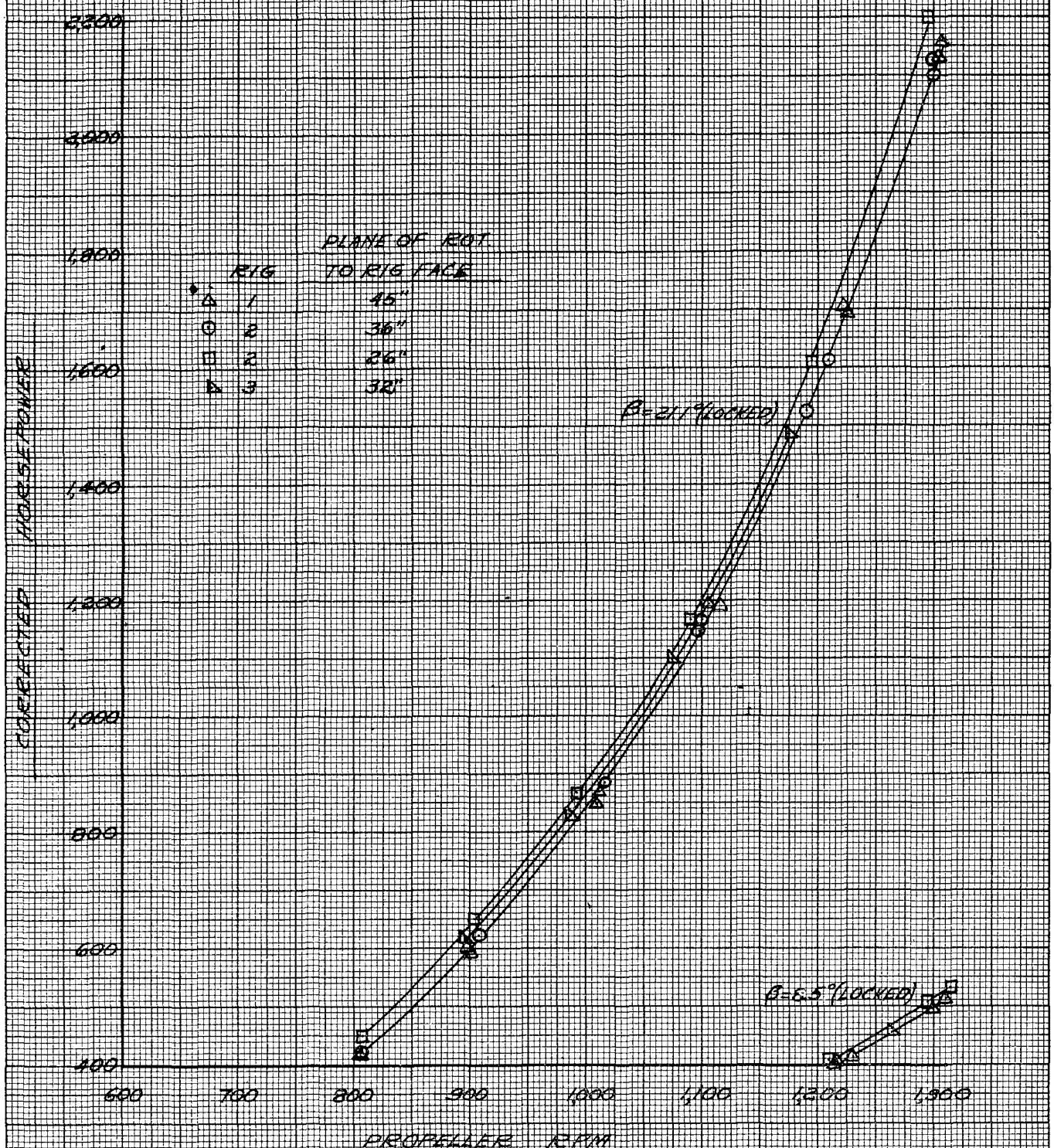

UNCLASSIFIED

FIG. 33

EFFECT OF DISTANCE FROM PLANE OF ROTATION TO RIG FACE ON A FOUR BLADED PROPELLER
DIA = 13'-0" TIP = 500

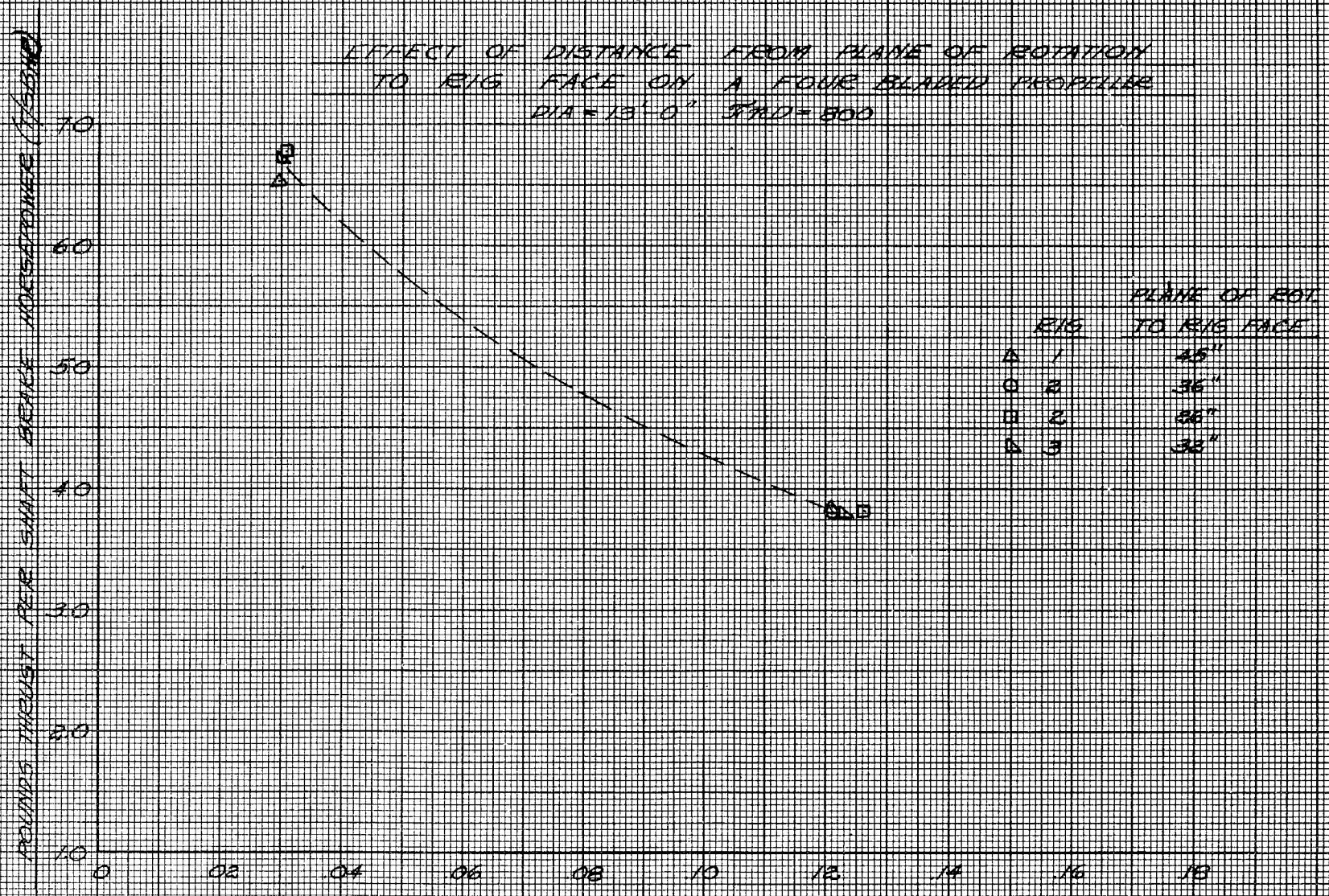

UNCLASSIFIED

FIG. 34

COMPARISON OF PROPULSIVE THRUST AND SHAFT THRUST FOR THREE-BLADED PROPELLERS AT $\pi n D = 900$

		D	AF	t/b	C_{L_i}	
PROPULSIVE THRUST	○	10'-1"	79	.088	38	REF 3
	△	10'-4"	84	.079	32	REF. 2

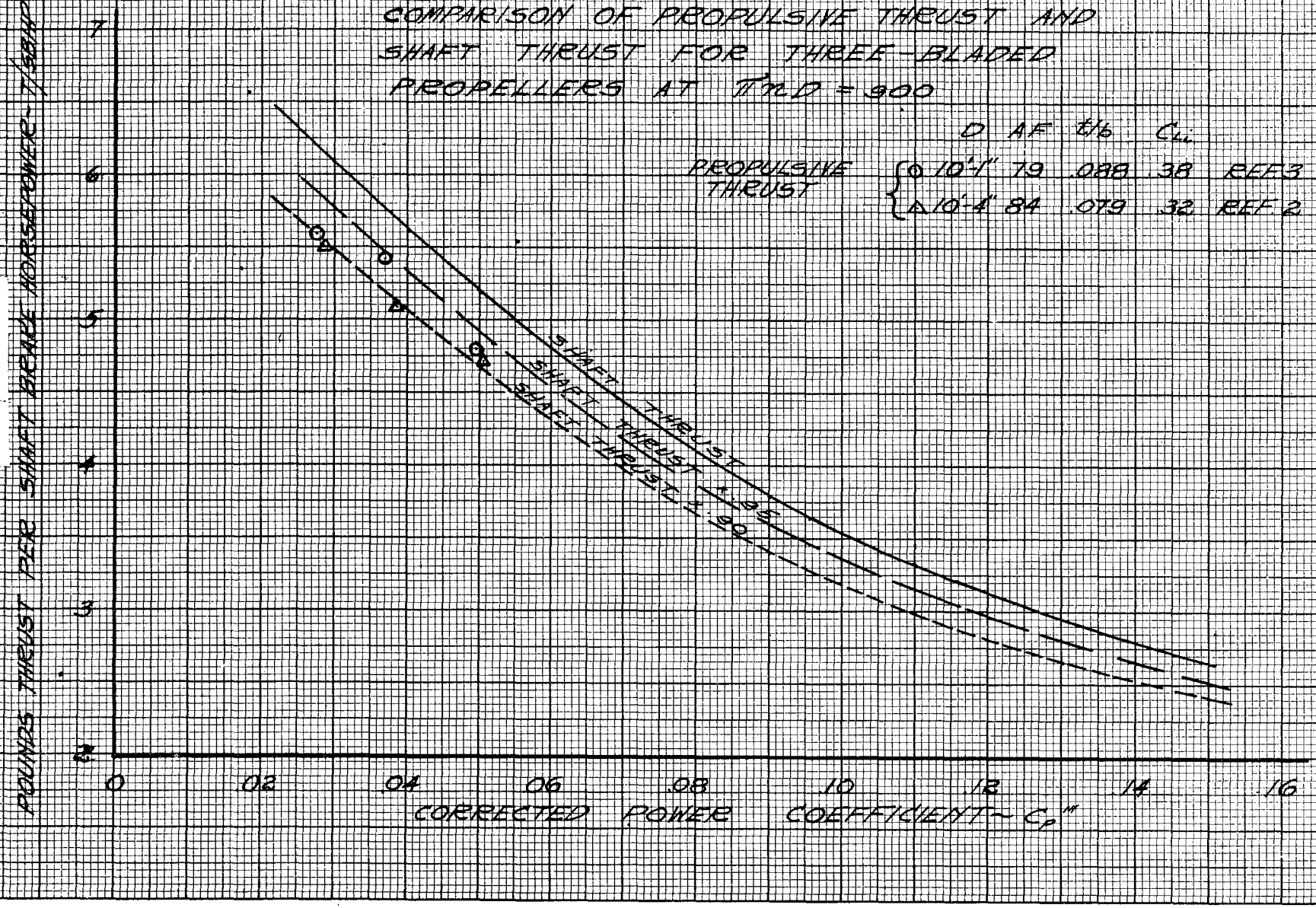

FIG. 35

EFFECT OF TIP SPEED ON THRUST PER HORSEPOWER AT SEVERAL VALUES OF POWER COEFFICIENT

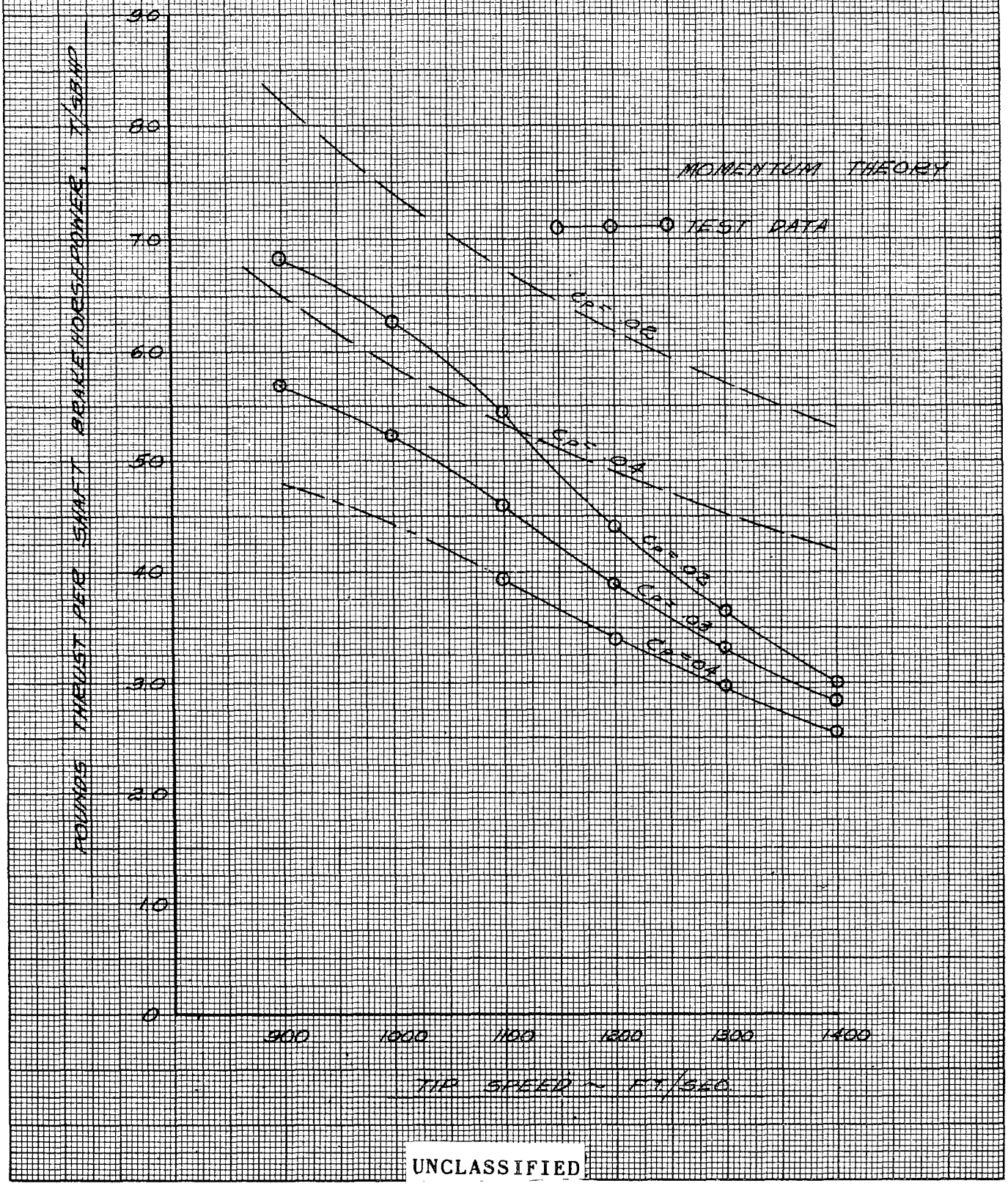

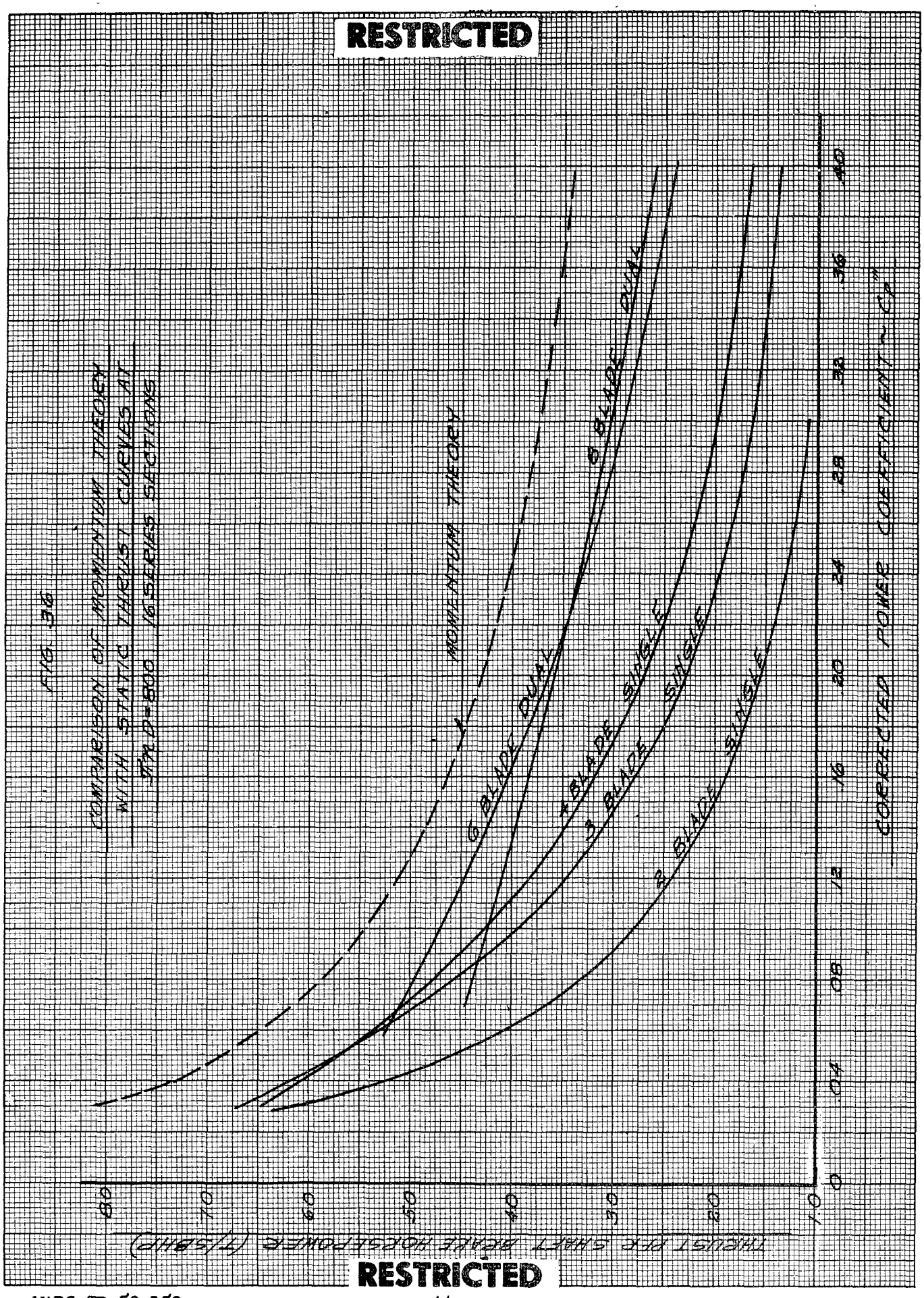

FIG. 36
COMPARISON OF MOMENTUM THEORY WITH STATIC THRUST CURVES AT J_{TIP} = 0.600 16 SERIES SECTIONS

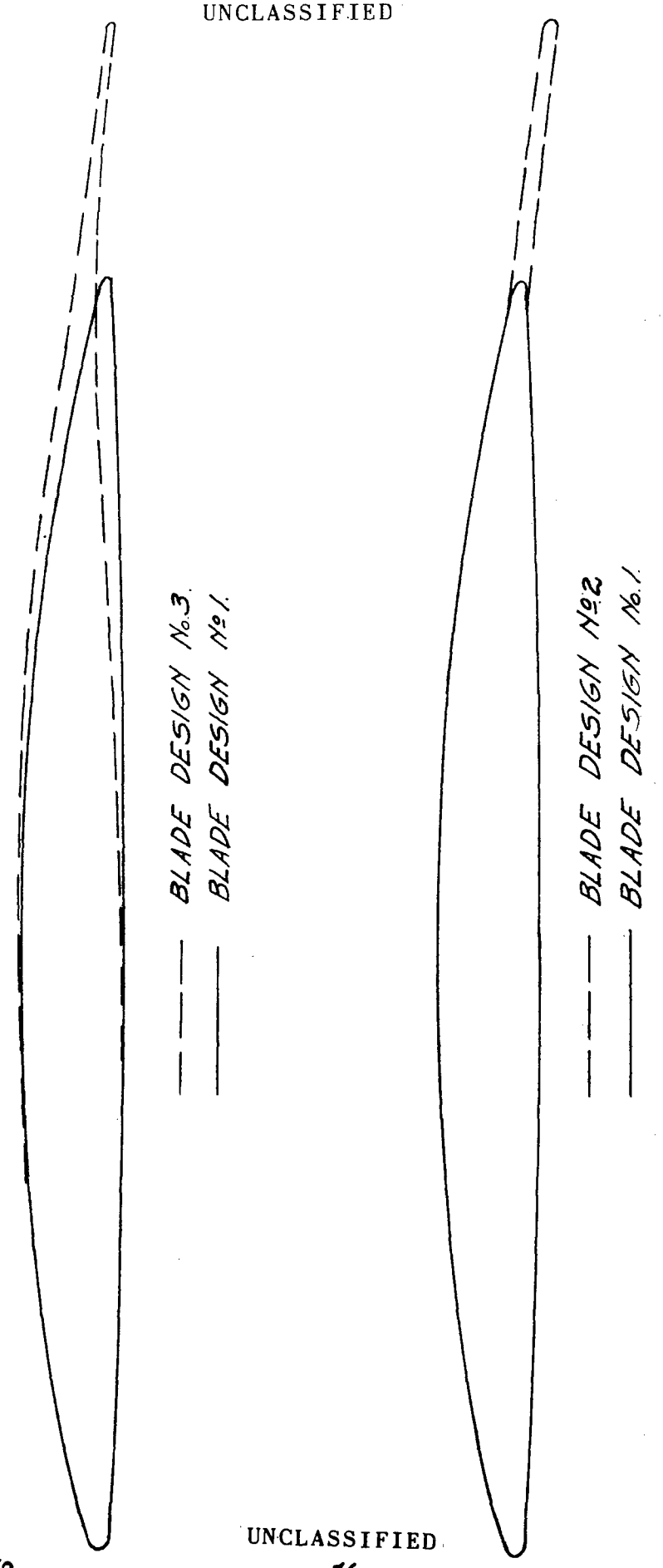

FIG. 37a
SECTION COMPARISON OF THE No.3 AND No.2 BLADE WITH THE No.1 BLADE

FIG. 37b

EFFECT OF TRAILING EDGE EXTENSION ON STATIC THRUST CHARACTERISTICS OF SEVERAL TWO BLADED PROPELLERS AT $\mathcal{R}_{MD}$ = 900

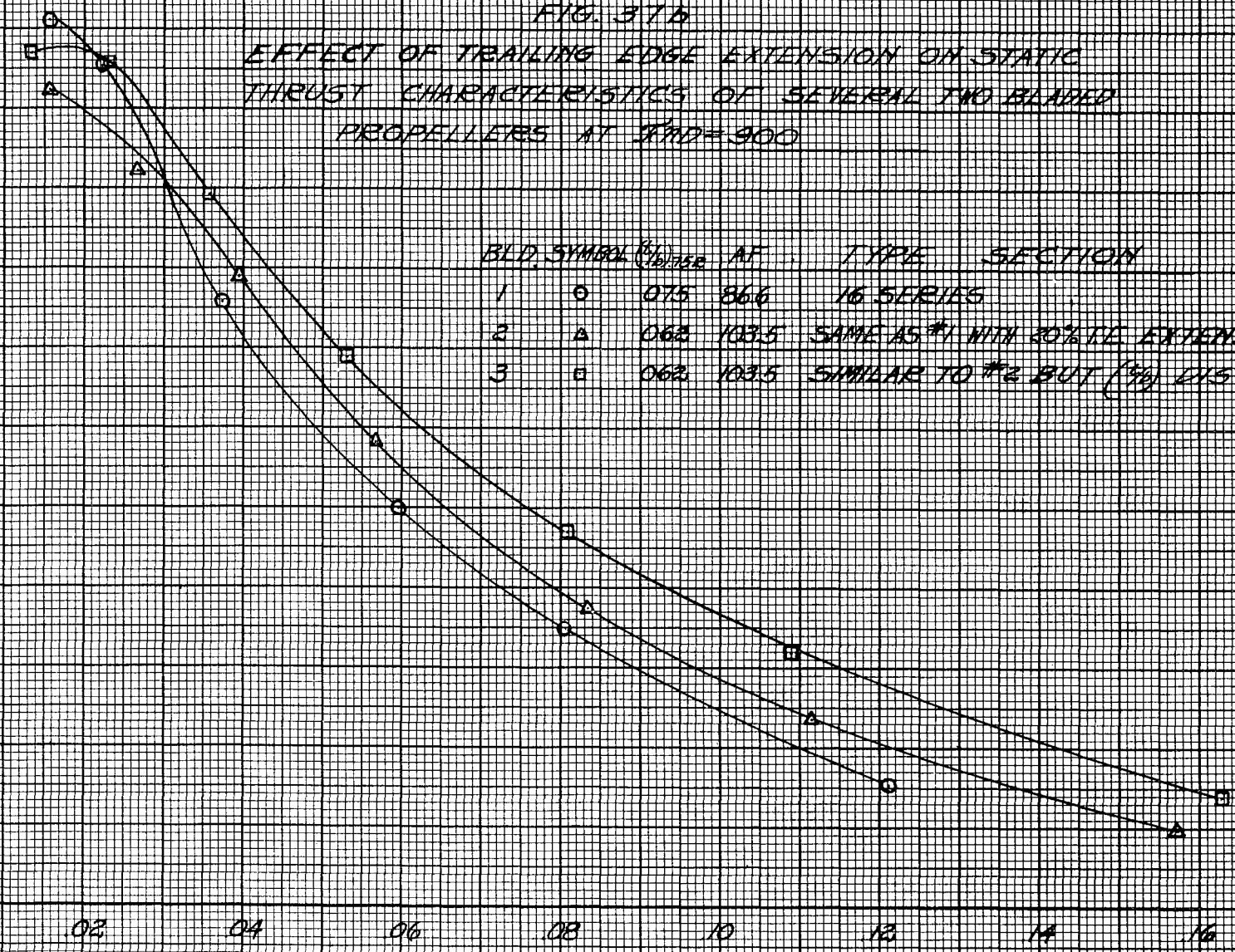

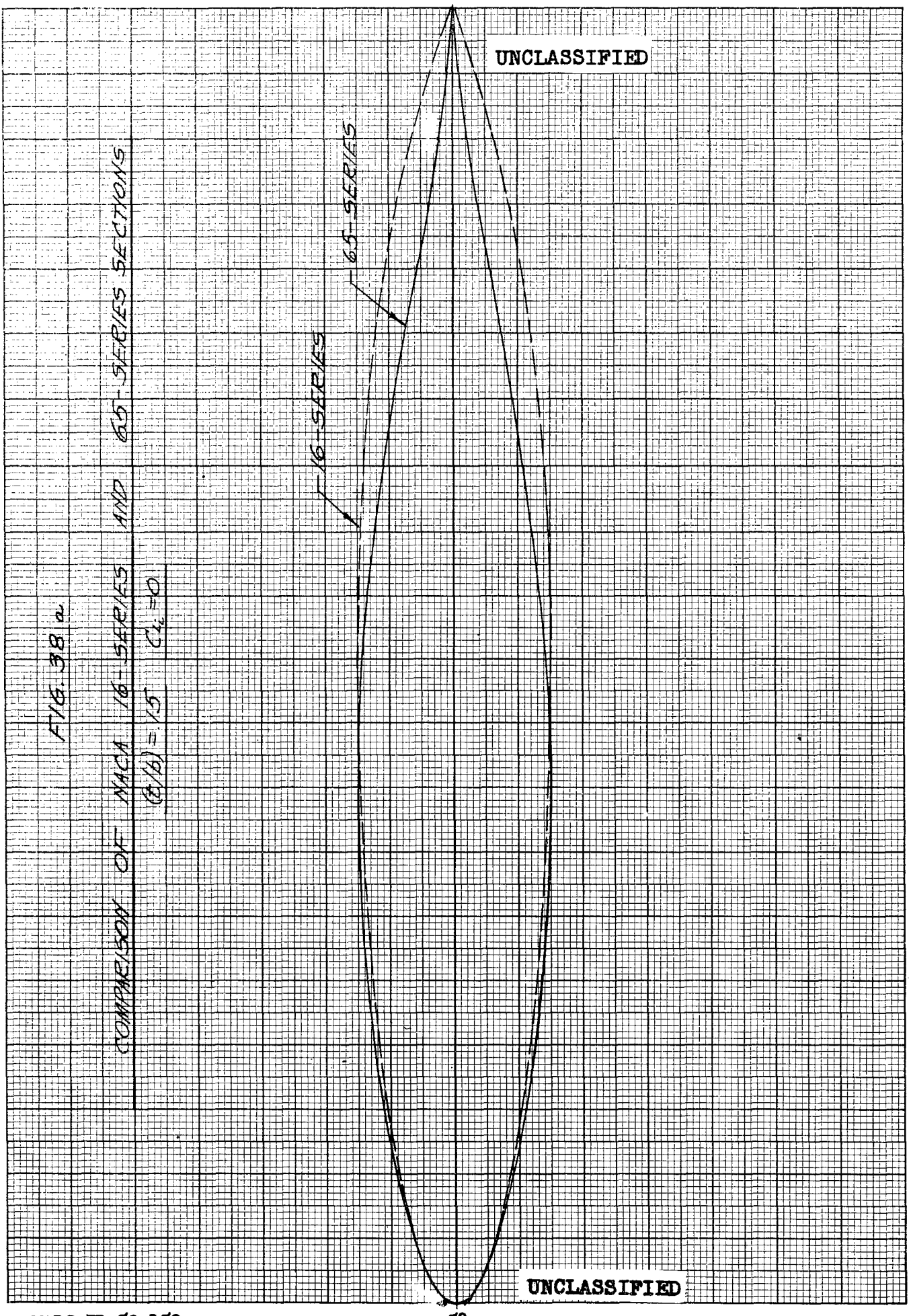

FIG 38 a

COMPARISON OF MACH 16-SERIES AND 65-SERIES SECTIONS

$(t/b) = .15$ $C_L = 0$

UNCLASSIFIED

FIG. 38b

COMPARISON OF A THREE BLADED 16 SERIES WITH A THREE BLADED 65 SERIES PROPELLER HAVING THE SAME AF, C_{L_i} AND $(t/b)_{75R}$

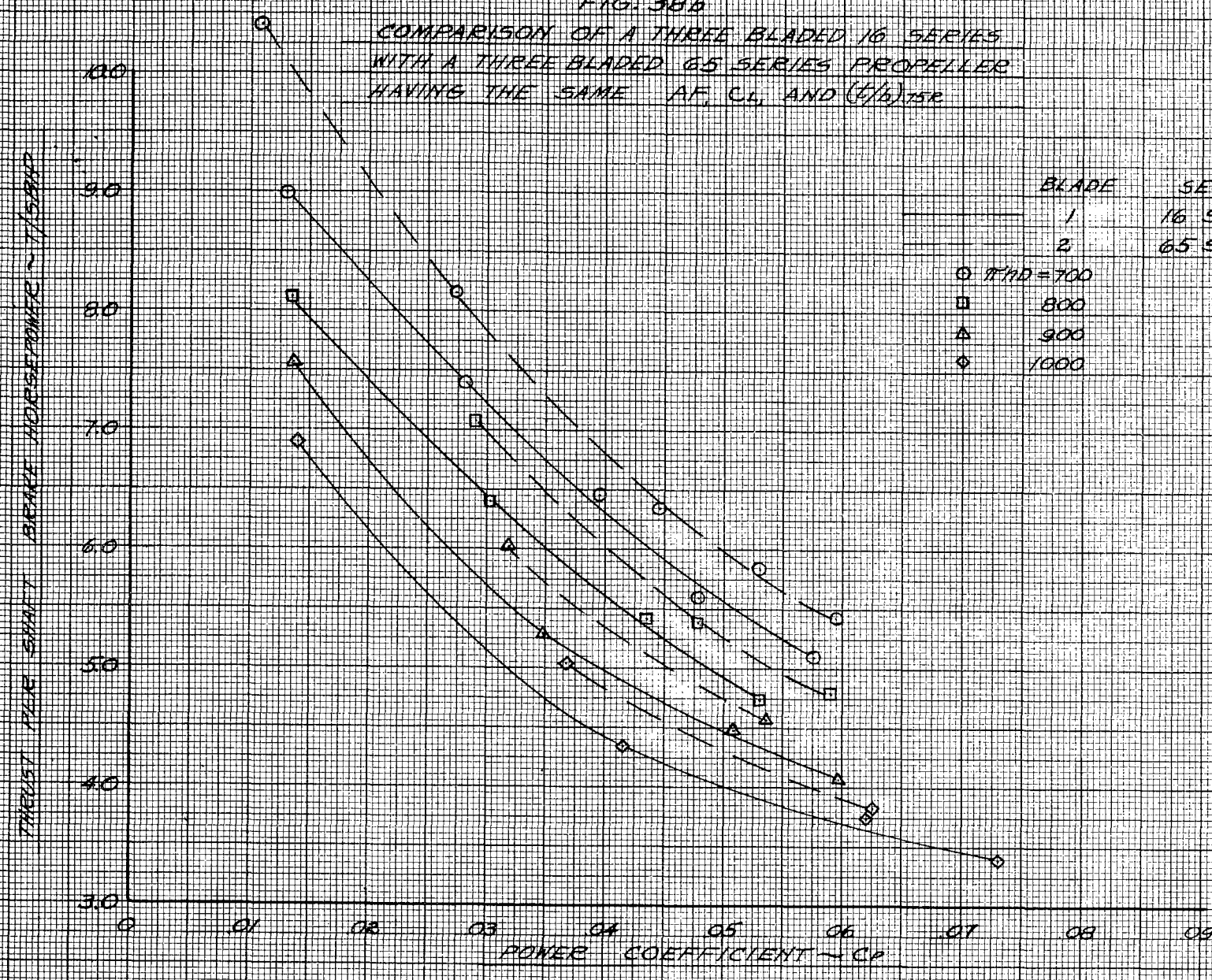

UNCLASSIFIED

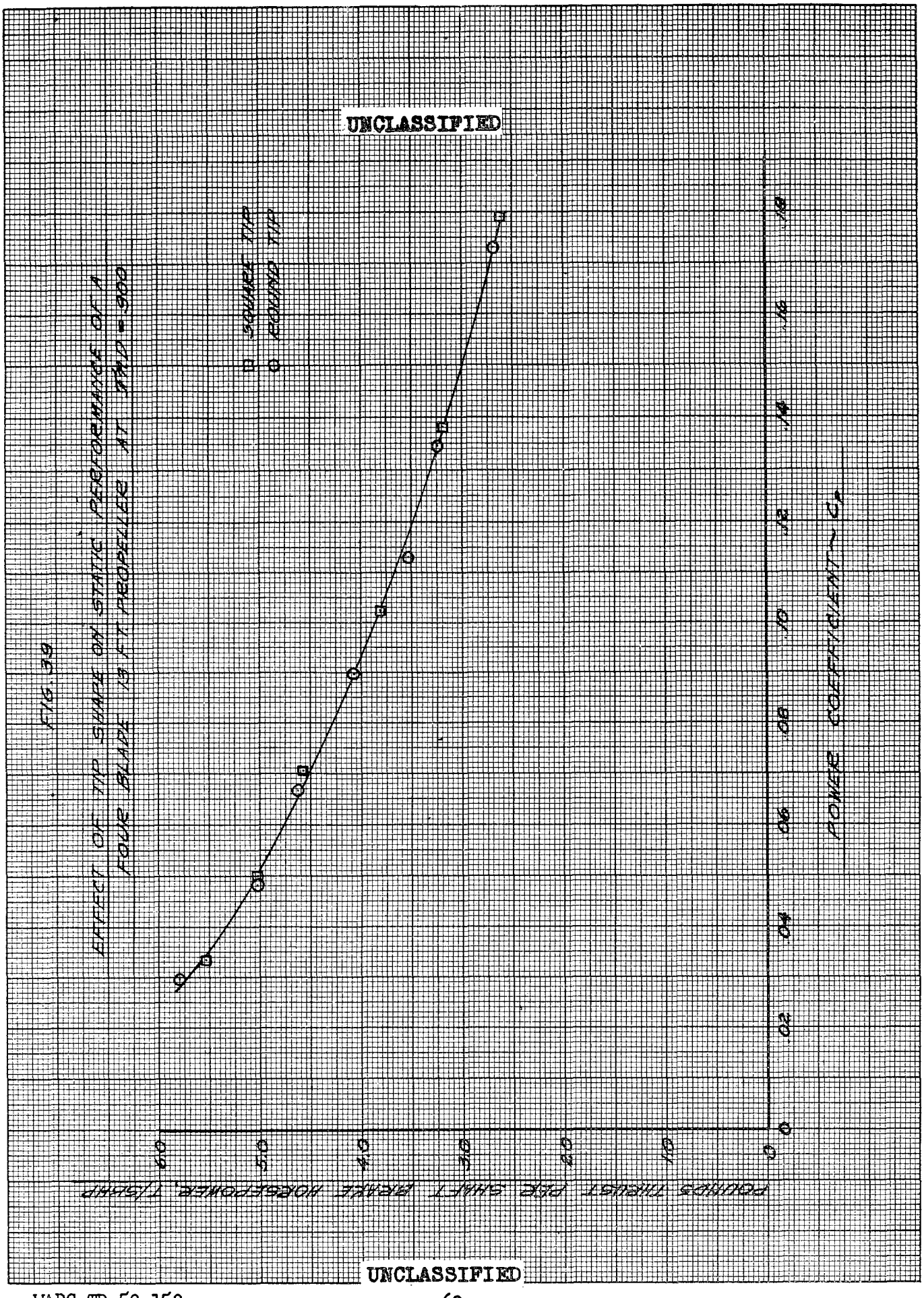

FIG. 39
EFFECT OF TIP SHAPE ON STATIC PERFORMANCE OF A FOUR BLADE 13 FT PROPELLER AT RPD = 900

UNCLASSIFIED

FIG. 40

COMPARISON OF NEW METHOD WITH PREVIOUS (3026) METHOD

16 SERIES $AF = 120$, $(C_H)_{REF} = .065$, $C_L = .40$

$\mathcal{R}_{AD} = 900$

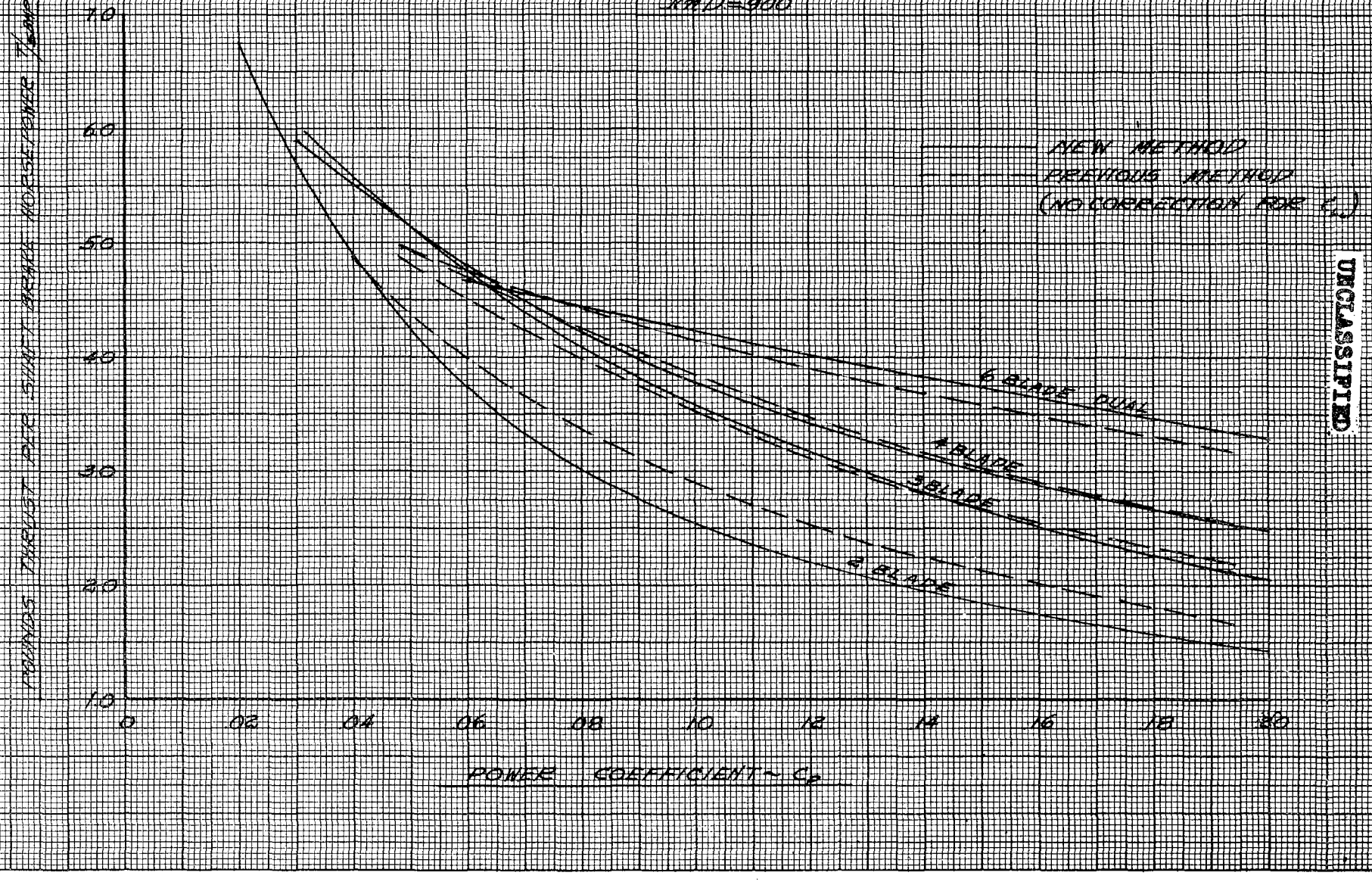

UNCLASSIFIED

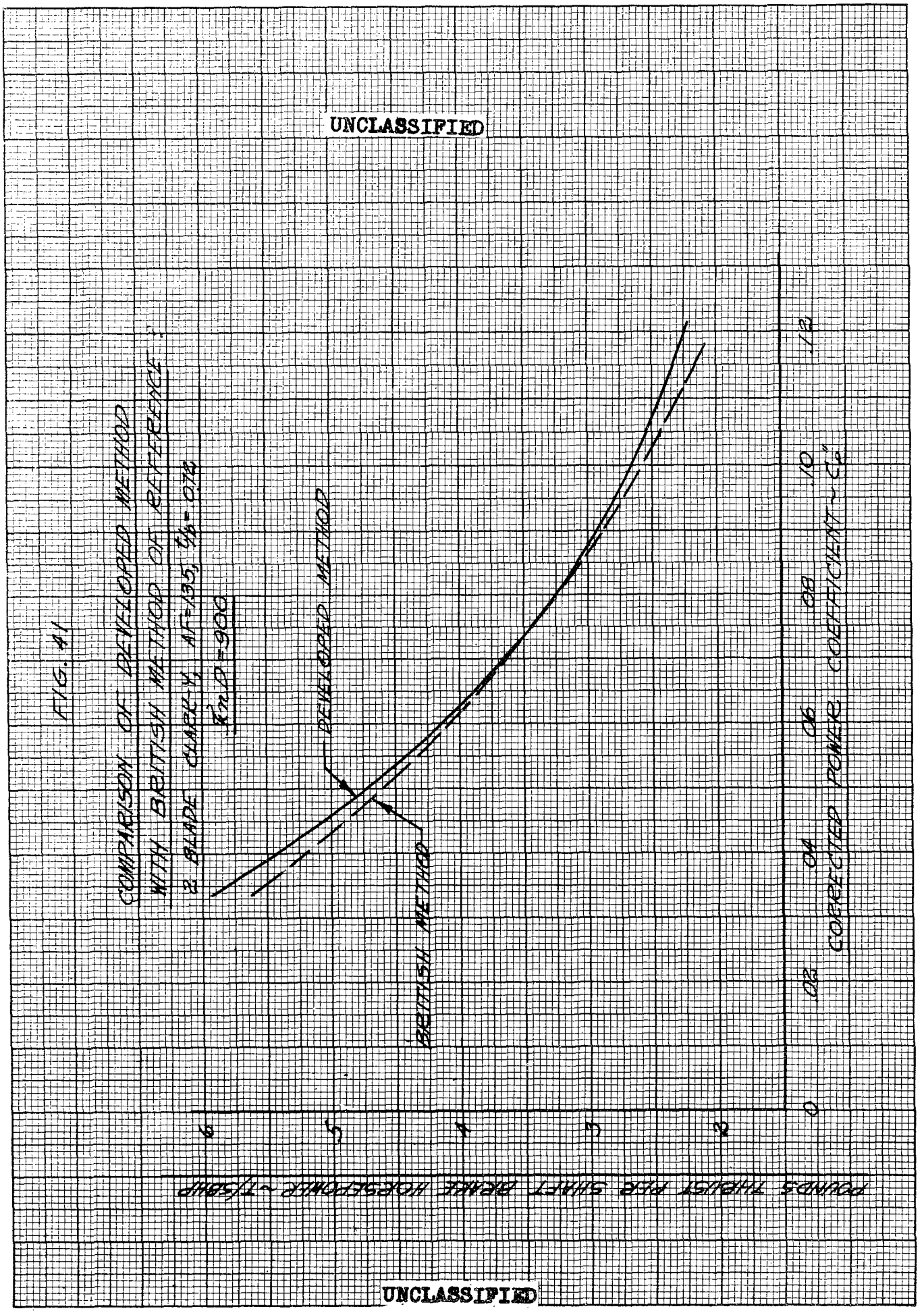

FIG. 41
COMPARISON OF DEVELOPED METHOD WITH BRITISH METHOD OF REFERENCE
2 BLADE CHARTS, AF=135, $\frac{t}{b}$ = .078
$K_n D$ = 900

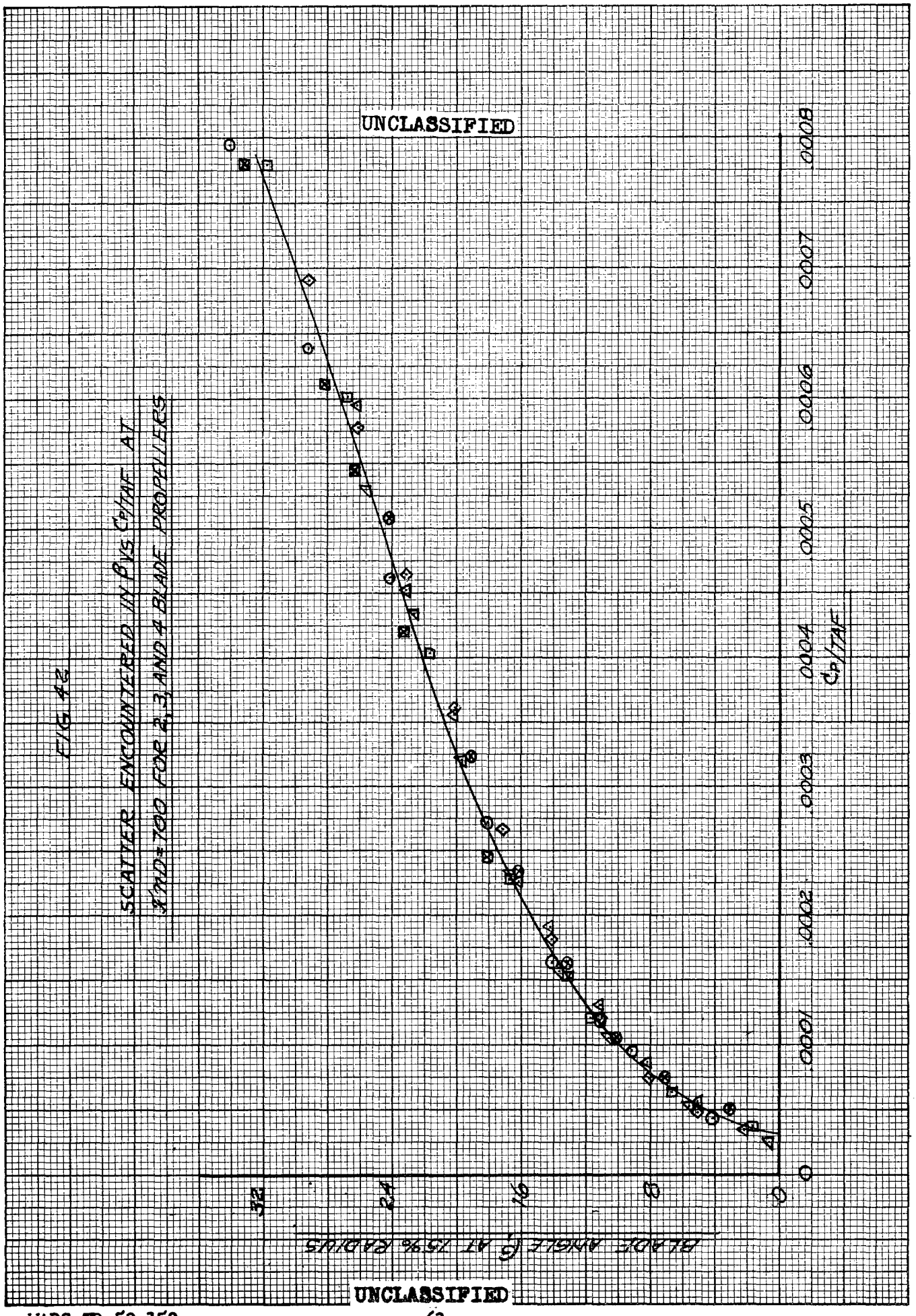

FIG. 42

SCATTER ENCOUNTERED IN P_{VS} C_P/TAF AT $N/\sqrt{\theta}$=700 FOR 2, 3, AND 4 BLADE PROPELLERS

UNCLASSIFIED

FIG. 43

STATIC BLADE ANGLE AT 75% RADIUS FOR 2, 3, AND 4 BLADE PROPELLERS, SINGLE ROTATION

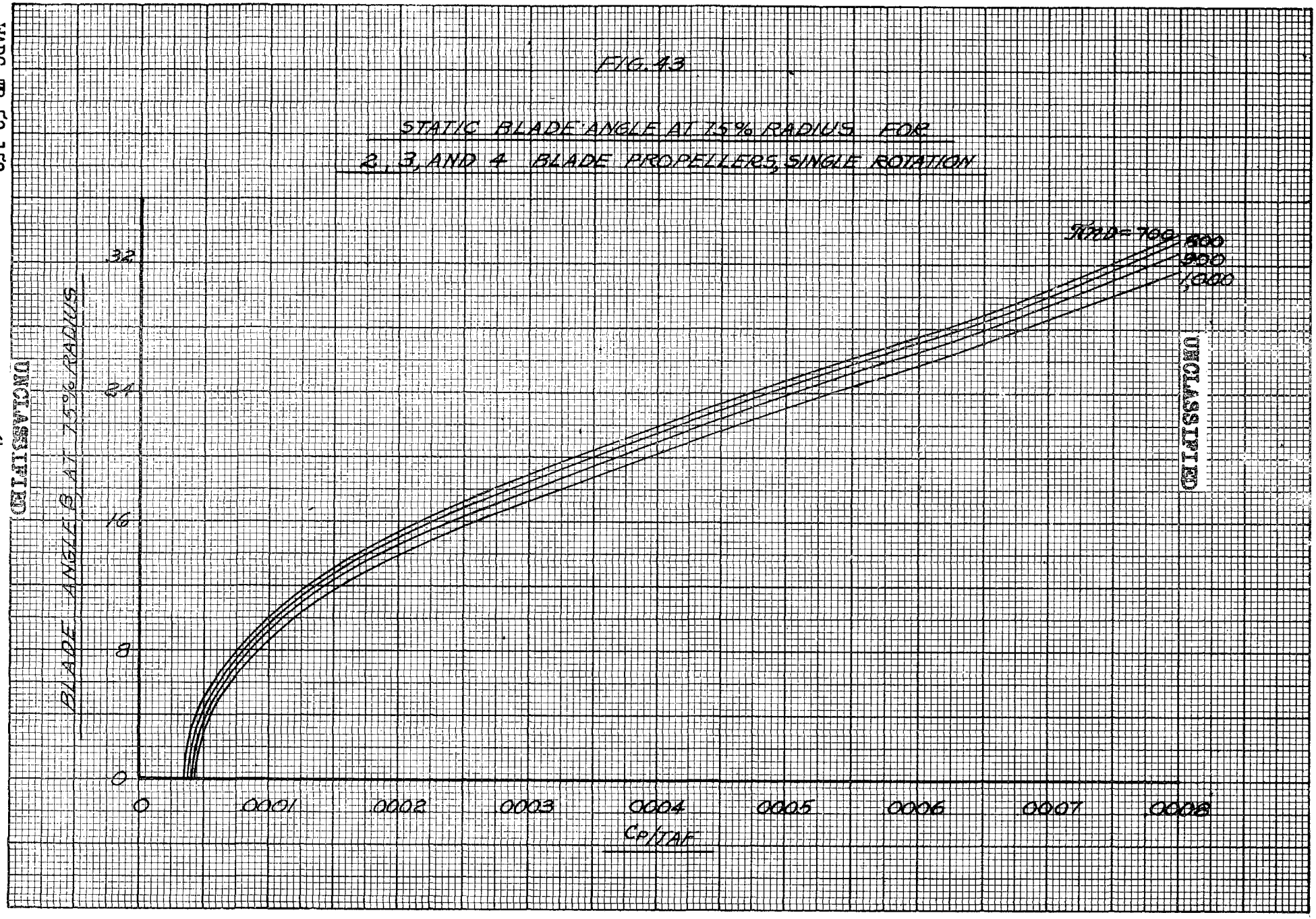

UNCLASSIFIED

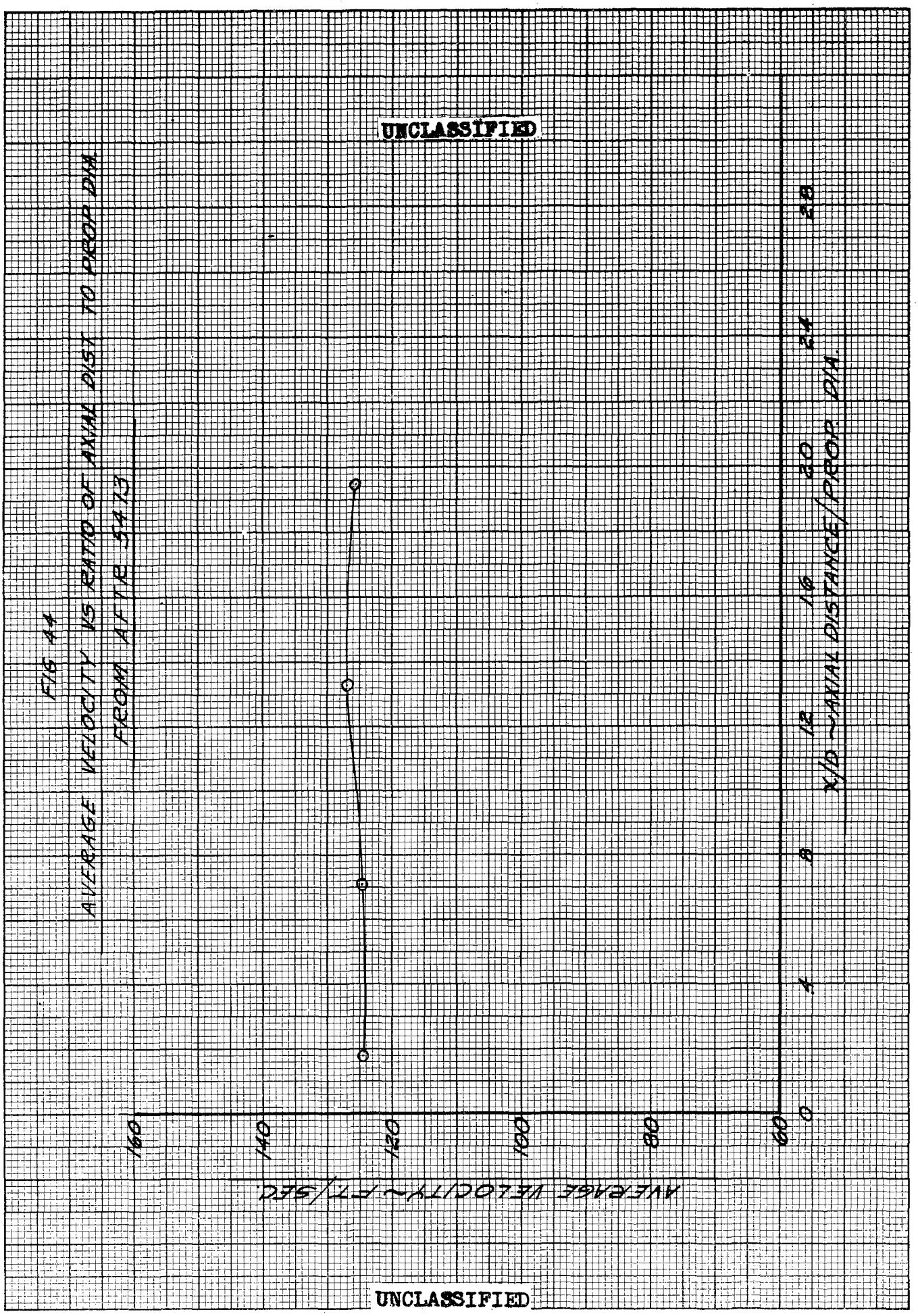
AVERAGE VELOCITY IS RATIO OF AXIAL DIST TO PROP DIA.
FROM AFTR 5413
X/D ~ AXIAL DISTANCE/PROP. DIA.
0
4
8
12
16
20
24
28
AVERAGE VELOCITY ~ FT/SEC
60
80
100
120
140
160

FIG 44

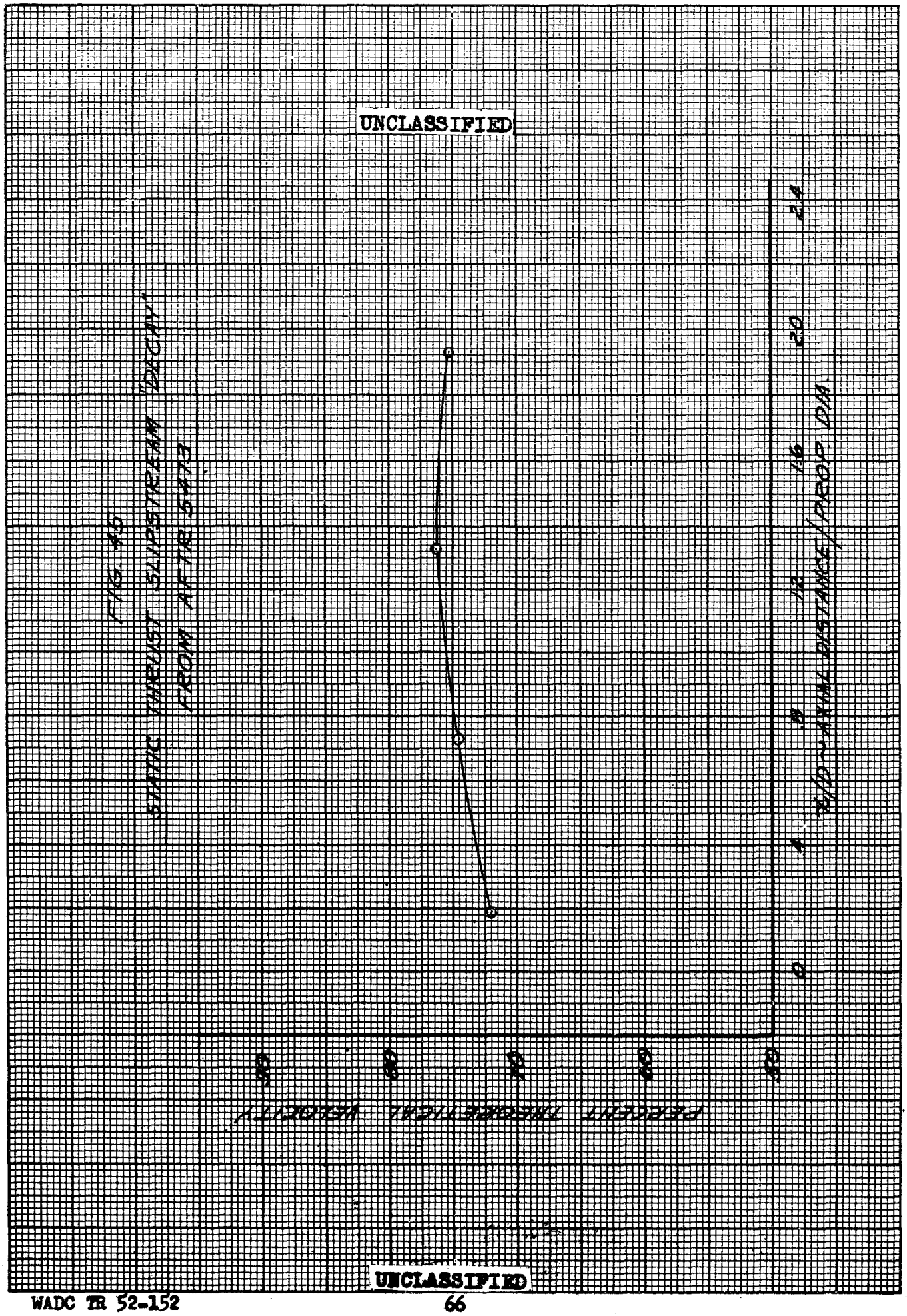

FIG 45
STATIC THRUST SLIPSTREAM DECAY
FROM AFTR 5473

UNCLASSIFIED

FIG 46

GENERALIZED RATIO OF NEGATIVE THRUST TO POSITIVE THRUST FOR SEVERAL FOUR-BLADED SINGLE ROTATION PROPELLERS

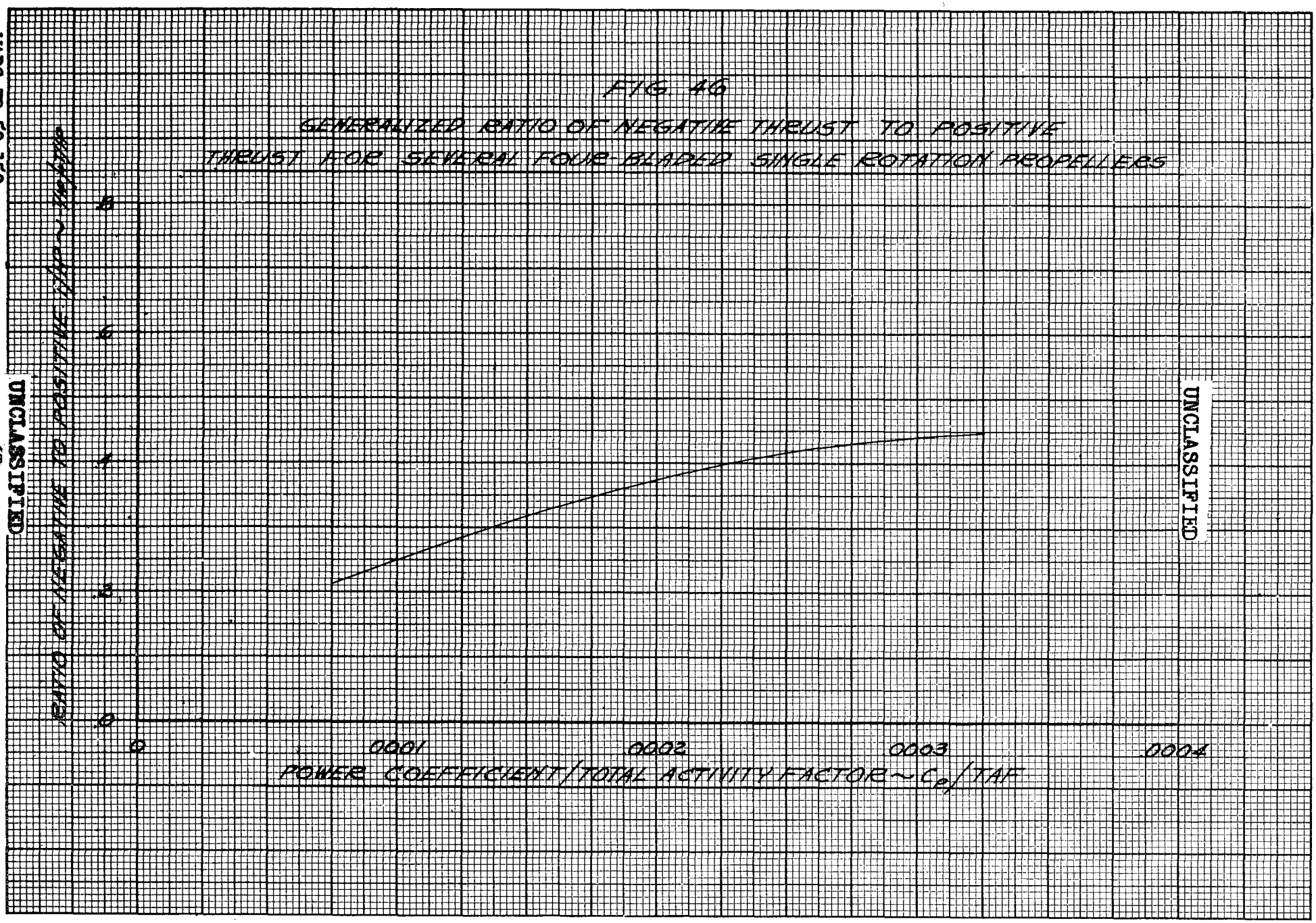

UNCLASSIFIED

BIBLIOGRAPHY

1. Platt, Robert J. Static Tests of Four Two-Blade NACA Propellers Differing in Camber and Solidity. NACA RM 18H25a, December 1948.

2. Corson, Blake W. and Mastrocola, Nicholas Static Characteristics of Curtiss Propellers Having Different Blade Sections. NACA Wartime Report L-568, August 1941.

3. Corson, Blake W. and Mastrocola, Nicholas Static Characteristics of Hamilton Standard Propellers Having Clark-Y and NACA 16-Series Blade Sections. NACA Wartime Report L-529, August 1941.

4. Gilman, Jean Static Thrust and Torque Characteristics of Single and Dual-Rotating Tractor Propellers. NACA Memorandum Report, June 1944.

5. Working Charts for the Computation of Propeller Thrust Throughout the Take-Off Range. NACA ARR 3G26, July 1943. (Extended by Propeller Laboratory)

6. Enos, L. H. Static Thrust Characteristics of Propellers Using Clark-Y, R.A.F. 6 and 2400 Profiles. Air Corps Technical Report No. 4319, June 1937.

7. Haines, A. B. and Chater, P. B. Revised Charts for the Determination of the Static and Take-Off Thrusts of a Propeller. British RAF Report No. Aero 2135.

8. Numerous Electric Motor Whirl Tests at Propeller Laboratory, Wright Air Development Center, Wright-Patterson Air Force Base, Ohio

9. Wood, John H. and Swihart, John M. The Effect of Blade Section Camber on the Static Characteristics of Three NACA Propellers. NACA RML51L28 (Confidential)

10. Dernbach, Anthony F. Propeller Performance Calculation Procedure As Used by Propeller Laboratory, AAF Materiel Command. Engineering Division Memorandum Report No. ENG-52-587-16-3, 3 July 1943. (Obsolete)

11. Long, R. F. B-29 Propeller Velocity Survey. United States Air Force Technical Report No. 5473, April 1946.

DISTRIBUTION LIST

Publications and Forms Branch, Publishing Division,
Air Adjutant General, WCAPP - (1)

ASTIA Document Service Center, DSC-SA - (2)

Aerodynamics Branch, Propeller Laboratory,
Directorate of Laboratories, WCLBY - (8)

Administration Office, Propeller Laboratory,
Directorate of Laboratories, WCLBA - (1)

Aerodynamics Branch, Aircraft Laboratory,
Directorate of Laboratories, WCLSR - (1)

Design Branch, Aircraft Laboratory,
Directorate of Laboratories, WCLSD - (1)

Flight Data Branch, Weapons System Division
Deputy for Operations, WCOSF - (1)

Rotating Engine Branch, Power Plant Laboratory,
Directorate of Laboratories, WCLPR - (1)

Assistant for Plans Office, Weapons System Division
Deputy for Operations, WCOWP - (1)

Director, Air University Library
Maxwell Air Force Base, Alabama - (1)

Research and Development Board
Committee on Aeronautics
Attn: Panel on Aircraft Propulsive System
Washington 25, D. C. - (1)

Chief, Bureau of Aeronautics
Department of the Navy
Attn: Dr. Ivan Driggs
Washington 25, D. C. - (2)

National Advisory Committee for Aeronautics
1724 F Street, N. W.
Washington 25, D. C. - (3)

General Electric Company
Lockland, Ohio - (1)

Consolidated-Vultee Aircraft Corporation
Government Aircraft Plant No. 4
P. O. Box 371
Fort Worth, Texas - (1)

North American Aviation, Inc.
Los Angeles International Airport
Los Angeles 45, California - (1)

Aircraft Industries Association of America, Inc.
610 Shoreham Building
Washington 5, D. C. - (1)

Boeing Airplane Company
Seattle 14, Washington - (1)

Lockheed Aircraft Corporation
2555 North Hollywood Way
P. O. Box 551
Burbank, California - (1)

Douglas Aircraft Company, Inc.
3000 Ocean Park Boulevard
Santa Monica, California - (1)

Wright Aeronautical Division
Curtiss-Wright Corporation
Wood-Ridge, New Jersey - (1)

Westinghouse Electric Corporation
32 North Main Street
Dayton, Ohio - (1)

Pratt and Whitney Aircraft Division
United Aircraft Corporation
362 South Main Street
East Hartford 8, Connecticut - (1)

Allison Division
General Motors Corporation
Indianapolis 6, Indiana - (1)

Republic Aviation Corporation
Farmingdale, Long Island, New York - (1)

McDonnell Aircraft Corporation
P. O. Box 516
Municipal Airport
St. Louis 3, Missouri - (1)

Glenn L. Martin Company
Baltimore, Maryland - (1)

Hamilton Standard Division
United Aircraft Corporation
362 South Main Street
East Hartford 8, Connecticut - (1)

Curtiss-Wright Corporation
Propeller Division
Caldwell, New Jersey - (1)

Aeroproducts Division
General Motors Corporation
Dayton Municipal Airport
Vandalia, Ohio - (1)